ABSTRACT

LEE, SA YONG. Analysis of Properties of Synthetic Mineral Microparticles for Retention and Drainage System. (Under the direction of Dr. Martin A. Hubbe).

Over the past 20 years there has been a revolution involving the use of nano- or macro-sized particles as a component of drainage and retention systems during the manufacture of paper. More recently a group of patented technologies called Synthetic Mineral Microparticles (SMM) has been invented and developed. This system has potential to further promote the drainage of water and retention of fine particles during papermaking. Prior research, as well as our own preliminary research showed that the SMM system has advantages in both of drainage and retention, compared with montmorillonite (bentonite), which is one of the most popular materials presently used in this kind of application. In spite of the demonstrated advantages of this SMM system, the properties and activity of SMM particles in the aqueous state have not been elucidated yet.

To help understand the molecular mechanisms involved in SMM technology, streaming current and potentiometric titration were employed to characterize the charge behavior of SMM, depending on the synthetic conditions, which included variation of the Al/Si ratio, partial neutralization of Al species, salt addition and shear rate. Surface area of SMM and the distribution of SMM particle size were investigated with scanning electron microscopy in order to elucidate the relationship between the morphology and coagulation behavior of SMM, *versus* the pre-stated synthetic conditions, as well as to estimate the optimal conditions to produce SMM as a retention and drainage aid for use during papermaking.

Through the streaming current titration experiments it was found that pH variation, caused by the change of Al/Si ratio and partial neutralization of aluminum's acidity, profoundly affects the charge properties of SMM. These effects can be attributed to the variation of Al-ion speciation and the influence ionizable groups on the Si-containing particle surfaces. The relationship between Al/Si ratio and isoelectric pH, measured by potentiometric titration, was estimated through statistical estimation, using a factor, the OH/Al ratio. This procedure permits estimation of the Al/Si ratio values at which the SMM particles can be expected to have net negative charges, as required for a microparticle system for promotion of retention and dewatering during papermaking.

It was found that the structural characteristics of SMM particles could be explained in terms of the effects of ionic charges on colloidal stability of primary particles during formation of the SMM.

Finally, a combination of moderate pH condition (from 5 to 8), relatively low Al/Si ratio (from 0.63 to 0.88), and partial neutralization of Al species in the range of OH/Al ratio between 0 to 1 were concluded to produce an optimal SMM product in terms of a fine-particle retention and effectiveness as a drainage aid component.

ANALYSIS OF PROPERTIES OF SYNTHETIC MINERAL MICROPARTICLES FOR RETENTION AND DRAINAGE SYSTEM

by

SA YONG LEE

A dissertation submitted to the Graduate Faculty of
North Carolina State University
in partial fulfillment of the
requirements for the degree of
Doctor of Philosophy

WOOD AND PAPER SCIENCE

Raleigh, NC

2006

Approved by:

Dr. Olando J. Rojas	Dr. Lucian A Lucia
Dr. Joel J. Pawlak	Dr. Martin A. Hubbe Chair of Advisory Committee

BIOGRAPHY

The author was born in April 1973 in Seoul, Republic of Korea. He received his Bachelor of Science degree in Forest Products in 1998 from College of Agricultural and Life Science, Seoul National University, Seoul, Republic of Korea. Then he obtained a Master of Science degree in Forest Products in 2000 from College of Agricultural and Life Science, Seoul National University, Seoul, Republic of Korea. In August 2002, he moved to Raleigh and continued his Ph. D study at North Carolina State University. His interested research areas are (a) properties and performances of synthetic mineral microparticle (SMM) in wet-end system as a system of retention and drainage during paper making, (b) chemistry between aluminum and silica, and (c) colloidal properties of sodium aluminosilicate.

ACKNOWLEDGMENTS

Sa Yong Lee would like to express his best gratitude to his chair advisor, Dr. Martin A. Hubbe, for advising him not only on the technical matters with regard to the research but also learning American culture. He also would like to express his appreciation to his committee members Dr. Lucian A. Lucia, Dr. Orlando J. Rojas and Dr. Joel J. Pawlak for supporting the research project by giving valuable advice and scientific ideas. He emphasizes that without their great support the research would never have been performed with success.

The author would like to state his appreciation to the Specialty Minerals Co. and the National Research Initiative of the USDA Cooperative State Research, Education and Extension Service, and the Department of Wood and Paper Science for supporting the entire project. He would like to thank all the faculty, instructors, and staff who gave precious experiences to him at NC State University, especially Dr. John A. Heitmann and Dr. Dimitris S. Argyropoulos. Also, he is grateful to his friends, especially Dr. Junhua Chen, Dr. Min Zhang, Takao Sezaki, Taweewat Tripattharanan, and Yun Wang in the wet-end research group and Dr. Sunkyu Park, Dr. Jung Myoung Lee, Dr. Jooyoun Kim, Changwoo Jeong, Mathias Erik Vilhelm Lindstrom, Junlong Song, and Gang Hu in Department of Wood and Paper Science. Their assistance encouraged and inspired him to continue improving himself and spend a fulfilling time at NC State University.

Finally, he wishes to thank his family for their continuing support and encouragement throughout his life and appreciate the invaluable love of his spouse, Mee Hyang Park and his daughter, Sojin Lee.

TABLE OF CONTENTS

Page

LIST OF FIGURES

Page

CHAPTER 3.

CHAPTER4.

LIST OF TABLES

Page

CHAPTER 1

Introduction

Over the past 20 years there has been a revolution of using nano- or micro-size particles, such as colloidal silica, montmorillonite (bentonite), and micropolymers, as part of drainage and retention systems in the paper industry [1-13]. During the last 10 years a collection of patented technologies called Synthetic Mineral Microparticles (SMM) has been invented and developed to further increase the retention of fine materials used in paper manufacturing and the speed of drainage to promote the production rate [14-16].

Prior research and patents done by the inventors in Specialty Mineral Co. showed that the SMM system has advantages in both drainage and retention, compared with montmorillonite (bentonite), which is very popular as a material used for microparticle systems in paper industry [16].

Even though this SMM system has some advantages, the properties and activity of SMM in the aqueous state has not been elucidated yet. Additionally, some of the metal species dictated in patents, including $Al_2(SO_4)_3$, $ZnCl_2$, and $FeCl_3$, have SO_4^{2-}, Zn^{2+}, and Fe^{3+}, which are not regarded by papermakers as welcome species, due to the environmental concerns. For this reason, $AlCl_3$ was selected in the present study as the major metal species to sythesize SMM suspensions.

The purpose of this introductory section is to review past research findings related to various aspects of microparticles, including the SMM system. In this introduction, the role and

mechanism of microparticle system during papermaking is fundamental and will be discussed first. The SMM system, in particular will be reviewed second, describing the method of synthesis. Finally, chemistries of aluminum and silica which are used to synthesize SMM system will be considered as the background to understand properties of SMM and to anticipate the factors that can affect the properties of SMM.

1. MICROPARTICLE SYSTEM

Before the adoption of microparticle systems, paper technologists had developed techniques in order to overcome certain problems which papermakers encounter during production. For example, papermakers face challenges in retaining fine particles efficiently, while still achieving uniform formation of the paper [17]. To meet such goals papermakers traditionally have employed a step-wise procedure including, (1) dispersion of papermaking additives before addition in order to improve the functionality of each additives and to avoid excessive usage of dispersants and surface-active agent, (2) chemical coagulation in the fiber suspension to achieve gains in retention and drainage and surface-site preparation to make fibers and other solid additives suitable for interaction with retention aid, (3) flocculation by polyelectrolytes to improve retention, and (4) selective deflocculation to improve uniformity.

Microparticulate retention and drainage aid systems have become increasingly popular, starting in the early 1980's, because they are so markedly effective to conserve the retention rate achieved by the steps mentioned in previous phrase as well as to promote dewatering, which is primarily considered among the various papermaking factors to increase the production rate.

1.1. Species of Microparticle System

Fig. 1.1 shows the relative sizes of the microparticle products that have become the most widely used within the paper industry [18]. The drawing of a large, plate-like particle in the right side of Fig. 1.1 illustrates the shape of an alkali montmorillonite, or bentonite particle. Bentonite is one of the most popular microparticle types within the paper industry. Bentonite is being used to promote retention and drainage with a highly cationic charged polymer in wet-end during papermaking [7-9]. The width of bentonite, as shown in Fig. 1.1, is almost as large as mineral fillers used in papermaking or pigments in coating color, but the thickness of it is as thin as molecular dimensions [10].

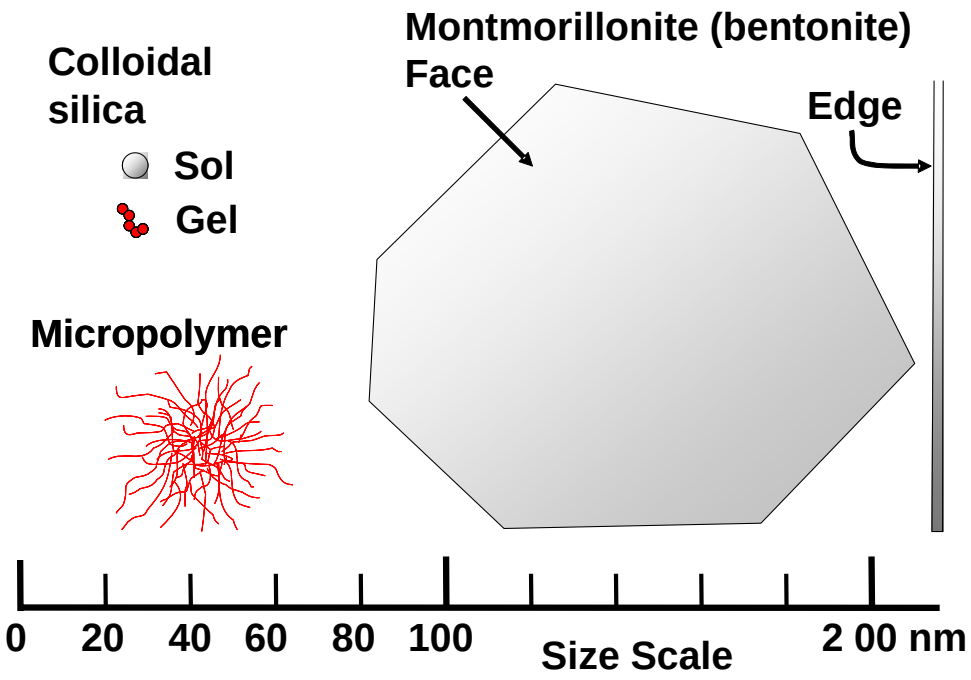

Hubbe, *Micro and Nonoparticles*, Ch. 1, TAPPI Press, *2005*

Fig. 1.1. Relative sizes of commercially available microparticle additives for paper manufacturing [18].

Colloidal silica, depicted in the upper left of Fig. 1.1, is the other popular microparticle. According to Iler [19], these particles generally fall into two major classes, “sol” and “gel.” “Sol” means that the primary particles exist separately from each other, whereas “gel” means that the primary particles coagulate together into chains or clusters. Sol-type colloidal silica products have been used as papermaking additives from the 1980s [1-2]. Gel-type colloidal silica products have been used at least since the 1990s [3-6].

A highly cross-linked water-soluble polymer, sometimes referred to as a “micropolymer” shown in the lower left of Fig. 1.1, is being used to obtain the similar effects with bentonite and colloidal silica [5, 11-13]. This is a highly negative charged substance and has a merit of adding smaller amount on the weight basis to get a certain degree of retention and drainage, in comparison with other microparticles.

1.2 Surface Charge of Microparticles

All of the microparticles commonly used in the paper machine wet end to improve retention and drainage have a highly negative charged surface [18]. As shown in Fig. 1.2, the negative charge of colloidal silica can be attributed to the dissociation of acidic hydroxyl groups in the pH range between about 3 and 7 [19-21]. Usually the negative charge and high surface area is significant for achieving a high effectiveness in terms of retention and drainage [18]. The negative surface charge of oxide materials, including silica, is expected to decrease with decreasing pH. In order to maintain a strong negative charge under neutral to acidic papermaking conditions, it was found that aluminum-containing colloidal silica particles

could be used [22-23]. The isomorphic substitution of tetravalent silicon atoms by trivalent Al in crystalline sites causes an increased negative charge at moderately acidic conditions, near to neutral pH.

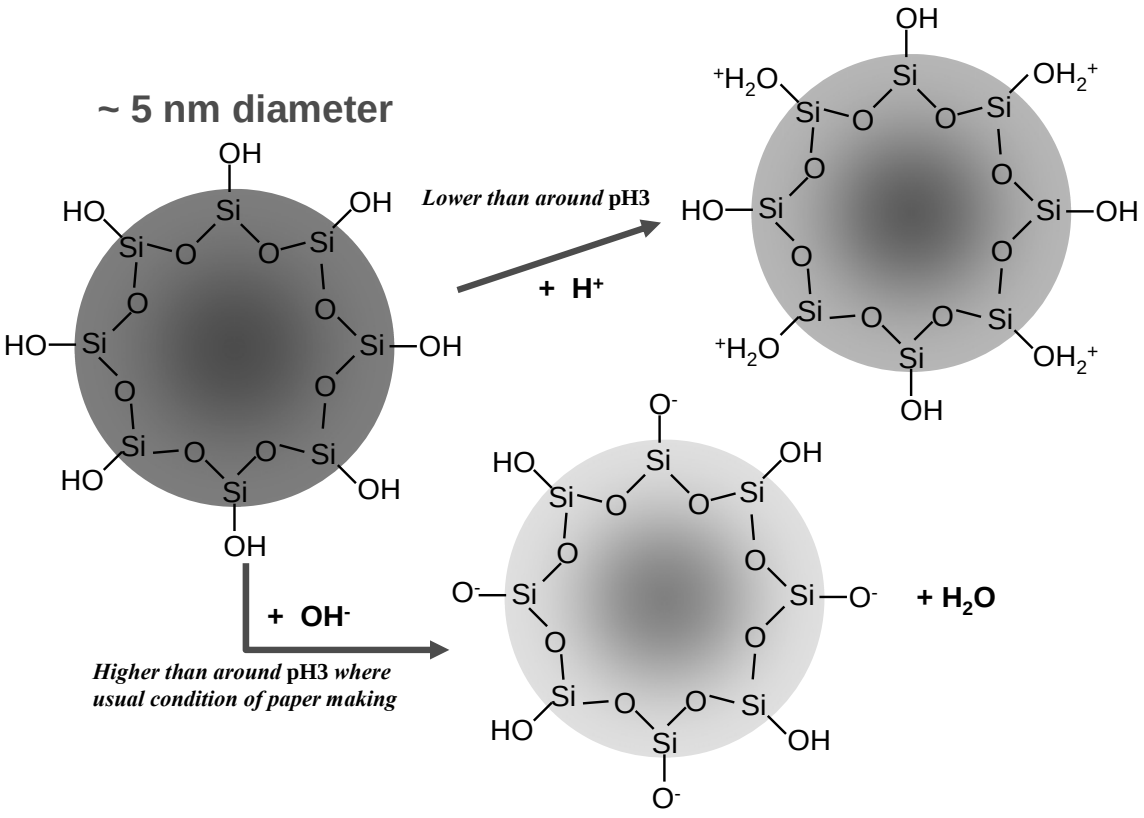

Fig. 1.2. Surface charge of silica sol or gel; Negative charge of particle surface due to dissociation of acidic hydroxyl groups [19-21].

1.3. Synthesis of Colloidal Silica and Considerable Factors for SMM

Fig. 1.3 shows Iler's graphical depiction of the process for chemical synthesis of colloidal silica particles [19]. Having a high pH, the initial alkali silicate solution is stable. Addition of acid reduces the pH of a sodium silicate solution and makes products unstable in solution and

susceptible to precipitation. Thereby, when one adds salts, which make the electrical repulsion weaker, the particles will have a greater tendency to become gelled and fused together. At the end of the process, the colloidal silica suspension may be chemically stabilized to prevent further growth or gellation by adjusting the pH or salt concentrations.

Even though the compositions and preparation of SMM additives differ in detail from Iler's depiction in Fig. 1.3, there are some variables, such as pH, addition of salts, and the Al/Si ratio, which can be used to obtain primary particles that are of controlled size and degree of fusion.

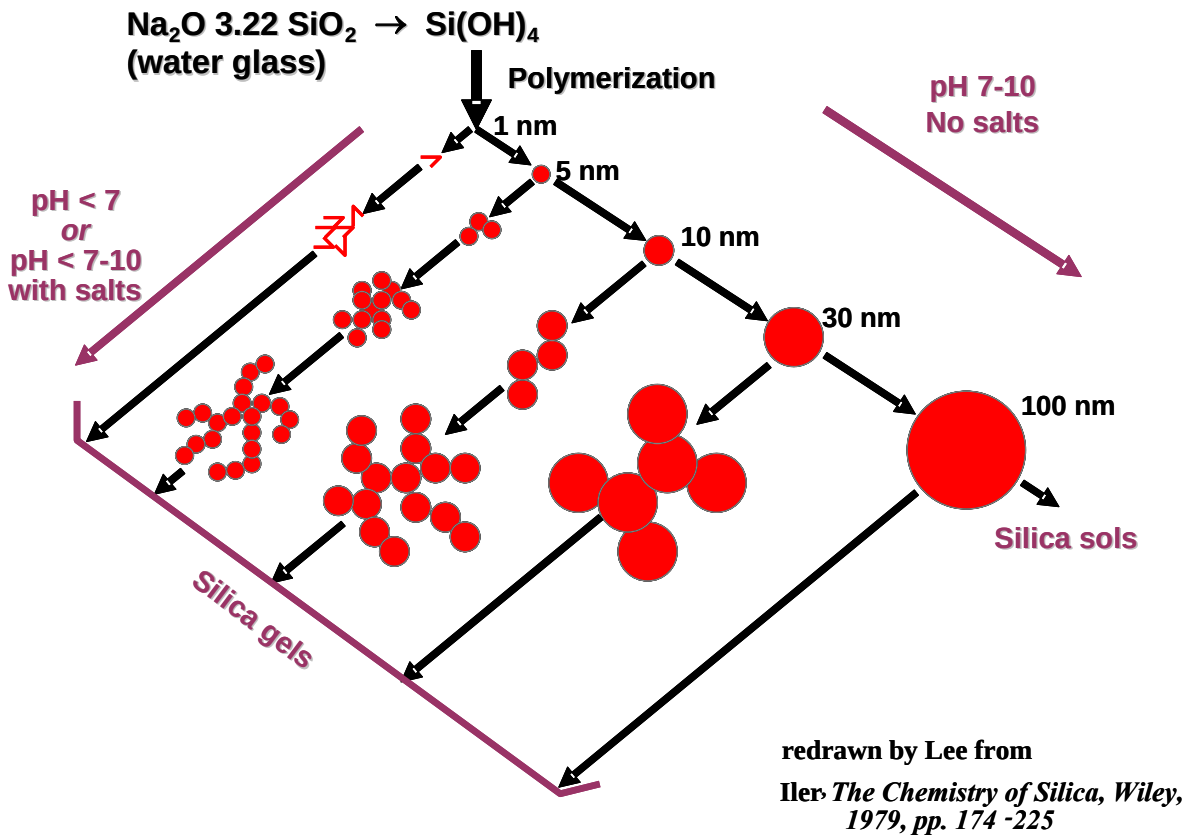

Fig. 1.3.Conventional synthesis schemes for colloidal silica particles of two main classes [19].

1.4. Sequential Addition of Microparticles within Wet-End

Fig. 1.4 illustrates a typical scheme for implementing a microparticle retention and drainage program in a paper mill [18]. The sequential addition of cationic polymer and the microparticle produces a synergistic effect that shows better retention and drainage performance than the effect of using the polymer alone. Commonly, the cationic polymer is added ahead of a pressure screen. The screening action breaks the polymer bridges between fibers, and redisperses the fibers from each other. The separated sequential addition of cationic polymer and microparticles has some positive effects, such as excellent mixing of the first additive and avoiding the severe flocculating effect of the polymeric additive which would be expected to cause bad formation. There are many examples in the field and in the published literature where the order of addition is either the same as what is shown in Fig. 1.4 [18, 7-9, 24-33] or the opposite order [7-8,27,34-42].

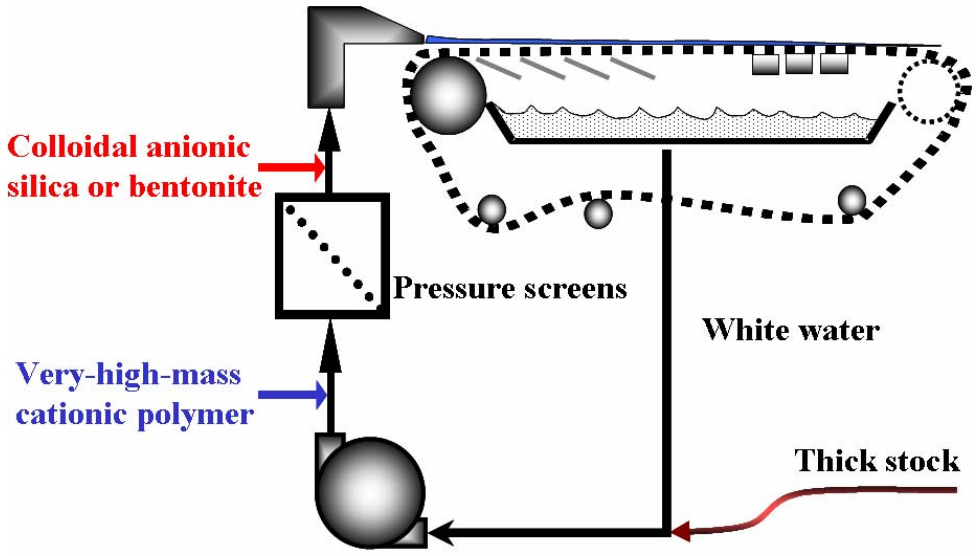

Hubbe, *Micro and Nanoparticles*, Ch. 1, TAPPI Press, 2005

Fig. 1.4. Typical addition scheme for microparticles, preceded by a very-high mass cationic polymer and a high-shear unit operation such as screening [18].

1.5. How Microparticles Work for Retention and Drainage (Molecular Mechanism)

As shown in Fig. 1.5A, treatment of the furnish with a retention aid results in the formation of polymer bridges [48-49], which tend to hold fibers together in larger flocs. This effect often causes a more floccy formation appearance of the paper product [46]. However, as shown in Fig. 1.5, passage of the stock through a pressure screen tends to break up these flocs with the breakage of the initial polymer bridges.

There can be an advantage of less persistent fiber flocs, resulting in a more uniform paper product. However, it is true that breakage of some of the initial polymeric bridges tends to work against efficient retention of fine particles. The process tends to favor the survival of the bridges linking fiber surfaces to fine particles such as mineral fillers [31].

Fig. 1.5B and 1.5C show how post-screen addition of a microparticle is expected to affect bridging attachments between solids in the same papermaking suspension, which previously had been treated with very-high-mass cationic polymer. According to various studies, the new microparticle-induced bridges (Fig. 1.5C) are expected to be denser, and therefore less capable of holding onto water than the initial polymer bridge (Fig. 1.5A) [31,46,53-54]. Additionally, as shown in Fig. 1.5C and 1.5D, the microparticle-induced bridges are expected to be more reversible, capable of being broken by hydrodynamic shear, but also capable of coming together at the beginning of or during formation of wet-web. This reversibility is believed to be an important feature of advanced retention and drainage programs [55].

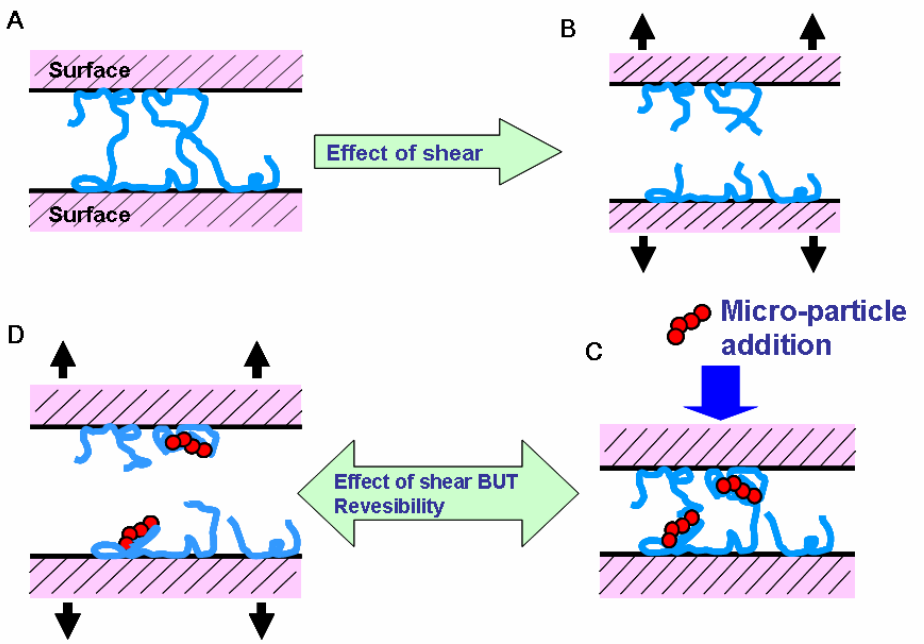

Fig. 1.5. Schematic illustrations of (A) the molecular mechanism of polymer bridging, (B) irreversible breakdown of some of the bridges when retention aid is added ahead of pressure screens, (B-C) the effect of subsequent addition of a microparticle to the system, and (C-D) the reversibility of microparticle-induced polymer bridges when exposed to high hydrodynamic shear, allowing the process of (B-C) to be repeated later.

Microparticle-induced fiber flocs can be expected to be broken and redispersed when the furnish passes through the high shear caused by the step diffusers in hydraulic headboxes and the headbox slice opening [56]. However, it has been shown that bridges mediated by microparticles are able to recover to a large extent [55], so it is also reasonable to expect that many bridging contacts are reestablished immediately before or during formation of the wet web. In terms of packing density of the web, such adhesive attachments are expected to have the same effect as they do on a macroscopic scale; sticky objects tend to form a relatively bulky, low-density packed structure, whereas slippery objects can slide past each other to form a denser mat of material [57-58]. Practical evidence of this mechanism includes an

observed porous and bulky nature of paper that results from a microparticle additive program [27,55], though it is important to note that much of the porosity is expected to disappear when the paper web is pressed and dried. The net benefits from this mechanism are faster drainage and more uniform paper.

As shown in Fig. 1.6, a positively charged chain of a retention aid molecule is expected to wrap itself around the highly negative surface of a microparticle and make itself denser with lower capability to hold onto water. This effect is expected to result in the expulsion of water from the polymer coils and bridges. Finally the contraction of macromolecules is expected to enhance the drainage speed. In addition to the pronounced drainage enhancement of microparticles [4,7-8,13,22,26-28,43,55,60-70], a further demonstration of this principle is an observed increase in density of polyelectrolyte material upon addition of microparticles, causing it to settle more rapidly in aqueous suspension [43,59].

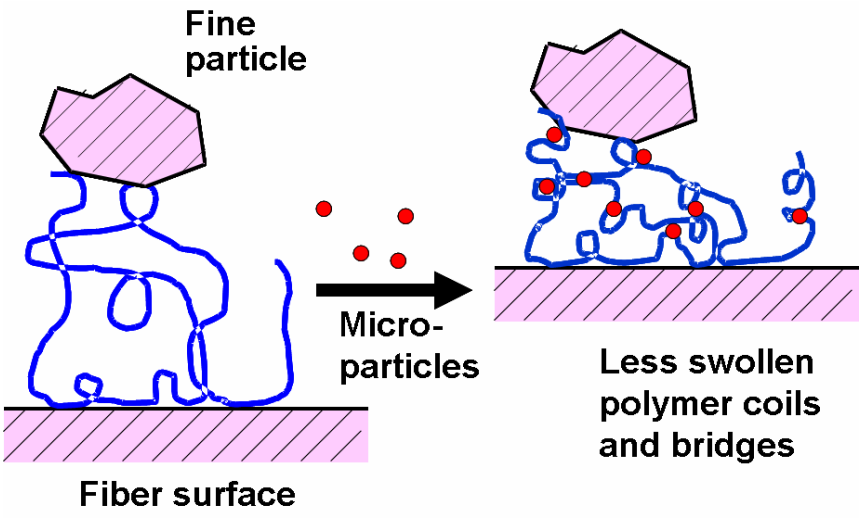

Fig. 1.6. Schematic illustration of how microparticles can cause contraction of loops of polyelectrolyte, including polymer bridges, so that the polymer material holds less water.

1.6. Balance of between the Amounts of Cationic Polymer and Microparticles

Fig. 1.7 shows the synergistic effect between an amylase type of cationic starch and colloidal silica in the case of a well-refined papermaking furnish [43]. Without colloidal silica, the measured freeness of the furnish was not affected very much by the starch addition. When colloidal silica was used, the Canadian Standard Freeness increased about 90 to 130 ml, depending on the dosages of cationic starch and colloidal silica. These results show that there needs to be a balance between the amount of cationic polymer and the amount of microparticle in order to get the most rapid dewatering. Several studies have confirmed the sensitivity of microparticle systems to the careful balancing of the dosages of oppositely charged additives [34, 44, 45, 47].

Some related results are shown in Fig. 1.8 [20]. However, in this example the polymer was a conventional retention aid, a very-high-mass cationic copolymer of acrylamide. The measured variable was fines retention, rather than freeness. Please note that the effectiveness of the retention aid depended not only on the amount of colloidal silica added, but also the structure of the microparticles. It made a big difference whether the particles were in the "sol" or "gel" form (Fig. 1.1). Thereby, the added amount and the structure of SMM can be expected to be important experimental factors.

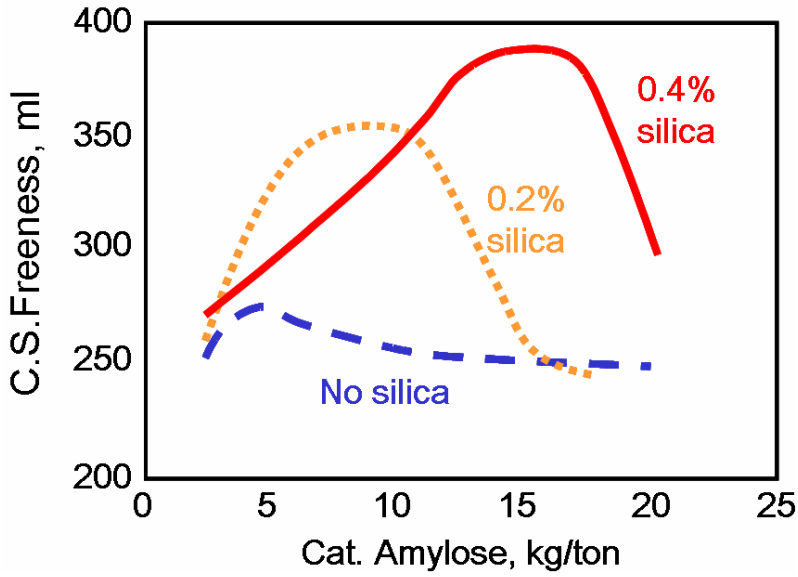

Carlson, *Proc. 24th EUCEPA Conf.*, 1990, 161.

Fig. 1.7. Effect of cationic amylose starch on the freeness of papermaking stock, with or without subsequent addition of silica microparticles - The synergistic effect between an amylose type of cationic starch and colloidal silica was varied, depending on the dosages of cationic starch and colloidal silica [43].

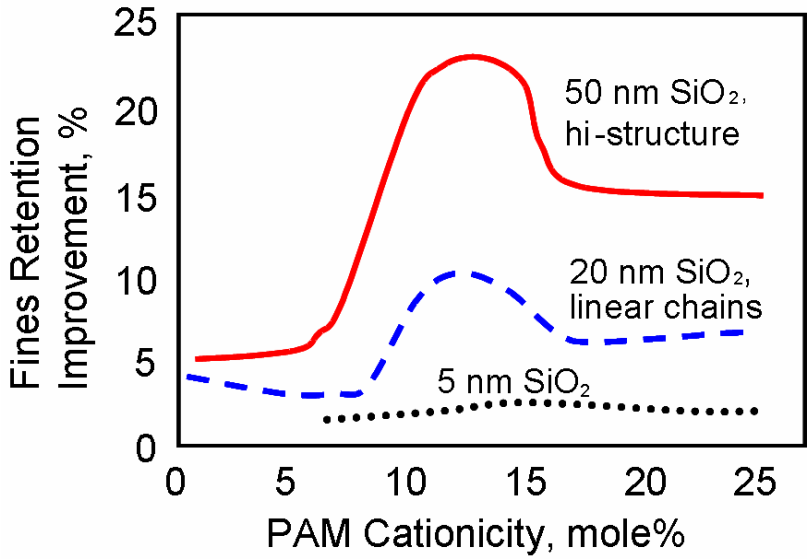

Moffet, *TAPPI J. 77*(12): 133 (1994)

Fig. 1.8. Effect of cationic acrylamide copolymer (retention aid) on retention of fiber fines, with or without subsequent addition of colloidal silica; it is affected by the structure of the microparticles [20].

2. SYTHETIC MENERAL MICROPARTICLES (SMM)

"Synthetic Mineral Microparticles" (SMM) is a patented system which can increase the rate of dewatering and promote the retention of fine particles more efficiently during the process of papermaking [14-16].

The relative simplicity of its synthesis process allows SMM to achieve certain advantages, such as on-site preparation, reduced cost, good retention and dewatering performances, an ability to optimize microparticle properties needed during paper production, and a more favorable balance of retention and paper uniformity.

The SMM technology is protected by the following US patents:

- US 6,184,258: Process for preparation of microparticles [14]
- US 5,989,714: Composition patent for microparticles [15]
- US 6,183,650: Water treatment by means of microparticles [16]

Of these three patents, US 6,184,258 shows the most basic invention. It is shown that highly effective microparticles can be synthesized by simple mixing a dilute solution of silicate ions and a dilute solution of aluminum ions. This is very similar to the synthesis procedures which are the main concern of this thesis project.

SMM can be envisioned as being a composite of small parts, based on a precipitation reaction between metal ionic species and silicate ions. The chemical process of synthesizing SMM can be illustrated by the following reaction between sodium metasilicate (SMS) and aluminum sulfate (alum):

$$y\mathrm{Na_2SiO_3} + x\mathrm{Al_2(SO_4)_3} \rightarrow \mathrm{Na_{2y-6x}Al_{2x}Si_yO_{3y}} + 3x\mathrm{Na_2SO_4}$$

As disclosed in the patents, the chemical nature of the additives and their relative concentrations in the mixture can be varied within relatively wide ranges.

2.1. Synthesizing Method of SMM

Sodium meta-silicate ($Na_2SiO_3 \cdot 5H_2O$) is used as base ingredient with k molal concentration. The value of x, the molar concentration of sodium meta-silicate ($Na_2SiO_3 \cdot 5H_2O$) in u gram mass of solution with k molal concentration is calculated by (1). MW_s is the molecular weight of sodium meta-silicate.

$$x = \frac{k \cdot u}{1000 + MW_s \cdot k} \tag{1}$$

The value of y, the molar concentration of metal ingredient in v gram weight of solution with l molal concentration was calculated by (2). MW_m is the molecular weight of the metal ingredient.

$$y = \frac{l \cdot v}{1000 + MW_m \cdot l} \tag{2}$$

The metal/Si ratio is given by $\alpha = \frac{m \cdot y}{n \cdot x}$, where m is the number of metal atoms in one molecule of metal ingredient and n is the number of Si atoms in one sodium meta-silicate molecule. Various molar ratio of metal to silicate can be used, for example Al/Si = 0.5, 0.63,

0.76, 0.88, 1.00, and 1.14, Zn/Si = 1.14, and Fe/Si = 0.76. The amounts of sodium meta-silicate and metal ingredient solutions were calculated by (3)

$$v = \frac{1000 + MW_m \cdot l}{m \cdot l} \cdot \frac{\alpha \cdot n \cdot k}{1000 + MW_s \cdot k} \cdot u \tag{3}$$

When the metal ingredient is aluminum chloride, in the case of 25 % neutralization of Al^{3+}, w ml of 1 M NaOH solution is calculated by (4) and added to the sodium meta-silicate solution during continuous stirring.

$$w = 0.75 \cdot y \cdot 1000 \tag{4}$$

Shear levels during synthesis of microparticle were varied as 500 rpm, 1500 rpm, and higher, for instance 13,000 rpm. To provide a concrete example of how these equations are used, 80 grams (u) of a 0.455 (k) molal aqueous sodium meta-silicate solution ($Na_2SiO_3 \cdot 5H_2O$) is added to a 250 ml beaker equipped with an rpm-controllable motor stirrer. 49.8 grams (v) of a 0.566 molal (l) aqueous aluminum chloride solution ($AlCl_3 \cdot 6H_2O$) is then rapidly added to the 500 rpm stirring meta-silicate solution at ambient temperature. 19.7 ml 1M NaOH (w) is added immediately for 25 % neutralization. The mixture is stirred for one minute, after which the reaction is terminated. The reaction results in a cloudy, white slurry, containing 2.1706 % of aluminum silicate microparticles. 1mM of sodium chloride (NaCl), based on the total weight of solution, can be added for salt concentration.

Based on the amounts of reagents, and assuming complete consumption of Si species, the reactions could be described by the following equations;

$x \cdot Na_2SiO_3 + y \cdot Al_2(SO_4)_3 \rightarrow Na_{2x-6y}Al_{2y}Si_xO_{3x} + 6y \cdot Na^+ + 3y \cdot SO_4^{2-}$,when x-3y >0 and

$\rightarrow Al_{(2x/3)}Si_xO_{3x} + 2x \cdot Na^+ + (2y - 2x/3) \cdot Al^{3+} + 3y \cdot SO_4^{2-}$,when x-3y <0.

$x \cdot Na_2SiO_3 + y \cdot AlCl_3 \rightarrow Na_{2x-3y}Al_ySi_xO_{3x} + 3y \cdot Na^+ + 3y \cdot Cl^-$, when $2x-3y > 0$ and

$\rightarrow x/3 \cdot Al_2(SiO_3)_3 + (y - 2x/3) \cdot Al^{3+} + 2x \cdot Na^+ + 3y \cdot Cl^-$, when $2x-3y < 0$.

$x \cdot Na_2SiO_3 + y \cdot ZnCl_2 \rightarrow Na_{2x-2y}Zn_ySi_xO_{3x} + 2y \cdot Na^+ + 2y \cdot Cl^-$, when $x-y > 0$ and

$\rightarrow x \cdot ZnSiO_3 + (y- x) \cdot Zn^{2+} + 2x \cdot Na^+ + 2y \cdot Cl^-$, when $x-y > 0$.

$x \cdot Na_2SiO_3 + y \cdot FeCl_3 \rightarrow Na_{2x-3y}Fe_ySi_xO_{3x} + 3y \cdot Na^+ + 3y \cdot Cl^-$, when $2x-3y > 0$ and

$\rightarrow x/3 \cdot Fe_2(SiO_3)_3 + (y - 2x/3) \cdot Fe^{3+} + 2x \cdot Na^+ + 3y \cdot Cl^-$, when $2x-3y < 0$.

2.2. Retention Performance of SMM

Table 1.1 compares the Britt Jar first-pass retention achieved in the laboratory during initial testing with an SMM product prepared by adding aluminum sulfate solution to sodium silicate solution at an Al/Si ratio of 0.5. All eight fiber furnishes considered were at 1 % consistency with 20 % of added filler. Percol®368 was the coagulant, followed by Percol®175 cationic acrylamide copolymer retention aid, and then microparticle addition always at the 5 lb/ton dosage.

It is worth noting that the results in Table 1 were obtained without any effort to optimize the conditions of mixing, overall concentration of the mixture or detailed chemistry other than the ratio of the two major components of the SMM colloidal dispersion.

Table 1.1. Performance of SMM in comparison with commercially available microparticles in four different fiber furnish environments.

Microparticle Type	Britt Jar First Pass Retentions (%)							
	Furnish & Filler Type*							
	Kraft A		Kraft B		Groundwood A		Groundwood B	
No Microparticle	29	37	40	37	53	51	55	28
SMM	**57**	**74**	**60**	**60**	**54**	**61**	**81**	**61**
Bentonite	50	75	64	64	73	72	84	77
Colloidal SiO_2	27	35	40	32	50	51	52	30

* Kraft A = 100 % softwood kraft; Kraft B = mixed kraft; Groundwood A and B are from different paper mills; PCC = Albacar® HO; Clay = Georgia water-washed; Bentonite = Hydrocol® O; Colloidal silica = Nalco® 8671.

2.3. Effect of SMM Al/Si Ratio

As shown in Fig. 1.9, the filler retention performance of SMM microparticles was only moderately sensitive to the Al/Si ratio. The furnish was 100 % softwood kraft with 20 % added filler. For tests involving water-washed clay filler, the furnish was first treated with 2 lb/ton of Percol®386 coagulant, followed by 1 lb/ton of Percol®175 cationic acrylamide copolymer retention aid, and finally 5 lb/ton of the microparticle on a dry basis. In the case of precipitated calcium carbonate (PCC, Albacar®HO) the additives were 1 lb/ton of Percol®175 retention aid followed by 5 lb/ton of microparticle. The highest retention was obtained at a critical Al/Si ratio. Fig. 1.10 shows confirmatory results for different pulp furnishes.

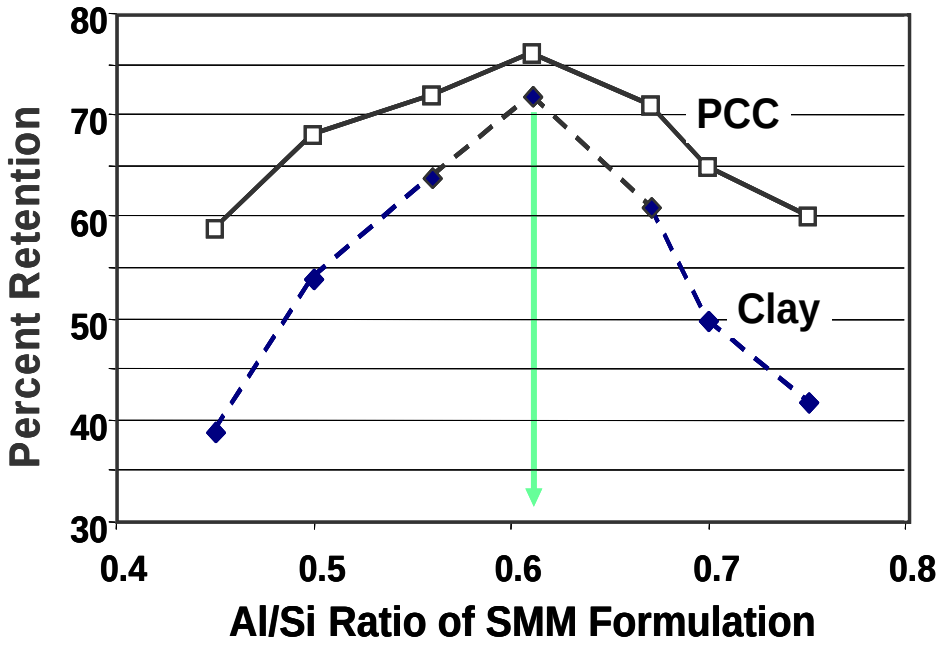

Fig. 1.9. Effect of Al/Si ratio of SMM microparticles on filler retention results in a bleached kraft furnish- There is a critical point of Al/Si ratio to get the maximum percent retention.

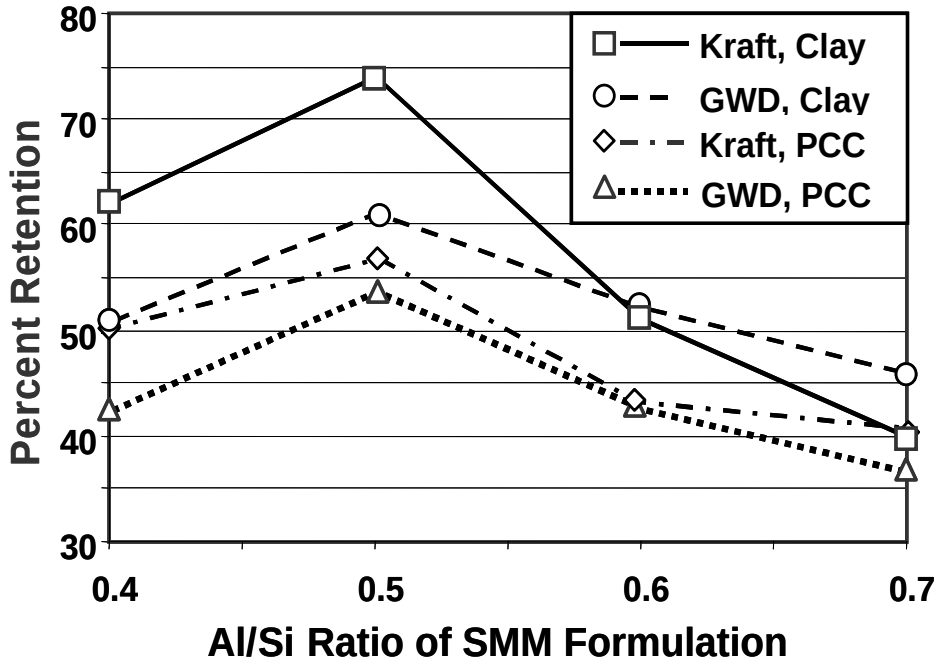

Fig. 1.10. Effect of Al/Si ratio of the SMM additive for enhancement of filler retention in furnish already treated with cationic retention aid.

3. ALUMINUM CHEMISTRY

As described in the previous section, $Al_2(SO_4)_3$, $ZnCl_2$, and $FeCl_3$ are used to synthesize SMM particles according to certain embodiments of the patents. However, the SO_4^{2-}, Zn^{2+}, and Fe^{3+} ionic species are sometimes avoided by papermakers due to the environmental regulations. For this reason, the present study was based on the use of $AlCl_3$ as the major metal species used to synthesize SMM. In order to understand the behavior of SMM in aqueous solution and to help in interpreting the results from experiments, the chemistry of aluminum ions will be reviewed in this section.

3.1. Aluminum used in Papermaking

In the early year 1807, Illig introduced aluminum sulfate, or "papermaker's alum" ($Al_2(SO_4)_3 \cdot 18H_2O$), in a method for improving the wetting resistance of paper by precipitating rosin size onto fiber surfaces [71-72]. Furthermore, papermakers found that alum can coagulate fine materials, increase the retention rate of those materials, and also promote more rapid dewatering. Such effects have been attributed to the highly cationic charge of aluminum ions under acidic papermaking conditions. Consequently, alum has become widely used as retention and drainage aid [73-77].

As neutral and alkaline papermaking systems gradually have become more popular, another aluminum compound, polyaluminum chloride (PAC), has been more widely used. A key advantage of PAC is that it can remain positive in surface charge even at pH values above 6.

Therefore, it is possible that positively charged aluminum ions are present even at neutral and weakly alkaline pH values of process water used in papermaking.

3.2. Chemistry of Aluminum Ions

The chemistry of aluminum ions in aqueous solution is very complicated. Aluminum ions undergo various hydrolysis reactions depending on pH. When solution pH is higher than 3, the hydrolysis of Al^{3+} begins [78]. Table 1.2 shows the reaction equilibrium constants of aluminum ions [79, 80]. Stole *et al.* reported that the monomeric aluminum species are formed according to the reactions in rows 1 and 2 of Table 1.2 when the ratio OH/Al is lower than 0.5, with a low total aluminum concentration of 10^{-2} to 10^{-5} mol/L [78]. When the OH/Al value is between 0.5 and 2.46, the monomeric species of aluminum ions can be oligomerized to species such as $Al_2(OH)_2^{4+}$, $Al_3(OH)_4^{5+}$, and $Al_{13}O_4(OH)_{24}^{7+}$ by following the reactions in the row 5, 6, and 7 of Table 1.2 [81-85]. Fig. 1.11 shows the beginning step of polymerization, and then aluminum ions undergo further complexation reactions.

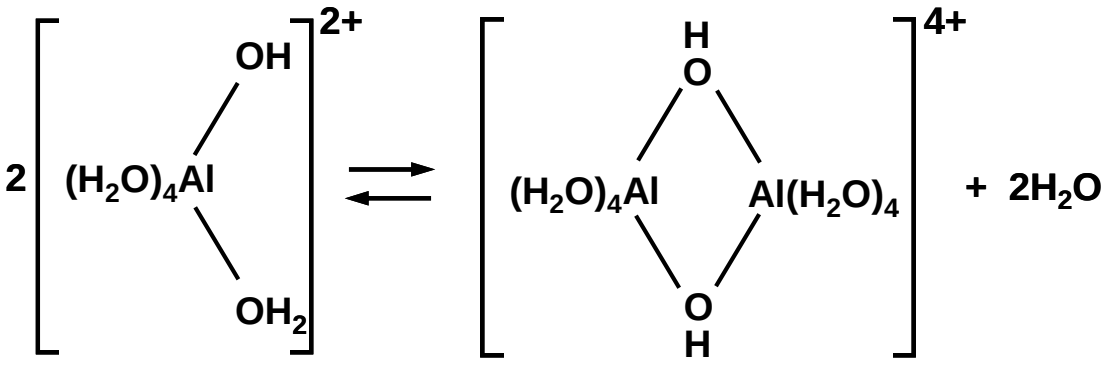

Fig. 1.11. The formation of aluminum ion dimmer.

Table 1.2. Hydrolysis of Al(III) in Aqueous Media [79,80].

Equilibrium Reaction	Log K at 25℃
$Al^{3+} + H_2O \rightleftharpoons Al(OH)^{2+} + H^+$	-5.0
$Al(OH)^{2+} + H_2O \rightleftharpoons Al(OH)_2^{+} + H^+$	-4.3
$Al(OH)_2^{+} + H_2O \rightleftharpoons Al(OH)_3 + H^+$	-5.7
$Al(OH)_3 + H_2O \rightleftharpoons Al(OH)_4^{-} + H^+$	-8.0
$2Al^{3+} + 2H_2O \rightleftharpoons Al_2(OH)_2^{4+} + 2H^+$	-7.7
$3Al^{3+} + 4H_2O \rightleftharpoons Al_3(OH)_4^{5+} + 4H^+$	-13.94
$13Al^{3+} + 28H_2O \rightleftharpoons Al_{13}O_4(OH)_{24}^{7+} + 32H^+$	-98.73
$Al(OH)_3$ (amorphous) $\rightleftharpoons Al^{3+} + 3OH^-$	-31.5 (estimated)
Note: K is the stepwise equilibrium hydrolysis constants for the respective reactions.	

3.3. Distribution of Aluminum Ionic Species Depending on pH

Various studies have been based on an assumption that pH is the primary factor governing the speciation of aluminum ions [86-87]. By assuming that no other stable hydrolyzed cationic species would coexist in the presence of precipitate, Haydin and Rubin calculated the effect of the pH on aluminum colloidal behavior [86]. As shown in Fig. 1.12, these authors were able to fit their data to certain assumed ionic and neutral species. They supported the existence of the polymeric ion $Al_8(OH)_{20}^{4+}$, which was first used to interpret colloid coagulation data by Matijević and Tezak [94]. At the same time, the probability of the existence of other polymeric ions was dismissed by their research. Arnson studied the

distribution of aluminum species as a function of pH under acidic conditions. The results are shown in Fig. 1.13 [88].

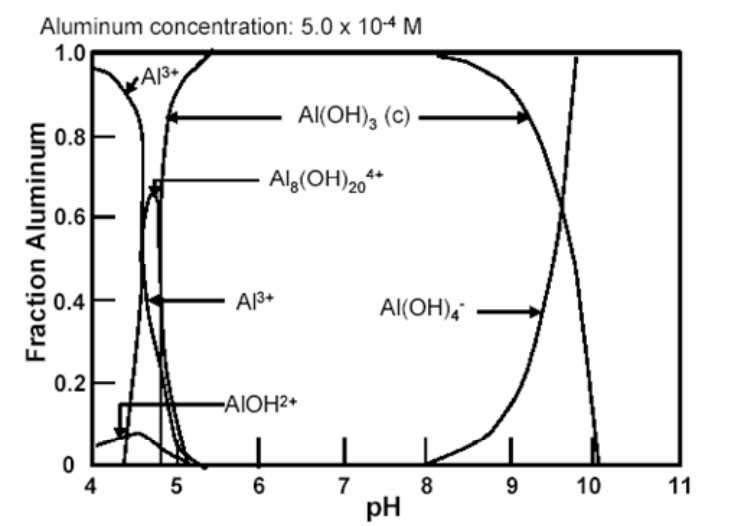

Smith, R.W. *Advances in Chemistry Series*, 106: 250-279, 1971

Fig. 1.12. Distribution of aluminum ionic species as a function of pH for $AlCl_3$ in both acid and alkaline pH range [93].

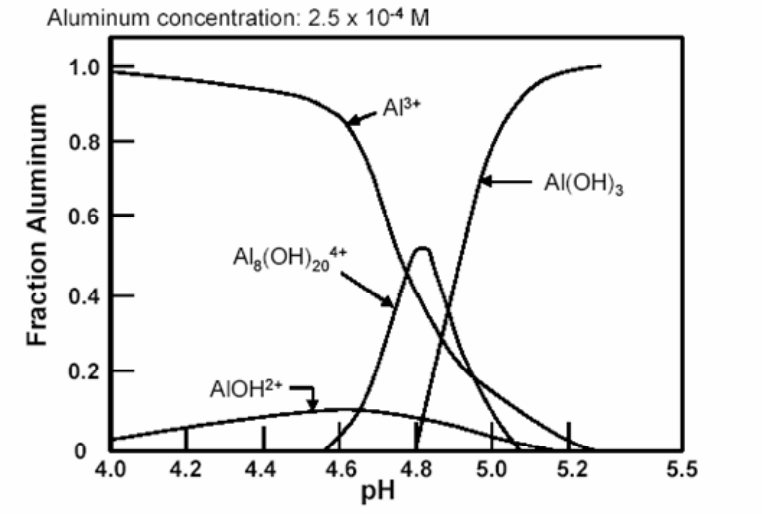

Arnson, T.R., Tappi Journal, 65(3): 125-130, 1982

Fig. 1.13. Distribution of aluminum ionic species as a function of pH for $AlCl_3$ under acidic condition [88].

After ^{27}Al NMR was found to be sensitive to the hydrolyzed aluminum species, as well as the unhydrolyzed ion $Al(H_2O)_6^{3+}$ in the aqueous solution, Akitt *et al.* adopted this technique to investigate the structure of aluminum ion species, combining with other test methods, such as spectrophotometric and potentiometer methods [83,87]. Bottero *et al.* also studied the effect of pH on aluminum chloride solutions using the ^{27}Al NMR technique. Fig. 1.14 shows a typical spectrum. NMR spectra were able to provide much clearer evidence of the existence of different aluminum ionic species. They stated that the Al_{13} species, $AlO_4Al_{12}(OH)_{24}(H_2O)_{12}^{7+}$, were the predominant polymeric species, instead of $Al_8(OH)_{20}^{4+}$ discussed previously. The proposed structure of $AlO_4Al_{12}(OH)_{24}(H_2O)_{12}^{7+}$ is shown in Fig. 1.15. Furthermore, other species present are confirmed as $Al(H_2O)_6^{3+}$, $Al(OH)(H_2O)_5^{2+}$, $Al(OH)_2(H_2O)_4^{+}$, $Al_2(OH)_x(H_2O)_{10-x}^{(6-x)+}$ [89-92] shown in Fig 1.16.

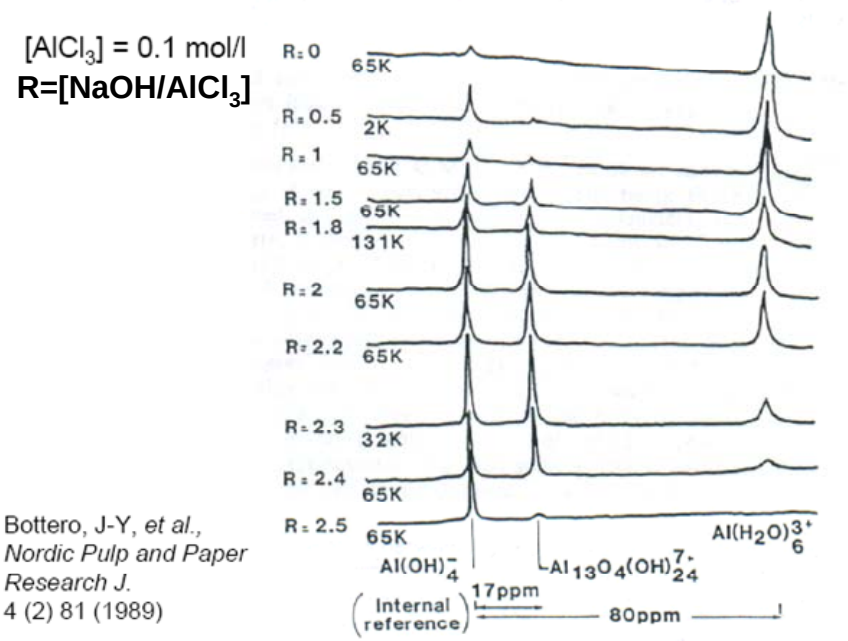

Fig. 1.14. The NMR spectra of aluminum species in aluminum chloride solution; R is ratio of molar concentration of OH^- to molar concentration of Al^{3+} in solution [90].

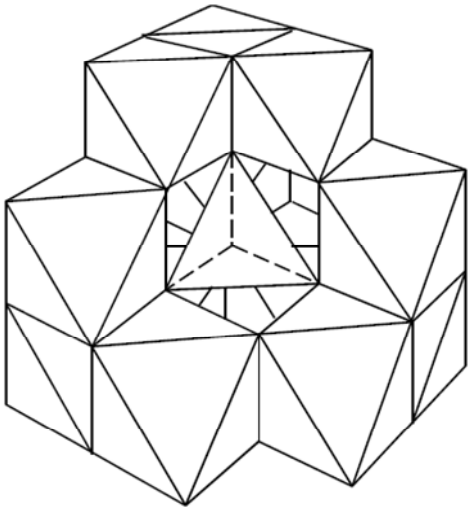

Base, C.F. and Mesmer, R.E., *The Hydrolysis of Cations*, John Wiley & Sons, New York, 1976

Fig.1.15. Representation of the $[AlO_4Al_{12}(OH)_{24}(H_2O)_{12}]^{7+}$ polynuclear species; demonstrating the tetrahedrally coordinated aluminum at the center of the cage-like structure comprising 12 octahedrally coordinated aluminum atoms joined by common edge [79, 95].

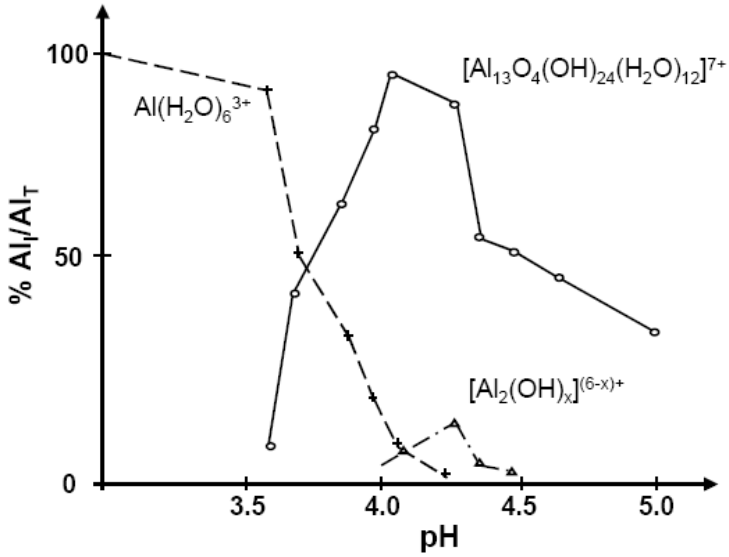

Bottero, J. Y., *et al*., *Progress in Water Technology, 13* (1): 601 (1980)

Fig. 1.16. The distribution of aluminum species in the solution measured with high resolution NMR, as depicted in Fig. 1.14 [89].

4. CHEMISTRY OF SILICA

4.1. Formation of Silanol Groups on Silica Surface

The concept of "combined, structurally bound" water has become widely used to describe the surface character of dispersed amorphous silica in aqueous solution. The concept helps to account for both theoretical and practical issues [19, 96-97]. OH groups that are bound through the valence bond with Si atoms on the silica surface, and in some cases with Si atoms inside the particles of silica, form silanol groups. In the 1930s, several researchers investigated the condensation processes of silicic acids [98-99], and slightly later, Carman showed that hydroxyl (silanol) groups, ≡Si–OH , should be present on the surface of silicate and silica [100].

Fig. 1.17 shows how silanol groups are formed on the surface of silica [101]. Firstly, silanol groups are formed during the condensation polymerization of $Si(OH)_4$ (Fig. 1.17(a)). In other words, this chemical change is expected to play a role in the growth of particles, as was depicted earlier in Fig. 1.3. In the solution supersaturated by the acid, $Si(OH)_4$ becomes converted into its polymeric form, which then changes into spherical colloidal particles containing ≡Si–OH groups on the surface. On the other hand, surface OH groups can be formed by rehydroxylation of dehydroxylated silica, as depicted in Fig. 1.17(b), when it is treated with water or aqueous solution. The surface silicon atoms tend to have a complete tetrahedral configuration. In an aqueous form, the free valence of this tetrahedral configuration becomes saturated with hydroxyl groups. However, two types of reactive sites

are present on the surface of silica by these reactions: strained siloxane bridges Si–O–Si (Fig. 1.18 b)) and silanols Si–OH (Fig. 1.18 a) and c)).

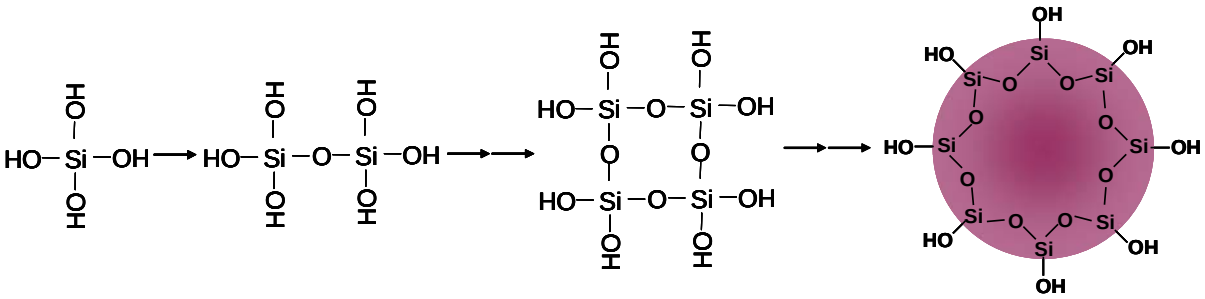

(a) Condensation Polymerization

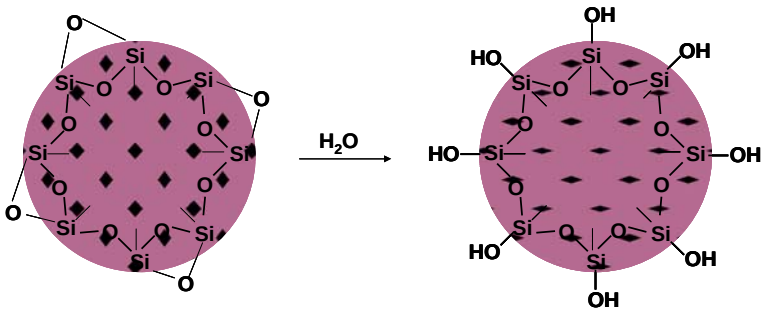

(b) Rehydroxylation

Zhuravles, L.T., *Colloids and Surface A: Physicohemical and Engineering Apects 173*: 38 (2005)

Fig. 1.17. The formation of silanol groups on the silica surface by (a) condensation polymerization of $Si(OH)_4$ and (b) rehydroxylation of dehydroxylated silica in aqueous solution [101].

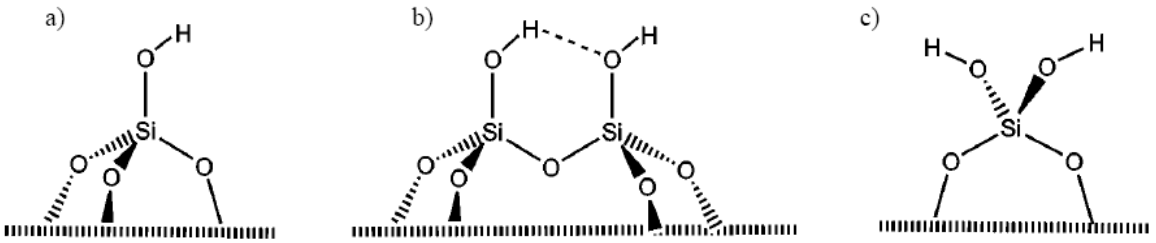

Pinkas, J., *Ceramics-Silikaty 49*(4): 287-298 (2005)

Fig. 1.18. Silanol groups at the silica surface: a) isolated, b) vicinal, and c) geminal [101, 102].

4.2. Ion Exchange on the Aqueous Surface of Silica

Numerous Scientists have studied the relationship between surface charge and chemical properties of silica sols and gels (depicted in Fig. 1.3), and aqueous conditions, e.g. pH, ion concentrations, and adsorption of akali ions. Bryant investigated the effect of particle size and electrolyte concentration of the titration curve of alkaline silica sols [103]. He concluded that the silica particles are dissolved at high pH, and that silica particles show different solubility behavior depending on various cations in water. Results were interpreted as a consequence of the preferential adsorption of cations. This result was strengthened by the researches of several scientists, Sears, Bolt, Tadros *et al.* and Strazhesko *et al.* [104-107].

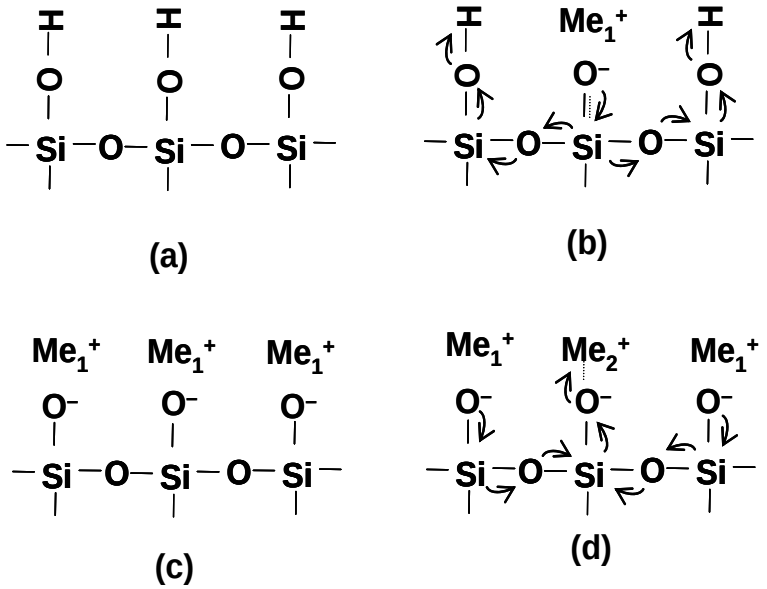

Me_1: Li, Na, K, Rb, Cs, Ca, Sr, Ba / Me_2: Be, Mg, Al

Strazhesko, D.N., Strelko, V.B., Belyakov, V.N. and Rubanik S.C., *Journal of Chromatography 102*: 191-195 (1974).

Fig. 1.19. Mechanism of cation exchange in silica gels; (a) the surface hydrogen in silanol group; (b) exchange of proton with strongly basic alkali metal, Me_1 and transference of electron density; (c) occurrence of a neighborhood of $Si–O^-$ Me_1^+ groups; (d) absorption of Me_2^+ ions due to a maximum degree of pi-interaction with the surface siloxane bonds [107].

Strazhesko *et al.* explained the mechanism of cation exchange in silica gels as depicted in Fig. 1.19. The surface of the common hydrogen form of silica gel can be represented as shown in Fig. 1.19(a). When the protons of a small proportion of the surface Si–OH groups are exchanged with strongly basic alkali metal or alkaline earth metal cations, Me_1^+ as depicted in Fig. 1.19(b), $Si–O^-\ Me_1^+$ groups occur with a negative charge on the oxygen. This negative charge can have an electric influence on the neighbor Si–OH groups by being transferred through the chain of Si–O bonds as arrows depicted in Fig. 1.19(b). This transference of negative electric influence can cause a neighborhood of $Si–O^-\ Me_1^+$ groups (Fig. 1.19(c)). However, Me_2^+ ions (Be, Mg and Al) could be adsorbed most effectively because those Me_2^+ ions provide a maximum degree of pi-interaction with the surface siloxane bonds and complete successfully with the silicon atoms for the electronic density on the oxygen [107].

4.3. Surface Charge of Silica.

In 1987, Milonjić investigated surface properties of colloidal silica by the potentiometric acid-base titration method [108]. Table 1.3 shows the theoretical concept of his works. In the preceding equation in Table 1.3, SOH_2^+, SOH, and SO^- denote positive, neutral and negative sites on the oxide surface, respectively, SOH_2^+-A^- and SO^--M^+ represent the surface complexes at the interface, while the superscript “int” denotes the intrinsic constants, and “S” refers to the oxide surface.

Table 1.3. Association-dissociation and counter-ion bounding reactions at/with the amphoteric surface hydroxyl groups SOH [108].

pH range below isoelectric point	pH range above isoelectric point
$SOH_2^+ \overset{K_{a1}^{int}}{\rightleftharpoons} SOH + H_S^+$	$SOH_2^+ \overset{K_{a2}^{int}}{\rightleftharpoons} SO^- + H_S^+$
$SOH_2^+ + A_S^- \overset{K_{A^-}^{int}}{\rightleftharpoons} [SOH_2^+\text{-}A^-]$	$SO^- + M_S^+ \overset{K_{M^+}^{int}}{\rightleftharpoons} [SO^-\text{-}M^+]$
$[SOH_2^+\text{-}A^-] \overset{{}^*K_{A^-}^{int}}{\rightleftharpoons} SOH + H_2^+ + A_S^-$	$SOH + M_S^+ \overset{{}^*K_{M^+}^{int}}{\rightleftharpoons} [SO^-\text{-}M^+] + H_S^+$
K_{a2}^{int}; intrinsic surface ionization constant defined by $pK_{a2}^{int} = pH - \log\frac{\alpha_-}{1-\alpha_-} + \frac{e\psi_0}{2.3kT}$, ${}^*K_{M^+}^{int}$; intrinsic surface complexation constant defined by $p{}^*K_{M^+}^{int} = pH - \log\frac{\alpha_-}{1-\alpha_-} + \log[M^+] + \frac{e(\psi_0 - \psi_\beta)}{2.3kT}$, α_-; the fraction of charged sites, ψ_0; the mean potential in the surface charges plane created by the amphoteric reaction of the potential-determining ions, ψ_β; the mean potential in the plane of specially sorbed cations, k; the Boltzman constant.	

Based on this concept, Milonjić calculated surface charge densities. Table 1.4 shows surface charge densities, $-\sigma_0$ (μC/cm^2) of colloidal silica particles as a function of the electrolyte (NaCl) concentration and pH at 25℃ using the results of potentiometric titration. The isoelectric point of investigated silica in this research was assumed to be pH 3. There are several reports of isoelectric pH values in the range 1.5–3 for SiO_2, in a tabulation of data complied by Parks [109] and 3.5 reported by Boltz [105] and Komura *et al*. [110]. Furthermore, Eisenlauer and Killman reported the value 2–3 [111] for the isoelectric point of colloidal silica. After these cited works were published, the main conclusions have been strengthened recently by scientists using similar or improved techniques, e.g. potentiometric

titration [21, 112-114], modeling the dissolution process of silica [115], Collidal Dinamics, AcoustoSizer using the dynamic mobility spectrums of materials [116], and X-ray photoelectron spectroscopy [117]. Considering their results, the surface charge of colloidal silica becomes negative slowly from isoelectric point to pH 7 [21] and rapidly with further increase of pH from 7 to higher values, as shown in Fig 1.20 and Fig 1.21.

Table. 1.4. Surface charge densities, $-\sigma_0$ (μC/cm^2), of colloidal silica particles as a function of the electrolyte (NaCl) concentration and pH at 25℃ [108].

Electrolyte	pH	Electrolyte Concentration (mol/L)					
		0.001	0.01	0.10	0.25	0.50	1.00
NaCl	6.5	0.31	0.94	1.86	2.32	2.02	2.50
	7.0	0.56	1.26	2.48	3.10	2.79	3.41
	7.5	0.91	1.76	3.38	4.00	3.69	4.58
	8.0	1.57	2.80	4.31	5.24	5.24	8.40
	8.5	2.83	4.12	5.86	7.10	7.41	10.76
	9.0	4.56	6.09	8.34	10.17	11.10	14.45
	9.5	7.85	9.42	13.27	15.44	16.96	21.51

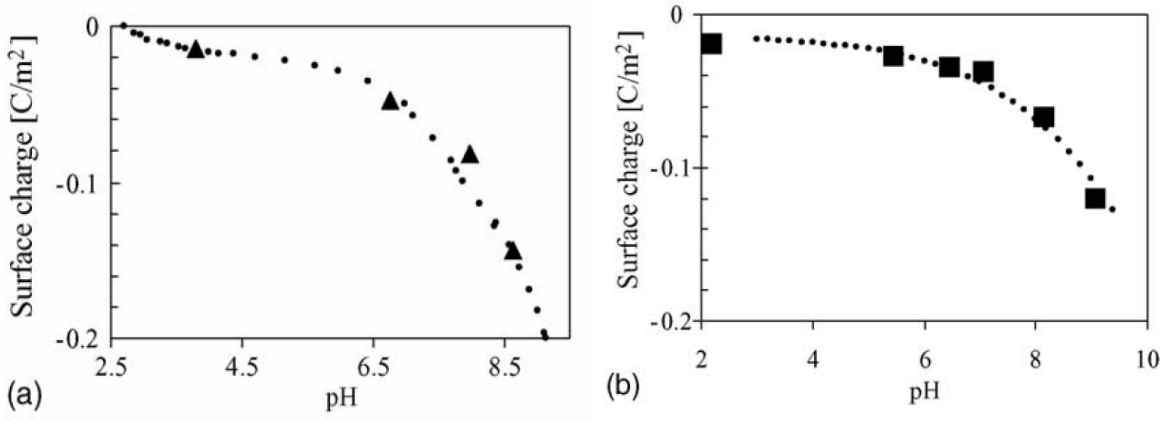

Cardenas, J.F., *Colloids and Surfaces A. 252*: 213-219 (2005)

Fig 1.20. Surface charge density of silica as a function of proton concentration determined by XPS (solid symbol) and potentiometric titration (dot line), (a) with 100 mM KCl and (b) with 20 mM NaCl [117].

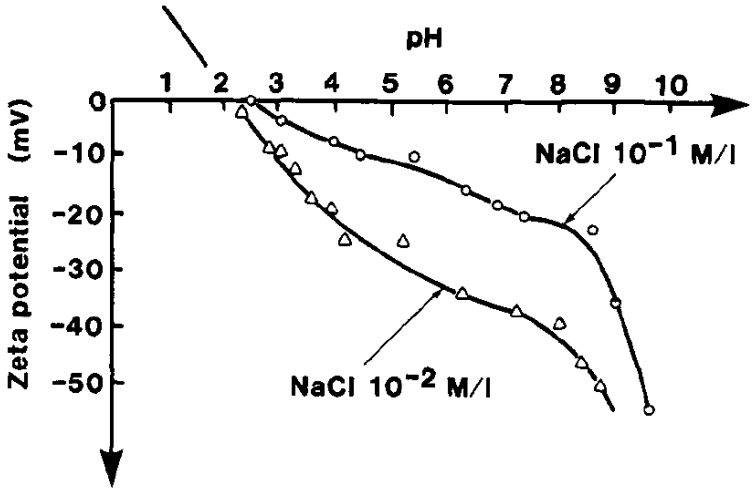

Axelos, M.A.V., Tchoubar, D., and Bottero, J.Y., *Langmuir 5*: 1186-1190 (1989)

Fig 1.21. Zeta-potential of Ludox HS silica in 10^{-1} and 10^{-2} NaCl by Small-Angle X-ray Scattering [118].

5. REFERENCES

1. On, C. and Thorn, I., "Progress in the Use of Colloidal Silica in Dual-Component Systems," *Eur. Papermaker 3* (2): 28 (1995)

2. Suden, O., Båtelson, P.G., Johansson, H.E., Larsson, H.M. and Svending, P.J., "Papermaking and Products Made Thereby," *U. S. Pat. 4,388,150*, June 14, 1983

3. Rushmere, J.D., "Polysilicate Microgels as Retention/Drainage Aids in Papermaking," *U. S. Pat. 4,954,220*, Sept. 4, 1990.

4. Harms, M., "Second Generation Microparticle Systems", *Wochenbl. Papierfabr. 126* (19): 922 (1998).

5. Honig, D.S., Harris, E.W., Pawlowska, L.M., O'Toole, M.P. and Jackson, L.A., "Formation Improvements with Water-Soluble Micropolymer Systems," *TAPPI J. 76* (9): 135 (1993).

6. Andersson, K., Larsson, B. and Lindgren, E., "Silica Sols and Use of the Sols," *U.S. Pat. 5,603,805*, Feb. 18, 1997.

7. Langley, J.G. and Litchfield, E., "Dewatering Aids for Paper Applications," *Proc. TAPPI 1986 Papermakers Conf*., 89 (1986).

8. Litchfield, E., "Dewatering Aids for Paper Applications," *Appita 47*(1): 62 (1994).

9. Langley, J. and Holroyd, D., "Production of Paper and Paper Board," *U. S. Pat. 4,753,710,* June 28, 1988.

10. Knudson, M. I., "Bentonite in Paper: the Rest of the Story," *Proc. TAPPI Papermakers Conf*., 141 (1993).

11. Honig, D.S., Farinato, R.S. and Jackson, L.A., "Design and Development of the Micropolymer System: An 'Organic Microparticle' Retention/Drainage System'," *Nordic Pulp Paper Res. J. 15*(5): 536 (2000).

12. Aloi, F.G. and Trksak, R.M., "Retention in Neutral and Alkaline Papermaking," in J. M. Gess, Ed., *Retention of Fines and Fillers during Papermaking*," TAPPI Press, 1998.

13. O'Brien, J.A., Lawrence, L.A. and Honig, D.S., "Making Highly Filled Alkaline Paper with a Micropolymer System," *Proc. TAPPI 1994 Papermakers Conf.*, 257 (1994).

14. Drummond, D.K., "Synthetic Mineral Microparticles for Retention Aid Systems," *U.S. Pat. 6,184,258 B1*, Feb. 6. 2001 (filed Feb. 7, 1997).

15. Drummond, D.K., "Synthetic Mineral Microparticles," *U.S. Pat. 5,989,714*, Nov. 23, 1999 (filed May 4, 1998).

16. Drummond, D.K., "Synthetic Mineral Microparticels and Retention Aid and Water Treatment Systems and Methods Using Such Particles," *U.S. Pat. 6,183,650 B1*, Feb. 6, 2001 (filed Oct. 13, 1999).

17. Rojas, O.J. and Hubbe, M.A., "The Dispersion Science of Papermaking," *Journal of Dispersion Science and Technology 25*(6): 713-732 (2004)

18. Hubbe, M.A., "Microparticle Programs for Drainage and Retention," in Rodriguez, Ed., *Micro and Nanoparticles in Papermaking*, Ch. 1, TAPPI Press, 2005.

19. Iler, R.K., *The Chemistry of Silica – Solubility, Polymerization, Colloid and Surface Properties, and Biochemistry*, J. Wiley & Sons, New York, 1979.

20. Moffett, R.H., "On-site production of a silica-based microparticulate retention and

drainage aid," *TAPPI J. 77*(12): 133-138 (1994).

21. Carroll, S.A., Maxwell, R.S., Bourcier, W., Martin, S. and Hulsey, S., "Evaluation of silica-water surface chemistry using NMR spectroscopy," *Geochimica et Cosmochimica Acta, 66*(6): 913-926 (2002).

22. Andersson, K., Sandström, A., Ström, K. and Barla, P., "The Use of Cationic Startch and Colloidal Silica to Improve the Drainage Characteristics of Kraft Pulps," *Nordic Pulp and Paper Res. J. 1*(2): 26-30 (1986).

23. Capozzi, A. M., "Innovations in Microparticle Technology," *PIMA 78*(6): 64 (1996).

24. Kiviranta, A. and Paulapuro, H., "Hydraulic and Rectifier Roll Headboxes in Boardmaking," *Paper Technol. 31*(11): 34 (1990).

25. Cauley, T.A., "The Hydrocol Microparticle System Comes to Standard News Production," *Proc. TAPPI 2000 Papermakers Conf. Trade Fair*, 545 (2000).

26. Wernås, B. and Litchfield, T., "Microparticle Flocculation Gaining Ground," *Svensk Papperstidn. 90*(15): 18 (1987).

27. McCourt, A.M., Ford, P.A. and Cauley, T.A., "A Practical View of Microparticle System in Supercalendered Paper," *Tappi Journal 776*(10): 165 (1993).

28. Schuster, M.A., Harrington, J.C., Liao, W.P. and Chen, F., "Method for Improving Retention and Drainage Characteristics in Alkaline Papermaking," *U. S. Pat. 5,415,740*, May 16, 1995.

29. Anon., "Hydrocol for Effective Retention," *Svensk Papperstidn. 90*(1): 39 (1987).

30. Dixit, M.K., Jackowski, C.W. and Maleike, T.A., "Retention Strategies for Alkaline Fine Papermaking with Secondary Fiber: a Case History," *Tappi Journal 74* (4): 107

(1991).

31. Ford, P.A., "Control the Wet End Balancing Act with Polymer/Pigment Microparticles," *Proc. TAPPI 1991 Papermakers Conf.*: 501, (1991).

32. Swerin, A. and Mähler, A., "Formation, Retention, and Drainage of a Fine Paper Stock During Twin-Wire Roll-Blade Forming. Implications of Fiber Network Strength," *Nordic Pulp Paper Res. J. 11*(1): 36 (1996).

33. Wågberg, L., Björklund, M., Åsell, I. and Swerin, A., "On the Mechanism of Flocculation by Microparticle Retention-Aid System," *TAPPI Journal 79*(6): 157 (1996).

34. Andersson, K. and Lindgren, E. "Important Properties of Colloidal Silica in Microparticulate Systems," *Nordic Pulp Paper Res. J. 11*(1): 15 (1996).

35. Main, S. and Simonson, P., "Retention Aids for High-Speed Paper Machines," *TAPPI J. 82*(4): 78 (1999).

36. Lindström, T., "Microparticle Technology – New Megatrend," *Svensk Papperstidn. 90*(1): 24 (1987).

37. Ford, P.A., "Highly Filled Papers using Polymer/Pigment Retention Systems," *Proc. TAPPI 1988 Papermakers Conf.*: 367 (1988).

38. Kajasvirta, R., "Supercoagulation in the Control of Wet-End Chemistry by Synthetic Polymer and Activated Bentonite," *Advanced Topics Wet-End Chem. Short Course Notes*, TAPPI Press: 35-38 (Oct. 11-13, 1989).

39. Chung, D.K., "Retention and Drainage Aid for Alkaline Fine Papermaking Process," *U. S. Pat. 5,126,014,* June 30, 1992.

40. Begala, A.J., "Papermaking Process with Improved Retention and Drainage," *U. S. Pat. 5,098,520,* March 24, 1992.

41. Smith, J.H., Jr., "Papermaking Process," *U. S. Pat. 5,221,435,* June 22, 1993.

42. Cauley, T.A., Langley, J.G. and Nixon, A., "Production of Paper," *U. S. Pat. 5,514,249*, Jul. 6, 1994.

43. Carlson, U., "Some Aspects of Microparticle Flocculation," *Proc. EUCEPA XXIV: The World Pulp and Paper Week, Paper Technol.*, Stockholm: 161, May 1990.

44. Miyanishi, T. and Shigeru, M., "Optimizing Flocculation and Drainage for Microparticle Systems by Controlling Zeta Potential," *Tappi Journal 80*(1): 262 (1997).

45. Honig, D.S., Turnbull, R.J. and Wheeler, C., "Retention Systems for Highly Filled Paper," *TAPPI 99 Proc.*: 1335 (1999).

46. Hubbe, M.A., "Reversibility of Polymer-Induced Fiber Flocculation by Shear. 1. Experimental Methods," *Nordic Pulp Paper Res. J. 15*(5): 545 (2000).

47. Hubbe, M.A., "Reversibility of Polymer-Induced Fiber Flocculation by Shear. 2. Multi-Component Chemical Treatments," *Nordic Pulp Paper Res. J. 16*(4): 226 (2001).

48. La Mer, V., K. and Healy, T. W., "Adsorption-Flocculation Reactions of Macromolecules at the Solid-Liquid Interface," *Rev. Pure Appl. Chem. 13* (Sept.): 11-133 (1963).

49. Gregory, J. and Sheiham, I., "Kinetic Aspects of Flocculation by Cationic Polymers," *Br. Polymer J. 6*(1): 47 (1974).

50. McKenzie, A. W., "Structure and Properties of Paper. XVIII. The Retention of Wet-End Additives," *Appita 21*(4): 104 (1968).

51. Hubbe, M. A., "Detachment of Colloidal Hydrous Oxide Spheres from Flat Solids Exposed to Flow. 2. Mechanism of Release," *Colloids Surf. 16*: 249 (1985).

52. Hubbe, M.A., "Retention and Hydrodynamic Shear," *Tappi J. 69*(8): 116 (1986).

53. Swerin, A. and Ödberg, L., "Flocculation of Cellulosic Fiber Suspensions by a Microparticlulate Retention Aid System Consisting of Cationic Polyacrylamide and Anionic Montmorillonite: Effect of Contact Time, Shear Level, and Electrolyte Concentration," *Nordic Pulp Paper Res. J. 11*(1): 22 (1996).

54. Hedborg, F. and Lindström, T., "Some Aspects on the Reversibility of Flocculation of Paper Stocks," *Nordic Pulp Paper Res. J. 11*(4): 254 (1996).

55. Lindström, T., "Some Fundamental Chemical Aspects on Paper Forming." in *Fundamentals of Papermaking,* Trans. 9th Fund. Res. Symp., Cambridge, C. F. Baker and V. W. Punton, Eds., Mech. Eng. Publ., Ltd., London, 311 (1989).

56. Kiviranta, A. and Paulapuro, H., "Hydraulic and Rectifier Roll Headboxes in Boardmaking," *Paper Technol. 31*(11): 34 (1990).

57. Kline, J.E., "The Application of the Verwey-Overbeek Theory to the Relative Sediment Volume of Kaolin-Water Dispersions," *Tappi 50*(12): 590 (1967).

58. Gruber, E., Gelbrich, M. and Schempp, W., "Morphological and Chemical Factors Related to Dewatering," *Wochenbl. Papierfabr. 125*(2): 66 (1997).

59. Burgess, M.S., Phipps, J.S. and Xiao, H., "Flocculation of PCC Induced by Polymer/Microparticle Systems: Floc Characteristics," *Nordic Pulp Paper Res. J. 15* (5): 572 (2000).

60. Vaughan, C.W., Adamsky, F.A. and Richardson, P.F., "New Approach to Wet End Drainage/Retention/Formation Technology and its Improvement of Paper Machine Production Rates and Runnability," *Wochenbl. Papierfabr. 126* (10): 458 (1998).

61. Lindström, T., Hallgren, H. and Hedborg, F., "Aluminum Based Microparticulate Retention Aid Systems," *Nordic Pulp Paper Res. J. 2* (4): 99 (1989).

62. Sophia, S.C., Johnson, K.A., Crill, M.S., Roop, M.J., Gotberg, S.R., Nigrelli, A.S. and Hutchinson, L.S., "Method for Dewatering Paper," *U. S. Pat. 4,795,531,* Jan. 3, 1989.

63. Gill, R. I. S., "Developments in Retention Aid Technology," *Paper Technol. 32*(8): 34 (1991).

64. Penniman, J.G. and Makhonin, A.G., "Optimizing Microparticulate Process Efficiency," *Proc. TAPPI 1993 Papermakers Conf.*,:129 (1993).

65. Breese, J., "Interactive Papermaking Chemistry Provides Machine Rebuild Options," *Pulp Paper 68*(4): 91 (1994).

66. Hoffmann, J., "Microparticle Systems – Mechanism and Application," *Wochenbl. Papierfabr. 122*(20): 785 (1994).

67. Swerin, A., Glad-Nordmark, G. and Sjödin, U., "Silica Based Microparticulate Retention Aid Systems," *Paperi Puu 77*(4): 215 (1995).

68. Vaughan, C.W., "A New Approach to Wet-End Drainage, Retention, and Formation Technology," *TAPPI J. 79*(7): 103 (1996).

69. Johnson, K.A., "A New Microparticle Retention and Drainage Program," *Proc. 51st Appita Annual Gen. Conf.*, Melbourne, 28 Apr.-2 May, 1997, Vol. 1, 325 (1997).

70. Stockwell, J.O., "Process of Making Paper," *U. S. Pat. 5,733,414,* Mar. 31, 1998.

71. Hunter, D. *Papermaking, the History and Technique of an Ancient Craft*, Dover Publish, New York, 1974.

72. Hunter, D. *A Papermaking Pilgrimage to Japan, Korea, and China*, Pyson Printers, New York, 1936.

73. Neimo, L. *Papermaking Chemistry*, Fapet Oy, Helsinki, 1999.

74. Walkush, J. C., Williams, D. G.., "The Coagulation of Cellulose Pulp Fibers and Fines as a Mechanism of Retention," *Tappi J., 57*(1): 112-116 (1974)

75. Strazdins, E., "Theoretical and Practical Aspects of Alum Use in Papermaking," *Nordic Pulp and Paper Res. J., 2*: 128-134 (1989).

76. Horoszko, W.L. and Smylie, S.E., "Aluminum Compounds-chemistry and Use," in *Retention of Fines and Fillers During Papermaking*, Gess, J. M., Ed., Tappi Press, Atlanta, Georgia: 323-232 (1998).

77. Eklund, D. and Lindstrom, T., *Paper Chemistry*, DT Paper Science Publications, Grankulla, Finland (1991).

78. Stol, R.J., van Helden, A.K. and de Bruyn, P.L., "Hydrolysis Precipitation Studies of Aluminium(III) Solutions 2. A Kinetic Study and Model," *Journal of Colloidal Interfacial Science 51*: 115-130 (1976).

79. Base, C.F. and Mesmer, R.E., *The Hydrolysis of Cations*, John Wiley and Sons., New York, (1976).

80. Öhman, L.-O. and Wågberg, L., "Freshly Formed Aluminum (III) Hydroxide Colloids – Influence of Aging, Surface Complexation and Silicate Substitution,"

Journal of Pulp and Paper Science 23(10): 475-480 (1997).

81. Furrer, G., Ludwig, C., Schindler, P. W., "On the Chemistry of the Keggin Al^{13} Polymer. 1. Acid-Base Properties," *Journal of Colloid and Interface Science 149* (1): 56 (1992).

82. Søgaard, E.G., "Production of the Coagulation Agent PAx-14. Contents of Polyaluminium Chloride Compounds," *Chemical Water and Wastewater Treatment*, Hahn, H.H., Hoffmann, E. and Ødegaard, H., Ed., Springer, Berlin, Germany: 3-16 (2002).

83. Akitt, J.W., Greenwood, W.N., Khandelwal, B.L. and Lester, G.D., "^{27}Al Nuclear Magnetic Resonance Studies of the Hydrolysis and Polymerisation of the Hexa-aquo-aluminium(III) cation. *Journal of the Chemical Society* Dalton: 604-610 (1973).

84. Bottero, J.Y., Cases, J.M., Fiessinger F. and Poirier, J.E., "Studies of Hydrolyzed Aluminium Chloride Solutions: 1.Nature of Aluminium Species and Composition of Aqueous solutions," *Journal of Physical Chemistry 84*(18): 2933-2939 (1980)

85. Allouche, I., Huguenard, C. and Taulelle, F., "3QMAS of Three Aluminium Polycations: Space Group Consistency between NMR and XRD," *Journal of Physical Chemistry of Solids 62*: 1525-1531 (2001)

86. Haydin, P.L. and Rubin, A.J., "Systematic Investigation of the Hydrolysis and Precipitation of Aluminum(III), in Aqueous-Environmental Chemistry of Metals," *Aqueous-Environmental Chemistry of Metals*, Rubin, A. J., Ed., Ann Arbor Science. Ann Arbor, MI (1976).

87. Akitt, J.W., Greenwood, N.N. and Lester, G.D., "Aluminum-27 Nuclear Magnetic Resonance Studies of Acidic Solutions of Aluminum Salts" *Journal of the Chemical Society A –Inorganic Physical Theoretical*, (5): 803 (1969).

88. Arnson, T.R., "The Chemistry of Aluminum Salts in Papermaking," *Tappi J., 65* (3): 125 (1982).

89. Bottero, J.Y., Porier, J.E. and Fiessinger, F., "Study of Partially Neutralized Aqueous Aluminum Chloride Solutions: Identification of Aluminum Species and Relation between the Composition of the Solutions and Their Efficiency as a Coagulant," *Progress in Water Technology, 1*(1): 601 (1980).

90. Bottero, J.Y. and Fiessinger, F., "Aluminum Chemistry in Aqueous Solution," *Nordic Pulp and Paper Res. J., 4*(2): 81 (1989).

91. Bottero, J. Y., Tchoubar, D., Cases, J. M., Fiessinger F., "Investigation of the Hydrolysis of Aqueous-Solutions of Aluminum-Chloride. 2. Nature and Structure by Small-Angle X-Ray-Scattering," *Journal of Physical Chemistry 86* (18): 3667 (1982).

92. Bottero, J. Y., Cases, J. M., Fiessinger, F., Poirier, J. E., "Studies of Hydrolyzed Aluminum-Chloride Solutions. 1. Nature of Aluminum Species and Composition of Aqueous-Solutions," *Journal of Physical Chemistry 84* (22): 2933 (1980).

93. Smith, R.W., "Relations among Equilibrium and Nonequilibrium Aqueous Species of Aluminum Hydroxy Complex," *Advances in Chemistry Series, 106*: 250 (1971).

94. Matijević, E. and Tezak, B., "Coagulation Effects of Aluminum Nitrate and Aluminum Sulfate on Aqueous Sols of Silver Halides in Statu Nascendi. Detection of Polynuclear Complex Aluminum Ions by Means of Coagulation Measurements," *Journal of Physical Chemistry, 57*(9): 951-954 (1953).

95. Bertsch, P.M., "Aqueous Polynuclear Aluminum Species," in Sposito, G Ed., *The Environmental Chemistry of Aluminum*, Ch.4, CRC Press, Inc., Boca Raton, Florida (1989).

96. Briggs, L.J., "On the adsorption of water vapor and of certain salts in aqueous

solution by quartz," *Journal of Physical Chemistry 9*(8): 617-640 (1905).

97. Mattson, S., "The Laws of Soil Colloidal Behavior: VIII. Forms and Functions of Water," Soil Science 33(4): 301-323 (1932).

98. Hofmann, U., Endell, K. and Wilm, D., "Radiographic and Colloid-Chemical Investigations of Clay," *Angewandte Chemie 47*: 0539-0547 (1934).

99. Rideal, E.K., "Introductory Address," *Transactions of the Faraday Society 32*(1): 3-10 (1936).

100. Carman, P.C., "Constitution of Colloidal Silica," *Transactions of the Faraday Society 36*: 964-973 (1940).

101. Zhuravlev, L.T., "The Surface Chemistry of Amorphous Silica. Zhuravlev Model," *Colloids and Surfaces A: Physicochemical and Engineering Aspects 173*: 1-38 (2000).

102. Pinkas, J., "Chemistry of Silicates and Aluminosilicates," *Ceramics-Silikaty 49*(4): 287-298 (2005).

103. Bryant, K.C., "Silica Sols. Part I. The Titration of Silica Sols," *Journal of the Chemical Society* (Aug): 3017-3020 (1952).

104. Sears, Jr. G.W., "Determination of Specific Surface Area of Colloidal Silica by Titration with Sodium Hydroxide," *Analytical Chemistry 28*(12): 1981-1983 (1956).

105. Bolt, G.H., "Determination of the Charge Density of Silica Sols," *Journal of Physical Chemistry 61*(9): 1166-1169 (1957).

106. Tadros, Th.F. and Lyklema, J., "Adsorption of Potential-Determining Ions at the Silica-Aqueous Electrolyte Interface and the Role of Some Cations," *Journal of Electroanalytical Chemistry 17*(3-4): 267-275 (1968).

107. Strazhesko, D.N., Strelko, V.B., Belyakov, V.N. and Rubanik S.C., "Mechanism of Cation Exchange on Silica Gels," *Journal of Chromatography 102*: 191-195 (1974).

108. Milonjić, S.K., "Determination of Surface Ionization and Complexation Constants at Colloidal Silica/Electrolyte Interface," *Colloids and Surface 23*: 301-312 (1987).

109. Parks, G.A., "Isoelectric Points of Solid Oxides, Solid Hydroxides and Aqueous Hydroxo Complex Systems," *Chemical Reviews 65*(2): 177-198 (1965).

110. Komura, A., Hatsutori K. and Imanaga H., "Acidic and Basic Properties of Silica at Interface with Aqueous-Electrolytes," *Nippon Kagaku Kaishi* (6): 779-784 (1978).

111. Eisenlauer, J. and Killmann, E., "Stability of Colloidal Silica (Aerosil) Hydrolysis: I. Preparation and Characterization of Silica (Aerosil) Hydrolysis," *Journal of Colloid and Interface Science 74*(1): 108-119 (1980).

112. Sonnefeld, J., Göbel, A. and Vogelsberger, W., "Surface Charge Density on Spherical Silica Particles in Aqueous Alkali Chloride Solutions, Part 1. Experimental Results," *Colloid and Polymer Science 273*(10): 926-931 (1995).

113. Sonnefeld, J., "Surface Charge Density on Spherical Silica Particles in Aqueous Alkali Chloride Solutions, Part 2. Evaluation of the Surface Charge Density Constants," *Colloid and Polymer Science 273*(10): 932-938 (1995).

114. Rodrigues, F.A., Monteiro, P.J.M. and Sposito, G., "The Alkali-Silica Reaction: The Surface Charge Density of Silica and Its Effect on Expansive Pressure," *Cement and Concrete Research 29*: 527-530 (1999).

115. Vogelsberger, W., Löbbus, M., Sonnefeld, J. and Seidel, A., "The Influence of Ionic Strength on the Dissolution Process of Silica," *Colloids and Surfaces A: Physicochemical and Engineering Aspects 159*: 311-319 (1999).

116. Franks, G., "Zeta Potentials and Yield Stresses of Silica Suspensions in Concentrated Monovalent Electrolytes; Isoelectric Point Shift and Additionsl Attraction," *Journal of Colloid and Interface Science 249*: 44-51 (2002).

117. Cardenas, J.F., "Surface Charge of Silica Determined Using X-ray Photoelectron Spectroscopy," *Colloids and Surfaces A: Physicochem. Eng. Aspects 252*: 213-219 (2005).

118. Axelos, M.A.V., Tchoubar, D., and Bottero, J.Y., "Small-Angle X-Ray-Scattering Investigation of the Silica Water Interface – Evolution of the Structure with pH," *Langmuir 5*(5): 1186-1190 (1989)

CHAPTER 2

Research Objectives

Considering the molecular mechanisms explained in Chapter 1, the factors which are expected to have important influence on the performance of microparticles in drainage and retention systems include (1) charge density, (2) specific surface area, (3) particle size, and (4) the structure of aggregation. In the case of the Synthetic Mineral Microparticle (SMM) systems, these factors can be varied by changing the aqueous conditions during synthesis. For example, the metal/Si ratio, the pH, the shear rate, and the salt concentration can be varied.

The following conceptual framework is proposed in order to help explain the main events affecting the physical and surface characteristics of SMM products. As already discussed in Chapter 1, the character of each of the reagents used in the formation of SMM suspensions is dependent on pH. Thus sodium silicate (Na_2SiO_3) and aluminum chloride ($AlCl_3$), which were chosen in the present work for synthesis of SMM, give rise to quite different ionic species with different charge densities, depending on pH. At pH higher than 10, the silica ions are in the stable form SiO_4^{4-}. An increase in the Al/Si ratio is expected to acidify the SMM suspension, due to the acidity of metal ions in aqueous solution with decreasing pH. Thus, at pH between 7 and 10, the silica ions are destabilized and start to form polymerized silica structures by condensation polymerization from $Si(OH)_4$, and silanol groups which are expected to exist on the surface of SMM shows negative charge properties. Additionally, the

Al-ions exist as a form of $Al(OH)_4^-$ which will be adsorbed on the silanol group and form aluminosilicate, with release of sodium ions.

When the Al/Si ratio is increased further, the pH falls, reaching a range of 4<pH< 7. Under such conditions the silanol groups on the surface of SMM are expected to have slightly negative charge properties. In case of aluminum, polymerized species, *e.g.* Al_{13}: $AlO_4Al_{12}(OH)_{24}(H_2O)_{12}^{7+}$, are expected to occur in a range 4<pH<5. These hydrolyzed aluminum ions destabilize the surface of silica and lead to bridging between primary particles of silica. Partial neutralization of Al^{3+} by NaOH during the synthesis of SMM is expected to shift pH values upward. An increase in pH promotes aluminum and favors formation of aluminum oligomers. Increasing pH also affects the charge and surface properties of silica particles due to the increase of sodium ion, Na^+.

There is relatively little published about the factors mentioned above in the case of the SMM system. Thus, the objective of this research is to investigate the surface charge properties and coagulation behavior of SMM suspensions, and to characterize the morphology. This information will be helpful in terms of optimizing the application of SMM system as a drainage and retention system to be applied within the wet end of a paper machine.

The negative surface charge of SMM appears to be very important with respect to its performance as part of a retention and dewatering system. It is proposed that this surface charge has a strong relationship with pH, which is varied by the changing the Al/Si ratio.

It is also proposed that size and aggregative structure of SMM, which has strong effect on the retention and drainage, is affected negatively or positively depending on the value of the Al/Si ratio, the degree of neutralization of the aluminum species employed in the reaction, and the shear rate applied during synthesis.

Finally, the maximum performance of SMM systems can be expected under synthetic conditions that result in small primary particle size, negative charge of the surface, and an aggregative structure. Performance, in this context, means that the microparticle can be used in sequence with a very high mass cationic polyelectrolyte to promote drainage and fine-particle retention, according to molecular mechanisms described in Chapter 1.

CHAPTER 3

Preliminary Test for the Confirmation of a Series of Patents of Synthetic Mineral Microparticles with Various Metal Species

1. INTRODUCTION

"Synthetic Mineral Microparticle" (SMM) is a patented system which can increase the rate of dewatering and promote the retention of fine particles more efficiently during the process of papermaking [1-3].

The SMM technology is protected by the following US patents:

- US 6,184,258: Process for preparation of microparticles [1]
- US 5,989,714: Composition patent for microparticles [2]
- US 6,183,650: Water treatment by means of microparticles [3]

Of these three patents, US 6,184,258 shows the most basic invention. It is shown that highly effective microparticles can be synthesized by simple mixing a dilute solution of silicate ions and a dilute solution of aluminum ions. This capability is illustrated by the results in Table 3.1, which compares the Britt Jar first-pass retention achieved in the laboratory during initial testing with an SMM product prepared by adding aluminum sulfate solution to sodium silicate solution at an Al/Si ratio of 0.5. It is worth noting that the results in Table 1 were obtained without any effort to optimize the conditions of mixing, overall concentration of the

mixture or detailed chemistry other than the ratio of the two major components of the SMM colloidal dispersion.

Table 3.1. Performance of SMM in comparison with commercially available microparticles in four different fiber furnish environments.

Microparticle Type	Britt Jar First Pass Retentions (%)							
	Furnish & Filler Type*							
	Kraft A		Kraft B		Groundwood A		Groundwood B	
No Microparticle	29	37	40	37	53	51	55	28
SMM	**57**	**74**	**60**	**60**	**54**	**61**	**81**	**61**
Bentonite	50	75	64	64	73	72	84	77
Colloidal SiO_2	27	35	40	32	50	51	52	30

Furnish: 1 % Consistency with 20 % of added filler,
Pulp: Kraft A = 100 % softwood kraft; Kraft B = mixed kraft; Groundwood A and B are from different paper mills,
Filler: PCC = Albacar® HO; Clay = Georgia water-washed;
Coagulant: Percol®368
Retention aid: Percol®175
Microparticels: SMM; Bentonite = Hydrocol® O; Colloidal silica = Nalco® 8671.

The filler retention performance of SMM microparticles was only moderately sensitive to the Al/Si ratio as shown in Fig. 3.1. The furnish was 100 % softwood kraft with 20 % added filler. For tests involving water-washed clay filler, the furnish was first treated with 2 lb/ton of Percol®386 coagulant, followed by 1 lb/ton of Percol®175 cationic acrylamide copolymer retention aid, and finally 5 lb/ton of the microparticle on a dry basis. In the case of precipitated calcium carbonate (PCC, Albacar®HO) the additives were 1 lb/ton of Percol®175 retention aid followed by 5 lb/ton of microparticle. The highest retention was

obtained at a critical Al/Si ratio. Fig. 3.2 shows confirmatory results for different pulp furnishes.

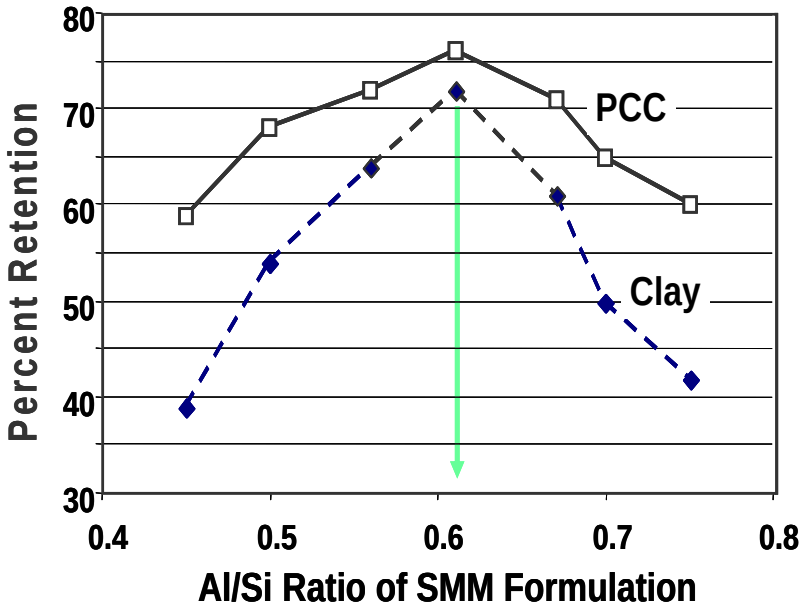

Fig. 3.1. Effect of Al/Si ratio of SMM microparticles on filler retention results in a bleached kraft furnish.

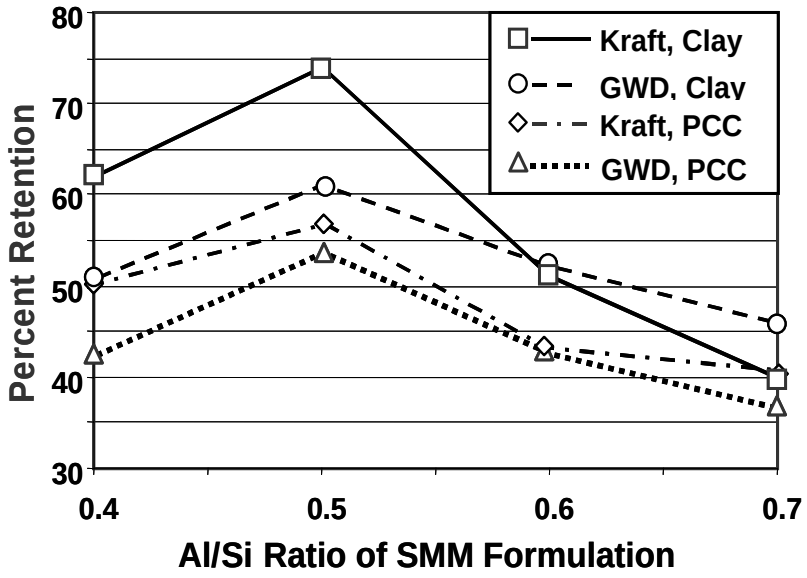

Fig. 3.2. Effect of Al/Si ratio of the SMM additive for enhancement of filler retention in furnish already treated with cationic retention aid.

The purpose of experiment in this chapter was to confirm the efficacy of representative synthetic mineral microparticle (SMM) formulations, covering a wide range of compositions, and discover effects of some key variables that have the potential to lead to unexpected advantages in terms of the effectiveness of the microparticles, when used in combination with a cationic polyacrylamide treatment of papermaking furnish.

2. EXPERIMENTAL

2.1. Furnish

A mixture of 75 % bleached hardwood kraft and 25 % bleached softwood kraft pulp was disintegrated for 10 min and co-refined to about 400 ml CSF. Then 10 %, by total furnish mass, of Albacar®5970 scalenohedral precipitated calcium carbonate (PCC) was added. Sodium sulfate solution (Na_2SO_4) of 1M concentration was added to achieve approximately 1000 μS/cm electrical conductivity at a filterable solids level of approximately 0.5 %.

2.2. Synthetic Conditions of SMM

Synthesis of SMM follows the synthetic method of SMM explained in Chapter 1. Only sodium meta-silicate ($Na_2SiO_3 \cdot 5H_2O$) was used as base ingredient in this set of tests with 0.445 molal concentration. Added metal solution ingredients in different tests included 0.566 molal aluminum sulfate ($Al_2(SO_4)_3$), 0.566 molal aluminum chloride ($AlCl_3$), 0.500 molal zinc chloride ($ZnCl_2$), and 0.500 molal ferric chloride ($FeCl_3$).

Various ratios of metal to silicate were used, e.g. Al/Si = 0.5, 0.76, and 1.0 molar ratio, Zn/Si = 1.14, and Fe/Si = 0.76. When the metal ingredients are aluminum chloride ($AlCl_3$) and aluminum sulfate ($Al_2(SO_4)_3$), w ml of 1 M NaOH solution was calculated by equation (1) for the 25 % neutralization of Al^{3+}, and added to the reacted suspension during continuous stirring.

$$w = 0.75 \cdot n \cdot y \cdot 1000 \tag{1}$$

where y is the molar concentration of metal ingredient, and n is the number of Al atoms in the metal-containing ingredient.

1mM NaCl, based on the total mass of solution, was added to adjust the salt concentration. Table 3.2 shows the grid of test conditions.

Based on the amounts of reagents, and assuming complete consumption of Si species, the reactions could be described by the following equations;

$x \cdot Na_2SiO_3 + y \cdot Al_2(SO_4)_3 \rightarrow Na_{2x-6y}Al_{2y}Si_xO_{3x} + 6y \cdot Na^+ + 3y \cdot SO_4^{2-}$,when x-$3y$ >0 and

$\rightarrow Al_{(2x/3)}Si_xO_{3x} + 2x \cdot Na^+ + (2y - 2x/3) \cdot Al^{3+} + 3y \cdot SO_4^{2-}$,when x-$3y$ <0.

$x \cdot Na_2SiO_3 + y \cdot AlCl_3 \rightarrow Na_{2x-3y}Al_ySi_xO_{3x} + 3y \cdot Na^+ + 3y \cdot Cl^-$, when $2x-3y > 0$ and

$\rightarrow x/3 \cdot Al_2(SiO_3)_3 + (y - 2x/3) \cdot Al^{3+} + 2x \cdot Na^+ + 3y \cdot Cl^-$, when $2x-3y < 0$.

$x \cdot Na_2SiO_3 + y \cdot ZnCl_2 \rightarrow Na_{2x-2y}Zn_ySi_xO_{3x} + 2y \cdot Na^+ + 2y \cdot Cl^-$, when $x-y > 0$ and

$\rightarrow x \cdot ZnSiO_3 + (y- x) \cdot Zn^{2+} + 2x \cdot Na^+ + 2y \cdot Cl^-$, when $x-y > 0$.

$x \cdot Na_2SiO_3 + y \cdot FeCl_3 \rightarrow Na_{2x-3y}Fe_ySi_xO_{3x} + 3y \cdot Na^+ + 3y \cdot Cl^-$, when $2x-3y > 0$ and

$\rightarrow x/3 \cdot Fe_2(SiO_3)_3 + (y - 2x/3) \cdot Fe^{3+} + 2x \cdot Na^+ + 3y \cdot Cl^-$, when $2x-3y < 0$.

Table 3.2. Test conditions.

Test No.	Metal Solution Ingredients	Ratio Metal Ion to Si	Shear, rpm	Salt	Neutralization
1	$Al_2(SO_4)_3$	0.76	500	None	None
2	$AlCl_3$	0.76	500	None	None
3	$ZnCl_2$	1.14	500	None	None
4	$FeCl_3$	0.76	500	None	None
5	$Al_2(SO_4)_3$	0.76	1500	None	None
6	$AlCl_3$	0.5	500	None	None
7	$AlCl_3$	1.0	500	None	None
8	$AlCl_3$	0.76	500	None	25 %
9	$ZnCl_2$	1.14	500	1 mM NaCl	None
10	$ZnCl_2$	1.14	1500	1 mM NaCl	None
11	$Al_2(SO_4)_3$	0.76	1500	1 mM NaCl	25 %
12	$Al_2(SO_4)_3$	0.50	1500	1 mM NaCl	25 %

2.3. Measurement of Drainage and Retention

2.3.1. Step-Wise Addition of Additives

For each set of retention and drainage experiments, 500 ml of stock from the master batch was placed in the Britt Jar and agitated with an impeller at 800 rpm. Then 0.05 % (1 lb/ton, solids basis) of Percol®175 cationic acrylamide copolymer, on furnish solids from a 0.1 % solution, was added. After 30 seconds, the stirring rate was increased to 1,250 rpm for 30 seconds, and then immediately reduced to 800 rpm. Next the selected microparticle formulation was added, followed by 30 seconds more of agitation. Various levels of synthetic

mineral microparticles, 0.25, 0.50, 0.75, and 1.00 % by solid basis of total furnish, were tested.

2.3.2. Turbidity Measurement to Evaluate Retention

An initial approximate 20 ml of filtrate was collected and discarded, because the fines and filler in this filtrate have high possibility of having been pressed through the screen by agitating motion of stirrer during the 1½ minute procedure. An aliquot of approximately 40 ml filtrate was collected in a 200 ml beaker and divided into two turbidity cuvettes (20 ml each). The turbidities of these two filtrates were evaluated based on the tenth appearance of digital output (about 3 seconds) after placement in the device. The cuvette was gently swirled and the turbidity was evaluated again.

In analysis of turbidity data, it will be assumed that a lower turbidity of filtrate implies a higher retention of particles. To account for the increase of turbidity due to microparticles, blank tests were done. 500g of water was placed in the Britt Jar. The same amounts of SMMs, synthesized in each conditions, and bentonite were added into the blank water. The turbidities of each filtrate was measured in the same way.

2.3.3. Gravity Drainage Time

After taking the turbidity samples, 200 ml of the slurry was placed in a filtration device, supplied with a 200 mesh screen of circular cross-section and a diameter of 3.9 cm. The time required for the water to drain from 200 ml to 150 ml was measured and recorded as the "gravity drainage time." Another sample was measured for the second value.

3. RESULTS AND DISCUSSION

3.1. Effect of Metal Species

Fig. 3.3(a) shows the results of turbidity to evaluate retention performances of each type of microparticle. The iron silicate, synthesized by adding the solution of ferric chloride ($FeCl_3$) to sodium meta-silicate solution, had the highest performance in the retention of fines and PCC through the all levels of addition. Zinc silicate and aluminosilicate synthesized by adding solution of either zinc chloride ($ZnCl_2$) or aluminum chloride ($AlCl_3$) showed similar retention performances. All species of SMMs performed better than bentonite through all addition levels. The retention performances of zinc silicate and two kinds of aluminum silicates were improved linearly according the increase of addition level of SMM.

The results of gravity drainage experiments are depicted in Fig. 3.3(b). Aluminum silicate synthesized from aluminum sulfate performed slightly better in drainage than bentonite at the higher addition level. Zinc silicate performed slightly better in terms of drainage at the 0.50 % addition level, under the same conditions of synthesis (500 rpm, no salt, no neutralization), though it should be noted that the metal/Si ratios were not held constant (Al/Si = 0.76, Zn/Si = 1.14, Fe/Si = 0.76).

Considering the results of both graphs, it is summarized that the SMMs synthesized by addition of metal species; aluminum chloride ($AlCl_3$), zinc chloride ($ZnCl_2$), and ferric chloride ($FeCl_3$), performed better than bentonite for retention and drainage.

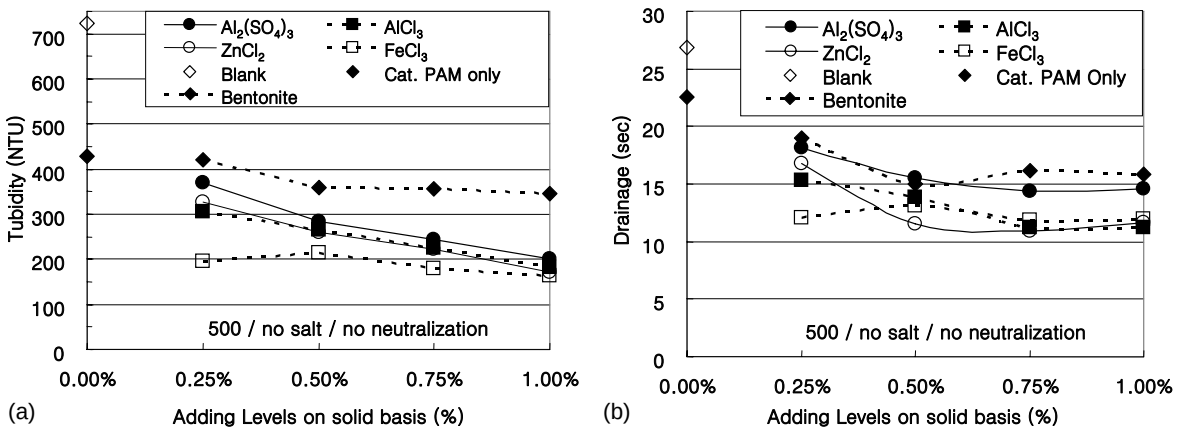

Fig. 3.3. Effects on filtrate turbidity and drainage times after replicate batches pulp-PCC suspension were treated with microparticles resulting from addition of metal solutions to sodium silicate solution under the following constant conditions: 500 rpm, no salt added, no neutralization; (a) results of turbidity measurements; (b) gravity drainage times.

3.2. Effect of Stirring Speed

Results in Fig. 3.4(a) show that an agitation speed of 1500 rpm produced results, in drainage, that were superior to 500 rpm during preparation of synthetic mineral microparticles in low addition levels, 0.25 and 0.50 %. Through the all of addition levels, both of 500 and 1500 rpm system performed better than bentonite.

Tentatively it is proposed that the higher performance of the material produced at 1500 rpm is due to a smaller primary particle size, which is equivalent to saying that the surface area per unit mass was higher, compared to the material produced at a lower speed of agitation. A higher surface area would explain why the microparticles produced at 1500 rpm were able to achieve relatively large retention effects at the lowest levels of microparticle addition considered. It is proposed that the higher hydrodynamic shear creates a larger number of

nucleation events, leading to a higher number of primary particles, which consume the available precipitating ions before they have grown as large as those produced under lower agitation. However, a smaller primary particle size does not in any way rule out the possibility of primary particles becoming fused together into gel structures. Past work has shown that more highly structured microparticles (chains, elongated clusters, *etc.*) can provide enhanced retention performance, when used in combination with a high-mass cationic polymer treatment [5]. This hypothesis is consistent with the observation that under pH 7, the microparticles formed at the higher agitation speed showed higher retention performance.

Part (a) of Fig. 3.4 also shows that the retention performance of SMM produced at 1500 rpm did not change when the amount added was increased above 0.25 % on a solids basis. Such behavior is highly desirable in a microparticle product, since there is no evidence of a reversal of the retention effect upon overdose of the microparticle. To explain this effect, retention aid systems based on high-mass acrylamide copolymers are well known for their largely irreversible behavior. Polyelectrolyte complex structures formed between highly structured microparticles and extended loops and tails of retention aid polymers would not be expected to easily become detached. Thus, any attachments mediated between polyelectrolyte-covered fibers and fines, upon initial addition of the structured microparticle additive would be expected to persist as higher incremental amounts of the microparticle are added [6-9].

Drainage rate results in Part (b) of Fig. 3.4 show an inverted order of effectiveness, compared to Part (a). The SMM formed at a lower rate of agitation approximately matched the

performance of bentonite, whereas the higher agitation rate yielded microparticles that were less effective at addition levels below 0.75 %. These results suggest that the latter particles have a higher degree of structure, an attribute that tends to favor retention performance over drainage performance [5].

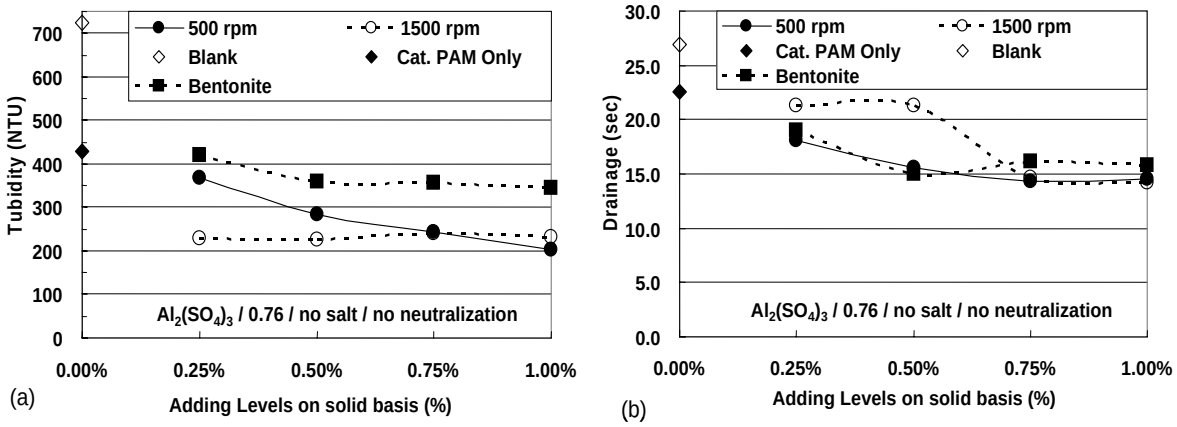

Fig. 3.4. Effects of the variations of stirring speeds, while holding other condition unchanged – $Al_2(SO_4)_3$, no salt added, no neutralization; (a) is the graph of the results of turbidity measurements and (b) shows the gravity drainage times.

3.3. Effect of Al/Si Ratio

A change in Al/Si ratio causes the pH to change, due to the high acidity of dissolved aluminum ions in aqueous form. As already reviewed in Chapter 1, the behaviors of silica and aluminum are complicated. High Al/Si ratio causes low pH synthetic conditions. Low pH decreases the amount of hydroxyl ion (OH^-), in aqueous solution. The hydroxyl ion is essential for deprotonation from silanol groups on the silica [10]. As a result of this, condensation of silica is limited, and the growth of silica particles is prevented. Under these circumstances, the primary particles remain small and the relative surface area of particle is

large. On the other hand, when the pH decreases into the range of 3.5 - 5, polymerized aluminum species are formed by the hydrolysis of Al-ions [11-14], and act as bridge ions to coagulate small size of primary particles [15].

As illustrated by the results in Fig. 3.5, there appears to be an optimum Al/Si ratio relative to retention and dewatering benefits of the synthetic microparticles. When we consider this fact, in Fig. 3.5, we can suppose that 0.76 and 1.0 Al/Si ratios are around the optimum value, which is supposed to be between 0.76 and 1.0, because the data of these 2 ratios have similar results caused by small primary particle and coagulation of primary particle to high structure.

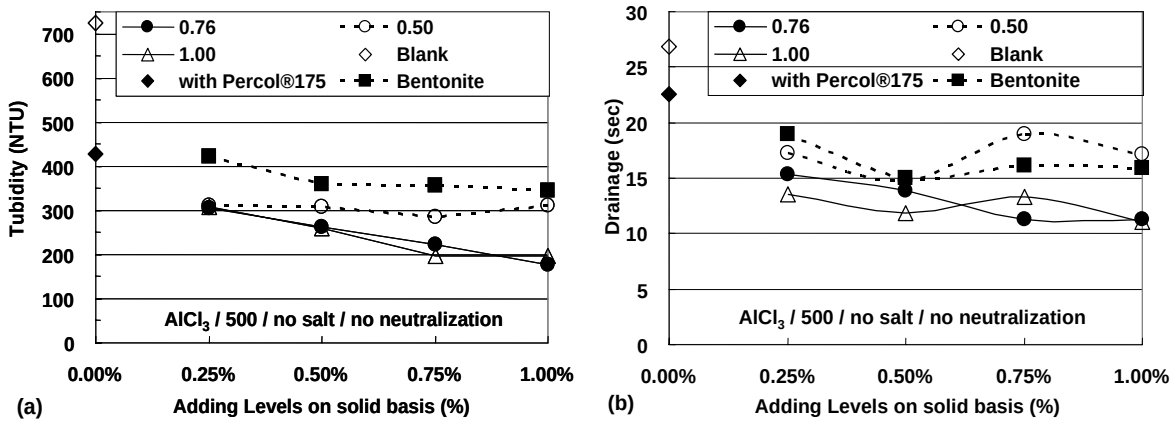

Fig. 3.5. Effects of variations of Al/Si ratio, while holding other conditions constant – $AlCl_3$, 500 rpm, no salt added, no neutralization; (a) is the graph of the results of turbidity measurements and (b) shows the gravity drainage times.

3.4. Effect of Salt

Fig. 3.6 shows no big change in the retention performance of $ZnCl_2$ as a function of changes in either salt addition or stirring speed. Zinc silicate showed a linear dependence of retention

performance on the increase of added amounts of microparticle. Considering drainage time, the most rapid drainage was achieved in the case of the zinc silicate that was formed in the absence of salt and with agitation at 500 rpm.

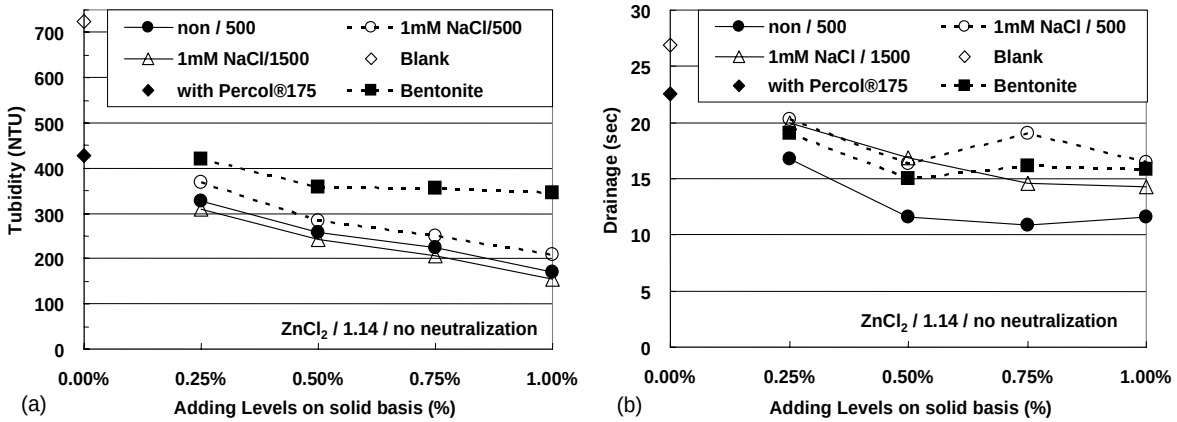

Fig. 3.6. Effects of variations of salt and stirring speed under the same other conditions– $ZnCl_2$, no neutralization; (a) is the graph of the results of turbidity measurements and (b) shows the gravity drainage times.

3.5. Effect of Neutralization

As shown in Fig. 3.7, partial neutralization of the aluminum chloride solution with NaOH before its addition to the sodium metasilicate solution rendered the microparticle product less effective in terms of both retention (Part a) and dewatering (Part b). When the Al/Si ratio was 0.76, neutralization moves the pH from 3.79 to 6. When pH is lower than 5, there are some aluminum ionic species, e.g. $Al_{13}O_4(OH)_{24}^{7+}$ and $Al_2(OH)_2^{4+}$, which can act as coagulants in SMM suspension. When the pH is 6, there is no cationic Al-ion species that can act as a coagulant. As a result of this, the micropaticles tend to remain more in a dispersed sol state, instead of forming a gel structure as shown in Fig. 3.8. In paper slurry, the higher gel

structure, which consists of the smaller microparticles, shows higher performance in retention and drainage [8]. This phenomenon is confirmed well by the lower turbidities and faster drainages in Fig. 3.7.

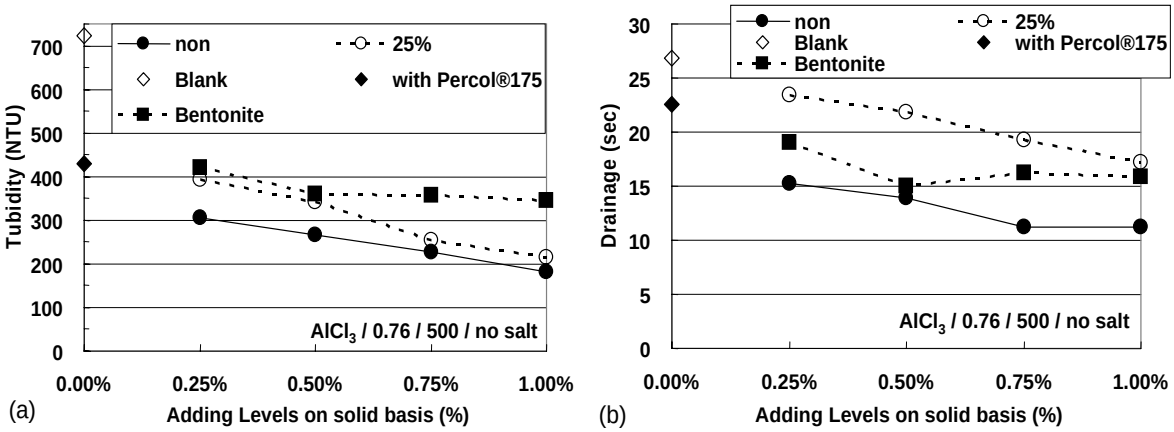

Fig. 3.7. Effects of neutralization under the same other conditions– $AlCl_3$, Al/Si=0.76, 500 rpm, no salt added; (a) is the graph of the results of turbidity measurements and (b) shows the gravity drainage times.

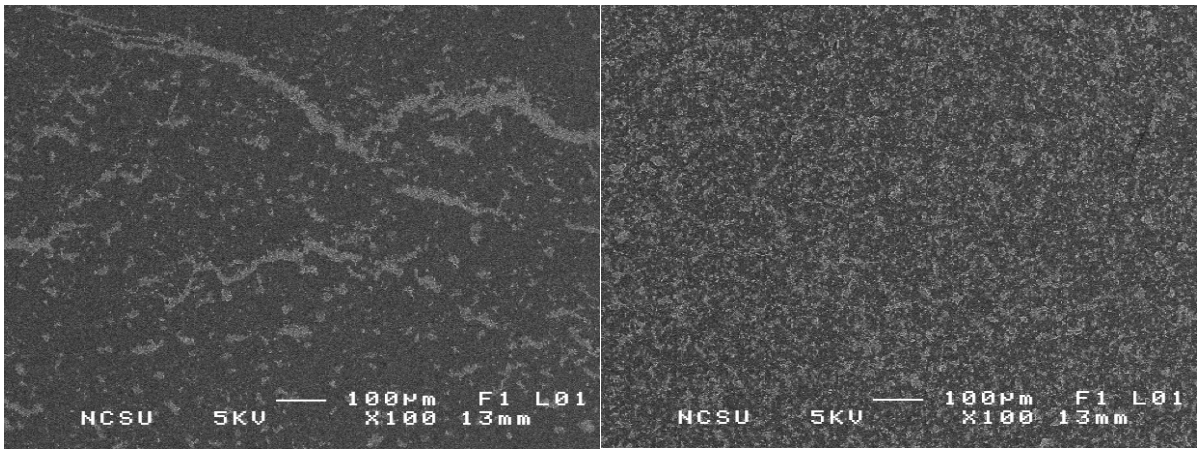

(a) (b)

Fig. 3.8. SEM pictures of SMMs synthesized under the conditions $AlCl_3$, Al/Si=0.76, 500 rpm, no salt added with (a) no neutralization and (b) 25 % neutralization with 1M NaOH.

4. CONCLUSIONS

Turbidity and gravity drainage time were measured using Britt-Jar test with representative synthetic mineral microparticle (SMM) formulations, in order to confirm the efficacy of SMM, covering a wide range of compositions, and discover effects of some key variables that have the potential to lead to unexpected advantages in terms of the effectiveness of the microparticles, when used in combination with a cationic polyacrylamide treatment of papermaking furnish.

An iron silicate showed highest retention performance, as well as suitably fast drainage time relative to other metal silicate and bentonite. Zinc silicate improved retention and drainage. SMM synthesized from aluminum sulfate ($Al_2(SO_4)_3$) did not show a benefit in retention and drainage, relative to bentonite. However, these three compositions have SO_4^{2+}, Zn^{2+}, and Fe^{3+}, which are not regarded by papermakers as welcome species, due to the environmental concerns. SMM synthesized from aluminum chloride ($AlCl_3$) performed better in drainage and retention than bentonite when the Al/Si ratios were 0.76 and 1.00 For these reasons, $AlCl_3$ was selected for the next series of studies as the major metal species to synthesize SMM suspensions.

In the results of retention and drainage at different stirring speed, the higher speed (1500 rpm) was proposed to produce small primary particles, whereas the lower speed (500 rpm) was expected to form a higher degree of structure in SMM suspension. However, it was found that when the Al/Si ratio and neutralization are considered, pH variation due to the change of Al/Si ratio can be a key factor to control the size of primary metal silicate particles

and the degree of coagulation of the primary particles. These effects appear to be due to the distribution of Al-ion species and different ionic behavior on the surface of silica through the pH variation.

5. REFERENCES

1. Drummond, D.K., "Synthetic Mineral Microparticles for Retention Aid Systems," *U. S. Pat. 6,184,258 B1*, Feb. 6. 2001 (filed Feb. 7, 1997).

2. Drummond, D.K., "Synthetic Mineral Microparticles," *U.S. Pat. 5,989,714*, Nov. 23, 1999 (filed May 4, 1998).

3. Drummond, D.K., "Synthetic Mineral Microparticels and Retention Aid and Water T reatment Systems and Methods Using Such Particles," *U.S. Pat. 6,183,650 B1*, Feb. 6, 2001 (filed Oct. 13, 1999).

4. Housecroft, C.E. and Sharpe, G., *Inorganic Chemistry*, Pearson Education Limited, E ssex, England (2001)

5. Moffett, R.H., "On-site production of a silica-based microparticulate retention and dr ainage aid," *TAPPI J. 77*(12): 133-138 (1994).

6. Hubbe, M.A., "Reversibility of Polymer-Induced Fiber Flocculation by Shear. 1. Exp erimental Methods," *Nordic Pulp Paper Res. J. 15*(5): 545 (2000).

7. Hubbe, M.A., "Reversibility of Polymer-Induced Fiber Flocculation by Shear. 2. Mul ti-Component Chemical Treatments," *Nordic Pulp Paper Res. J. 16*(4): 226 (2001).

8. Hubbe, M.A., "Microparticle Programs for Drainage and Retention," in Rodriguez, E

d., *Micro and Nanoparticles in Papermaking*, Ch. 1, TAPPI Press, 2005.

9. Hubbe, M.A., "Retention and Hydrodynamic Shear," *Tappi J. 69*(8): 116 (1986).

10. Iler, R.K., *The Chemistry of Silica – Solubility, Polymerization, Colloid and Surface Properties, and Biochemistry*, J. Wiley & Sons, New York, 1979.

11. Bottero, J.Y., Porier, J.E. and Fiessinger, F., "Study of Partially Neutralized Aqueous Aluminum Chloride Solutions: Identification of Aluminum Species and Relation bet ween the Composition of the Solutions and Their Efficiency as a Coagulant," *Progre ss in Water Technology, 1*(1): 601 (1980).

12. Bottero, J.Y. and Fiessinger, F., "Aluminum Chemistry in Aqueous Solution," *Nordi c Pulp and Paper Res. J., 4*(2): 81 (1989).

13. Bottero, J. Y., Tchoubar, D., Cases, J. M., Fiessinger F., "Investigation of the Hydrol ysis of Aqueous-Solutions of Aluminum-Chloride. 2. Nature and Structure by Small-Angle X-Ray-Scattering," *Journal of Physical Chemistry 86* (18): 3667 (1982).

14. Bottero, J. Y., Cases, J. M., Fiessinger, F., Poirier, J. E., "Studies of Hydrolyzed Alu minum-Chloride Solutions. 1. Nature of Aluminum Species and Composition of Aqu eous-Solutions," *Journal of Physical Chemistry 84* (22): 2933 (1980).

15. Iler, R.K., "The Effect of Surface Aluminosilicate Ions on the Properties of Colloidal Silica,"

CHAPTER 4

Charge Densities of Synthetic Mineral Microparticle Suspensions, Depending on Sythetic Conditions

ABSTRACT

Streaming current titrations with highly charged polyelectrolytes were used to measure the charge properties of SMM suspensions and to understand the interactions among SMM particles, fibers, fiber fines, and cationic polyacrylamide (cPAM) as a retention aid. It was found that pH variation, caused by the change of Al/Si ratio and partial neutralization of aluminum's acidity, profoundly affects the charge properties of SMM, due to the variation of Al-ions and the influence ionizable groups on the Si-containing particle surface.

1. INTRODUCTION

As already reviewed in Chapter 1, several types of microparticle retention and drainage aid systems have become popular, starting in the 1980's. As investigated in Chapter 3, the SMM, suspension, synthesized by adding aluminum chloride ($AlCl_3$) solution into the aqueous form of sodium metasilicate (Na_2SiO_3), showed a competent performance, in terms of retention and dewatering, which was compared to that of bentonite.

To improve retention and drainage, usually the microparticles need to be highly negative in charge under the wet-end conditions during paper producing [1]. It was found that aluminum-containing colloidal silica particles maintain a negatively charged surface from a neutral to a

slightly acidic papermaking condition [2-3]. The negative charge is attributable to isomorphic substitution of tetravalent silicon atoms by trivalent Al in crystalline sites causes an increased negative charge under moderately acidic conditions.

As introduced in Chapter 1, Milonjić showed that the surface of colloidal silica becomes increasing negative with increase of pH from 6.5 and with increase of the amount of added salt at ambient temperature [9]. Other scientists also have researched the charge properties and isoelectric point and concluded that the surface charge of colloidal silica becomes negative slowly from isoelectric point (pH 1.5–3) to pH 7 and rapidly with further increase of pH from 7 to higher values [8-20].

When an anionic aluminate ion, ($Al(OH)_4^{-1}$), reacts with the surface of silica at a tetrahedral coordination site, an aluminosilicate anion is formed, as depicted in the top part of Fig. 4.1. This aluminosilicate anion can form a higher structural aluminosilicate by condensation reaction, depicted in Fig. 4.1 (a) and (b), and leave as an ionic state on the surface of aluminosilicate as in Fig. 4.1 (c).

A multitude of minerals and synthetic materials can be composed of chains, rings, layers, three-dimensional arrays and amorphous forms that involve corner-sharing of SiO_4 and AlO_4 tetrahedral units. The isoelectronic relationship between $(SiO_2)_2$ and $[AlSiO_4]^-$ is the foundation of a vast range of aluminosilicate chemical species. Pentacoordinate AlO_5 moieties are less common, but not rare.

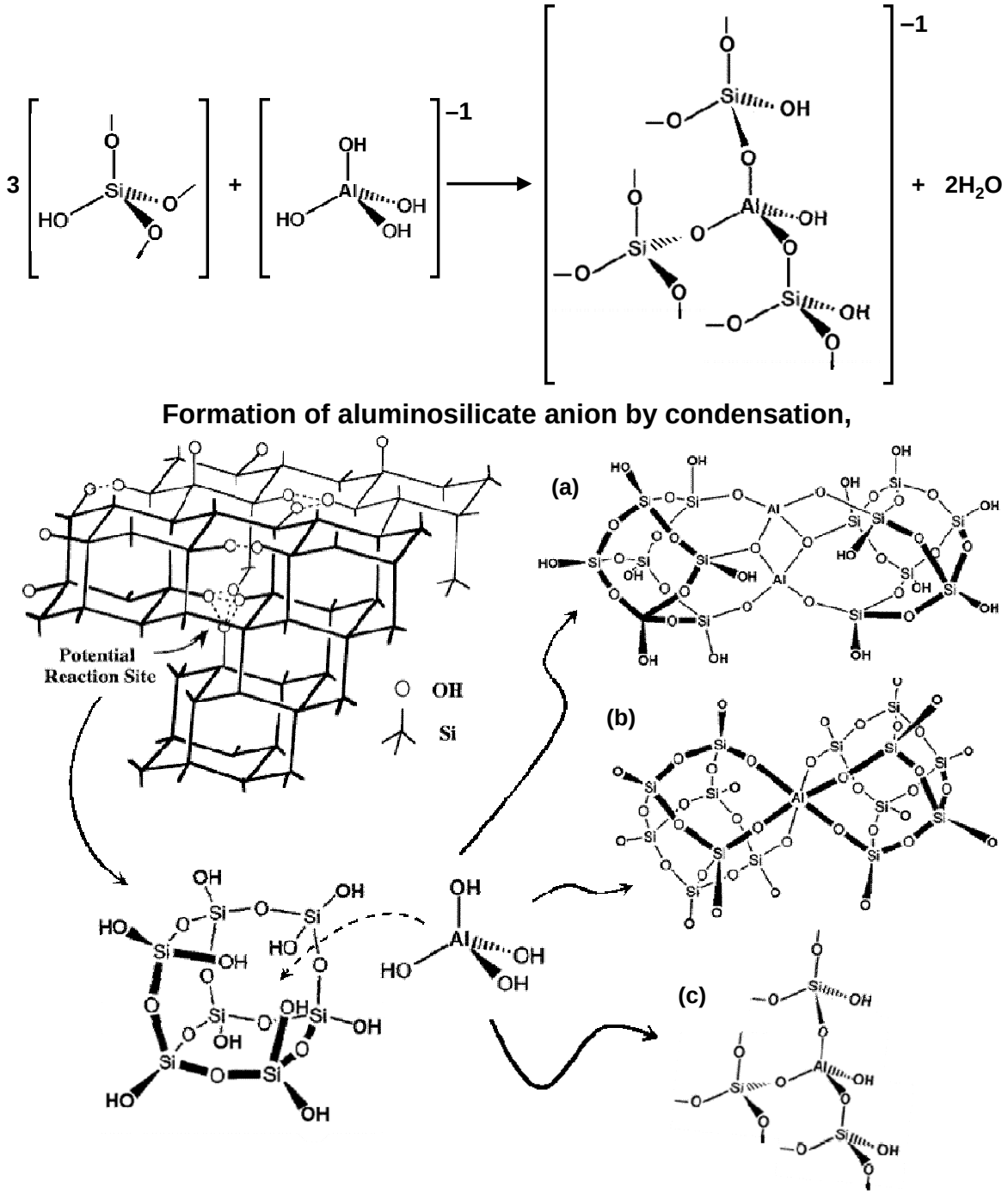

Fig. 4.1. The formation of the aluminosilicate by condensation of aluminate ion with the surface of silica; resulting in a higher structural aluminosilicate - (a) and (b), or an ionic state on the surface of aluminosilicate - (c) [15-17]

Since the aluminum III ion (Al^{3+}), and the silica ion (Si^{4+}) have similar size, it is easy to replace or condense an aluminum ion with a silica ion. However, an extra singly-charged cation must be present to maintain electrical neutrality. Sharing of all four oxygen atoms in the tetrahedral SiO_4 can form an infinite composition of SiO_2. On the other hand, when a part of the tetrahedral SiO_4 in the composition of SiO_2 is replaced by Al, aluminum silicate anions are formed, e.g. $[AlSi_nO_{2n+2}]^-$, $[Al_2Si_n\ O_{2n+2}]^{2-}$ [32].

2. MOTIVATIONS OF PRESENT WORK

Usually the negative charge and high surface area of the microparticles, commonly used in the paper machine wet end, are significant for achieving a high effectiveness in terms of retention and drainage [1]. Thus, it is necessary to maintain a strong negative charge under neutral to acidic papermaking conditions. The negative surface charge of SMM appears to be very important with respect to its performance as part of retention and dewatering system.

As already discussed in Chapter 1, the character of each of the reagents, sodium silicate (Na_2SiO_3) and aluminum chloride ($AlCl_3$), used in the formation of SMM suspensions in the present work, give rise to quite different ionic species with different charge densities, depending on pH.

It is proposed that an increase in the Al/Si ratio will acidify the SMM suspension, due to the acidity of metal ions in aqueous solution with decreasing pH. Thus, at pH between 7 and 10, the silica ions are destabilized and start to form polymerized silica structures by condensation polymerization from $Si(OH)_4$, and silanol groups which are expected to exist on the surface

of SMM particles, give rise to negative charge properties. Additionally, the Al-ions exist as a form of $Al(OH)_4^-$ which will be adsorbed on the silanol group and form aluminosilicate, with release of sodium ions.

When the Al/Si ratio is increased further, the pH falls reaching a range of 4<pH< 7. Under such conditions the silanol groups on the surface of SMM are expected to have slightly negative charge properties. In case of aluminum, polymerized species, *e.g.* Al_{13}: $AlO_4Al_{12}(OH)_{24}(H_2O)_{12}^{7+}$, are expected to occur in a range 4<pH<5. These hydrolyzed aluminum ions destabilize the surface of silica and lead to bridging between primary particles of silica. Partial neutralization of Al^{3+} by NaOH during the synthesis of SMM is expected to shift pH values upward. An increase in pH promotes aluminum and favors formation of aluminum oligomers. Increasing pH also affects the charge and surface properties of silica particles due to the increase of sodium ion, Na^+.

As shown by the results of drainage and retention experiments, using aluminum chloride for synthesis of SMM, as described in Chapter 3, there was an optimum Al/Si ratio, at which the effects of SMM addition were superior to those of bentonite. Thus, the net charge density of SMM was investigated to find the optimum synthetic conditions to make SMM have higher surface charge depending on the change of Al/Si ratio.

3. EXPERIMENTAL

3.1. Materials

SMM suspensions were synthesized in a manner consistent with the patents [2-4]. Sodium meta-silicate ($Na_2SiO_3 \cdot 5H_2O$) was used as base ingredient with 0.445 molal concentration. The added metal solution ingredient was 0.566 molal aluminum chloride ($AlCl_3$). The synthetic factors constituting this study were as shown in Table 4.1.

Table 4.1.. Factors Related to Microparticle Preparation.

Constant		**Variables**	
[Na_2SiO_3]:	0.445 molal solution	Al/Si ratios:	0.50, 0.63, 0.76, 0.88, 1.00, 1.14
		Salt:	None *vs*. 1 mM NaCl
[$AlCl_3$]:	0.566 molal solution	Neutralization:	None *vs*. 25 % with 1 N NaOH
		Shear rate:	1500 and 13,000 rpm.

The percent neutralization was defined as 100 times the ratio of added NaOH to $AlCl_3$, on a molar equivalent basis, noting that aluminum is tri-valent and the hydroxyl ion is monovalent. Thus, in certain tests partially neutralized aluminum-containing solutions were used during synthesis of SMM microparticle preparation.

Polyvinylsulfate, potassium salt (PVSK, Aldrich 27,196-9, Mw = Ca. 170,000) and poly-diallyldimethyl-ammonium chloride (P-DADMAC, Aldrich 40,901-4, Mw = Ca. 100,000 ~ 200,000) were used as titrants for measuring charge densities of SMM preparations

3.2. Measurement of Charge Densities of SMM

An SMM suspension was prepared, using the synthesis procedure described in the patents [2-4]. A speed-controlled motor was used to achieve a 1,500 rpm of agitation and a commercial blender was used for 13,000 rpm. The pH of the suspension was measured after synthesis.

3.2.1. Titration of Total Net Charge in SMM Suspension

For measuring the charge density, 10g of suspension was taken in a 200 ml beaker and diluted 5 times to 50g with deionized water. The pH of the diluted suspension was also measured. Titration was then performed on the diluted suspension. The weight concentration of solid was measured accurately by Thermogravimetric Analysis (TGA) for calculation of a charge density per unit solid mass of the suspension.

3.2.2. Charge Titration of Ionic Species in SMM Suspension

To measure the charge densities of particles and ionic species, 10g of microparticle suspension was placed in a centrifuge cell and diluted 5 times to 50g with deionized water. The pH value of each diluted suspension was also measured, and the diluted mixture in the cell was centrifuged. The supernatant was collected in another tared centrifuge cell. The mass and pH of the collected supernatant were recorded, and then the pH was adjusted to the pH of original diluted sample. The titration was performed subsequently. The mass concentration of supernatant was measured by TGA.

3.2.3. Charge Titration of SMM Solids

Deionized water was added to bring the total mass to 50 g in the centrifuge cell, which had the centrifuged solid from the SMM suspension. The solids in that cell were dispersed again

with a vortex generator and ultra-sonicator. Titration subsequently was performed on the redispersed suspension and the pH was measured, and then the pH was adjusted to the pH of the original diluted sample. The mass concentration of solids in the centrifuge cell was measured accurately by TGA for calculation of a charge density of the redispersed suspension.

4. THEORY

An increase in the Al/Si ratio is expected to acidify the SMM suspension. Figure 4.2 shows the relationship between pH and Al/Si ratio with or without 25 % neutralization of Al^{3+}. If it is assumed that the Si species are consumed quantitatively during synthesis, then the following chemical reaction equations between $AlCl_3$ and Na_2SiO_3 can be expected to describe the resulting chemical interactions:

$x \bullet AlCl_3 + y \bullet Na_2SiO_3$

$\rightarrow Na_{\boldsymbol{x}}Al_xSi_yO_{3y} + (2y–x) \bullet Na^+ + 3x \bullet Cl^-$,

when Al/Si ratio < 0.667 and no neutralization,

$\rightarrow Na_{\boldsymbol{x}}Al_xSi_yO_{3y} + (2y–0.25x) \bullet Na^+ + 3x \bullet Cl^- + 0.75x \bullet OH^-$,

when Al/Si ratio < 0.667 and 25 % neutralization,

$\rightarrow Na_{2y/3}Al_{2y/3}Si_yO_{3y} + \mathbf{(x–2y/3) \bullet Al^{3+}} + 4y/3 \bullet Na^+ + 3x \bullet Cl^-$,

when Al/Si ratio > 0.667 and no neutralization,

$\rightarrow Na_{2y/3}Al_{2y/3}Si_yO_{3y} + \mathbf{(x–2y/3) \bullet Al^{3+}} + (4y/3+0.75x) \bullet Na^+ + 3x \bullet Cl^- + 0.75x \bullet OH^-$,

when Al/Si ratio > 0.667 and 25 % neutralization.

where, x / y = Al/Si ratio

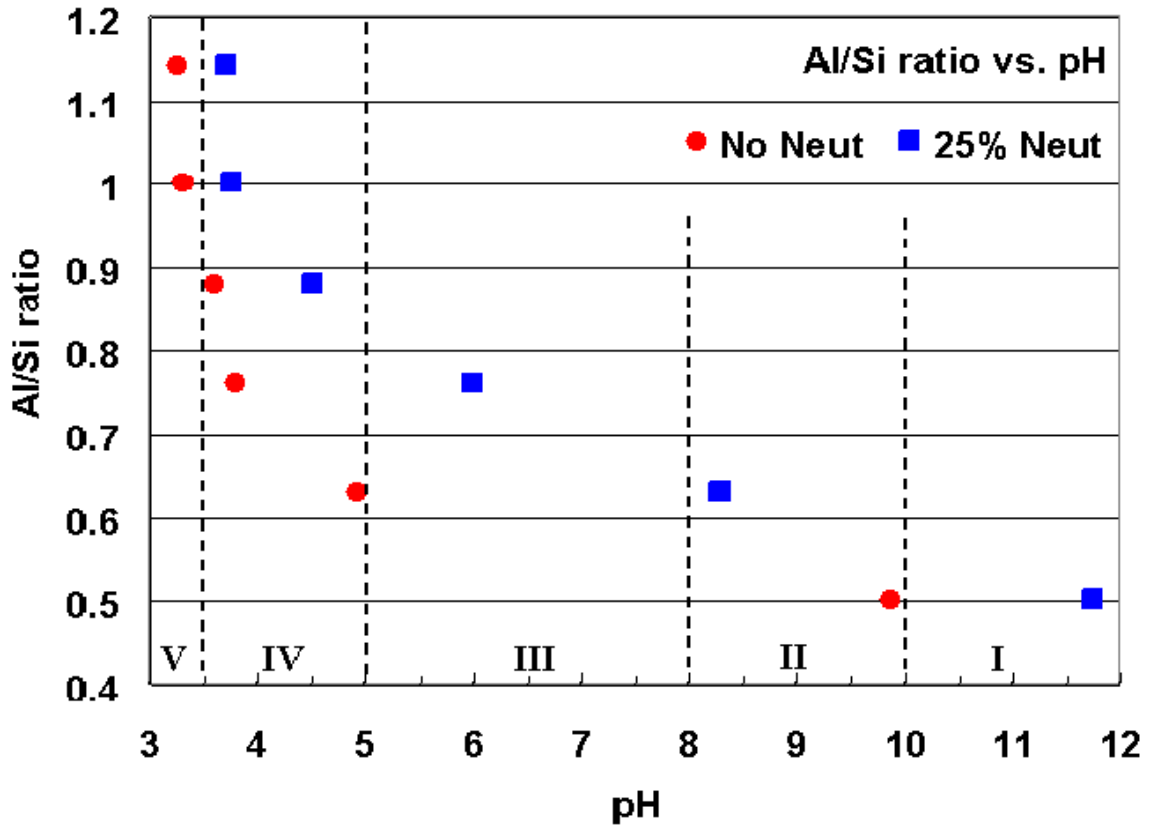

Fig. 4.2. The relationship between pH and Al/Si ratio with or without 25 % neutralization of Al^{3+}. The variable pH was plotted on the horizontal axis in order to better show the selected five ranges. However, it is understood that the Al/Si ratio was a controlled variable and the pH was a measured factor.

Figure 4.3 shows the expected residual ionic species in SMM suspension having different recipes. The concentration of Al^{3+} species in SMM suspension should increase with decreasing pH by increasing the Al/Si ratio as depicted in Fig 4.3. When the Al/Si is low, e.g. 0.50 and 0.63, Al^{3+} species cannot react with all of the SiO_3^{2-} ions that are present. For this reason, the residual SiO_3^{2-}, which does not react with Al^{3+}, is expected to exist inside of aluminosilicate sols (primary particle) or form colloidal silica.

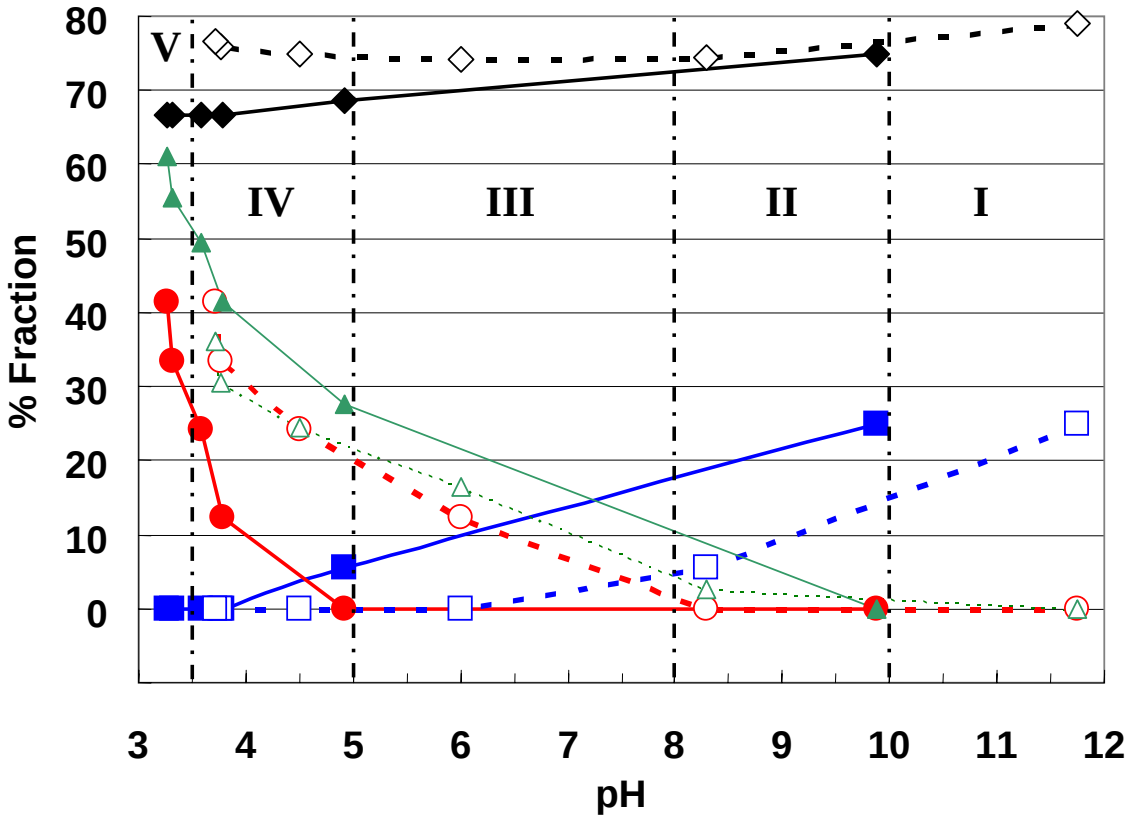

Fig. 4.3. Expected Residual Ionic Species in SMM suspension depending on pH, changed by molar ratio of Al/Si; solids – unneutralized samples; blank – 25 %neutralized samples; ●–Al^{3+}; ■–SiO_3^{2-}; ♦–Na^+;▲–Cl^- after deduction of molar concentration of Na^+ from molar concentration of Cl^-.

The residual sodium ion (Na^+) originates from the added sodium meta-silicate. Sodium ion can act as a neutralizer against the anion caused by the replacement or condensation of the aluminum ion with the silica ion. As a result of this phenomenon, sodium ions are consumed quantitatively in the same proportion with the consumption of aluminum ion. Then, the residual sodium ions, which are not consumed with aluminum ions, are expected to exist in the solution phase of the SMM suspension. These residual sodium ions then can react with silianol groups on the surface of colloidal silica or aluminosilicate.

The chloride ion (Cl^-) comes from aluminum chloride. The residual chloride ion, represented in Fig 4.3, was calculated by deduction of sodium ions, which could act as a salt with chloride ions. This residual chloride ion can compensate for the positive charge of aluminum ion in SMM suspension or be absorbed on the aluminum site or silica site by replacement of OH or O^-.

The distribution of ionic species is various, depending on the change of pH. However, the isoelectric point of silicate is reported to be lower than pH 4. As already discussed in Chapter 1, the distribution of aluminum ionic species is very delicate, depending on the change of pH. To clarify how such effects are likely to affect SMM synthesis, 5 zones, as drawn in Fig. 4.2 and 4.3, are assumed.

5. RESULTS AND DISCUSSION

5.1. Charge Densities of SMM Suspension

As shown in Fig. 4.4, the titration results were separated into two groups, non-neutralized and 25 % neutralized. In the case of non-neutralized conditions, the net charges of SMM suspensions changed from negative to positive at the point between 0.64 and 0.76 Al/Si ratios. In the other case of 25 % neutralized conditions, the changes in sign were shifted to between 0.76 and 0.88 Al/Si ratios. The net charges of SMM synthesized at 1,500 rpm shear rate were slightly lower in the positive area and higher in the negative zone, than the results at 13,000 rpm. It is proposed that the higher shear rate broke down the large particles or aggregated

structure and made more specific surface area. However, the difference between two results was not enough to significantly increase the charge properties of SMM with increasing shear.

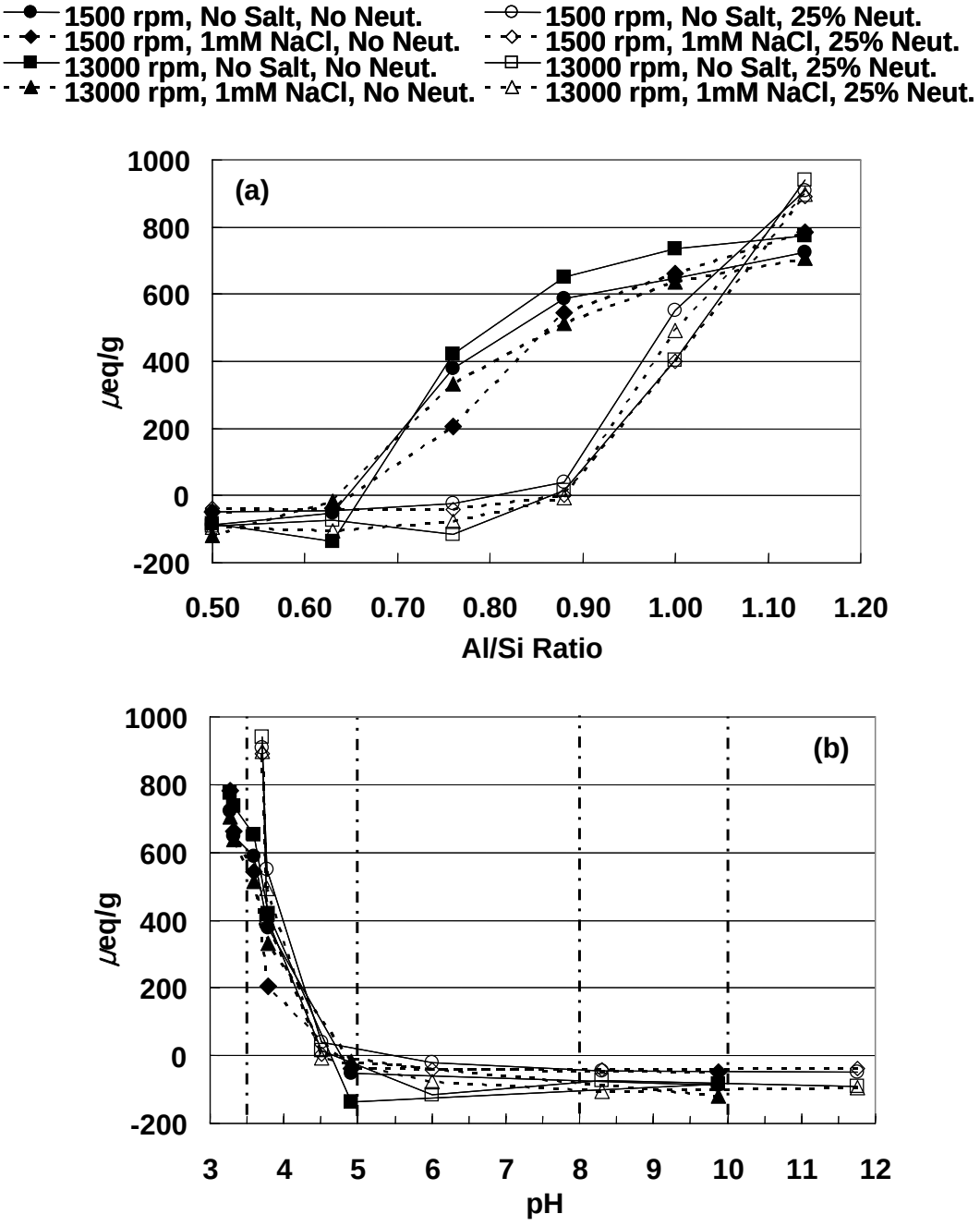

Fig. 4.4. The charge densities of SMM suspensions, synthesized of $AlCl_3$ and Na_2SiO_3 depending on (a) Al/Si ratio and (b) pH.

At this point, the charge properties of SMM need to be analyzed with respect to the zones in Fig. 4.2, and the residual aluminum species in Fig. 4.3. Two terms will be used in the discussion that follows, when describing partially or extensively hydrolyzed and hydroxylated aluminum species. When referring to the degree of polymerization of aluminum species, the term "high mass" implies that at least 13 aluminum atoms are associated in the same molecule. The word "low" will imply that 12 or fewer aluminum atoms participate in the predominant species that are present under the conditions being discussed. The term "gel," when used in discussing the aluminum compounds, will be taken to mean a colloid in which the dispersed phase of polymeric aluminum particles are aggregated with each other to produce a semisolid material.

(1) Zone I ($10<pH<12$): The main Al species are expected to be monomeric $Al(OH)_4^-$ ions [35-42]. The Si species are expected to be mainly $(SiO_4)^{4-}$ or $Si(OH)_4$. Those two species can easily form a sol type of sodium aluminosilicate by condensation reaction between two different species ($Al(OH)_4^-$ and $Si(OH)_4$) or only Si species. The size of a sol particle can grow easily due to the high pH and condensation reactions of residual silica species [7]. The existence of sodium chloride salt at a high concentration can prevent the sol from growing in size. High concentration of hydroxyl ion due to the high pH can deprotonate silianol groups on the sodium-aluminosilicate and make the surface charge negative, as depicted in Fig. 4.5. One synthetic condition (Al/Si=0.50; 25 % neutralization of Al^{3+}; pH=11.75) belongs to this zone.

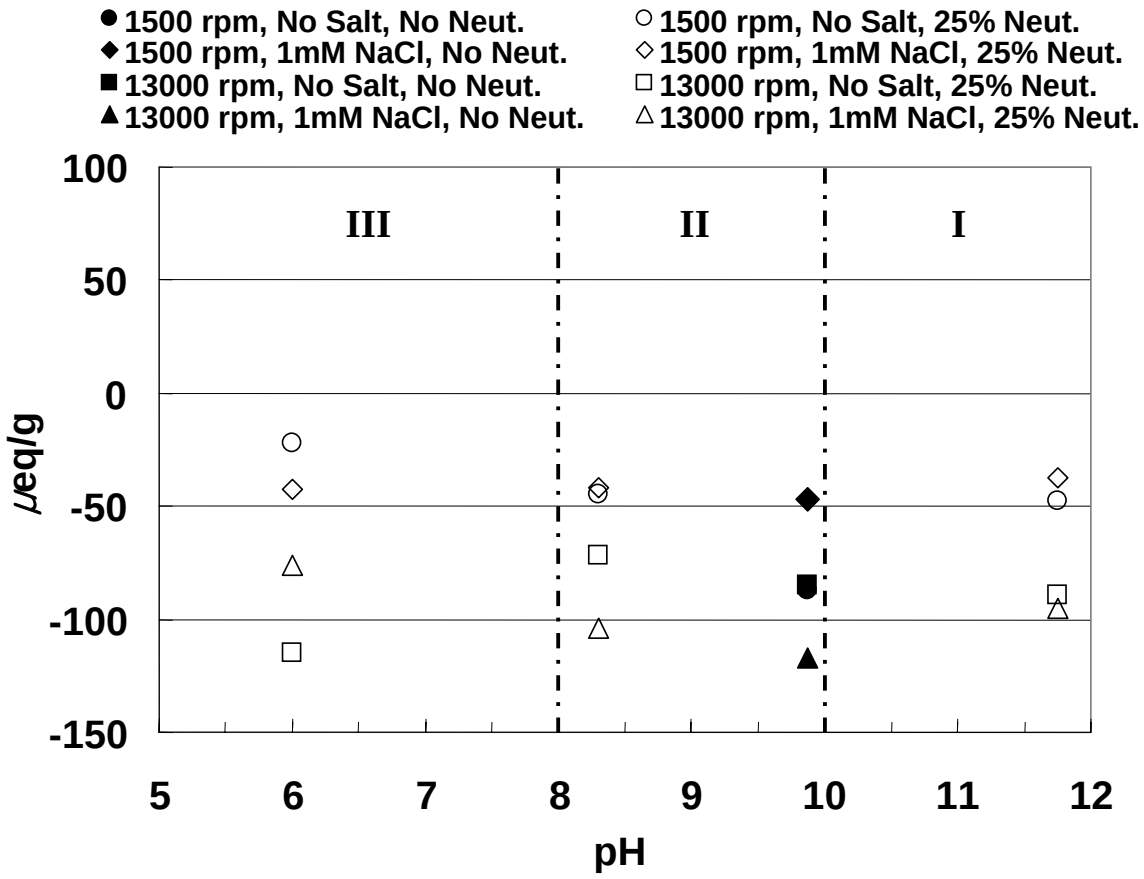

Fig. 4.5. The charge densities of SMM suspensions in zones I, II, and III, as depicted in Fig. 4.2 and 4.3.

(2) Zone II (8<pH<10): The main Al species can be gel types of polymeric Al species composed by $Al(OH)_3$, together with varying amounts of monomeric $Al(OH)_4^-$, which is formed by further hydrolysis [21-28,33]. The charge on the surface of hydroxyl polymeric Al is almost neutral and the gel form begins to dissolve and form $Al(OH)_4^-$. The behaviors of Si and residual ionic species are very similar with Zone I. Two synthetic conditions (Al/Si=0.50; non-neutralization; pH=9.9 and Al/Si=0.63; 25 % neutralization; pH=8.3) belong to this zone. The surface charges of SMM synthesis by those conditions shows negative charges due to the deprotonated silanol groups and the hydroxyl group attached to the aluminum on the surface of aluminosilicate.

(3) Zone III (5<pH<8): Only one synthetic condition (Al/Si=0.76; 25 % neutralization; pH=6.0) belongs to this zone. The main Al species are high mass polymeric Al and sol/gel $Al(OH)_3$. Monomeric Al decreases substantially in favor of high mass polymer [34-35], whose main species are Al_{13} – Al_{54}, [usually referred to as "large" polynuclear ions in the scientific literature related to aluminum chemistry] with high positive valence number from 5 to 32. The rate of formation of polymeric structure is very slow and the hydrolyzed polymeric Al ions are stable in this zone [33]. Further combination with –OH or –O on the surface of polymeric Al or silanol groups on the surface of aluminosilicate or colloidal silica can cause the sedimentation of these groups onto the surface with neutralization of negative charges on the silanol groups. By this way, the residual aluminum species are expected to exist on the surface of aluminosilicate as polymeric forms. The Si species fall in a range between $(SiO_4)^{4-}$ and $Si(OH)_4$. Condensation between Si species is not expected to be as rapid as in Zone I. Sol that is formed under the conditions of Zone I is expected to have relatively small particle size. The deprotonation rate of silanol groups on the surface of aluminosilicate or colloidal silica is lower than zone II due to the relatively low pH. However the negative charge of silanol groups tends to become nearer to zero when the pH becomes lower than 7. For this reason, a slightly negative charge on the surface of aluminosilicate still exists, as shown in Fig. 4.4 (a). In case of high shear rate (13000 rpm), it is supposed that the high shear destroyed the bridges between large polymeric Al species and the surface of aluminosilicate and then opened more silanol groups. This hypothesis can explain why the charge results of high shear (13000 rpm) were more negative than those of low shear (1500 rpm).

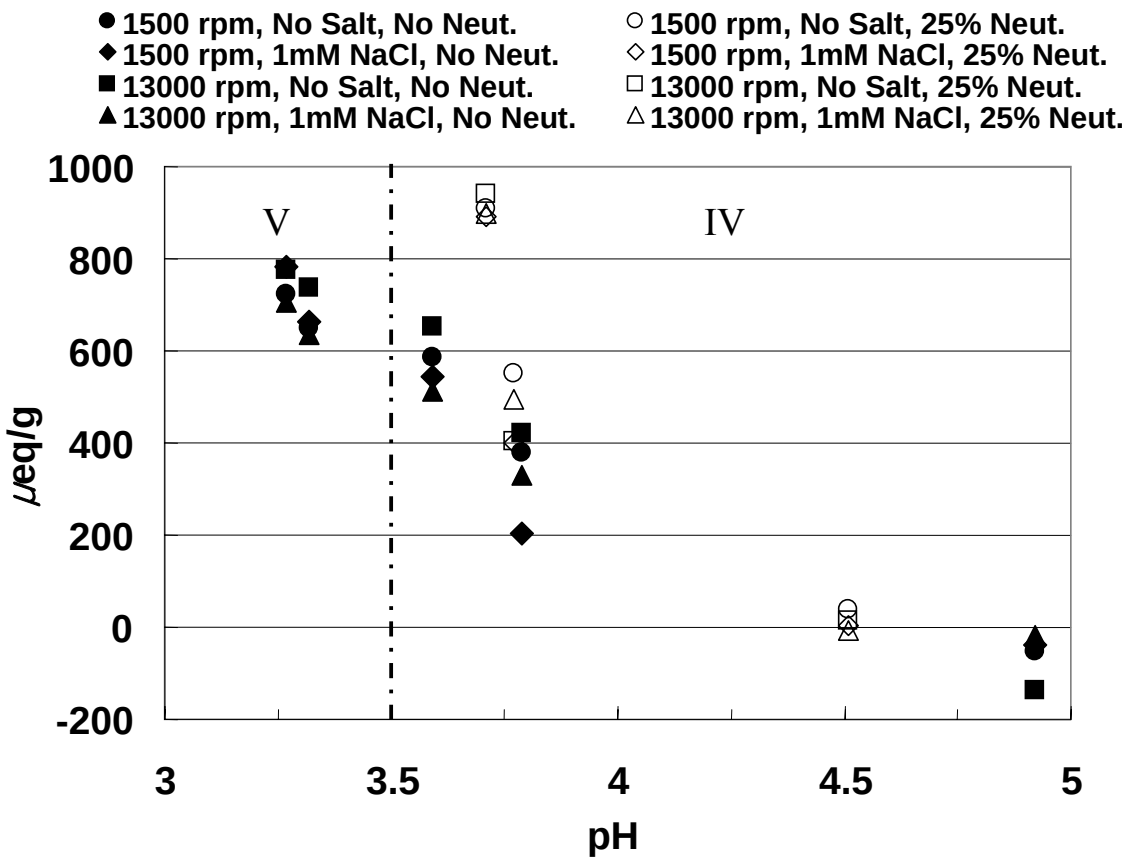

Fig. 4.6. The charge densities of SMM suspensions in zones IV and V, as depicted in Fig. 4.2 and 4.3.

(4) Zone IV (3.5<pH<5): Six synthetic conditions belong to this zone (Al/Si=0.63; non-neutralization; pH=4.9, Al/Si=0.88; 25 % neutralization; pH=4.5, Al/Si=0.76; non-neutralization; pH=3.79, Al/Si=1.00; 25 % neutralization; pH=3.77, Al/Si=1.14; 25 % neutralization; pH=3.71, Al/Si=0.88; non-neutralization; pH=3.59). The main Al species are small/middle size of polymeric Al. Monomeric Al forms HO–Al polymer to give Al_2–Al_{12} species, such as $Al_2(OH)_4^{2+}$, $Al_3(OH)_4^{5+}$, $Al_4(OH)_8^{4+}$, $Al_5(OH)_{13}^{2+}$, $Al_6(OH)_{12}^{6+}$, $Al_{10}(OH)_{22}^{8+}$, $Al_{13}(OH)_{30}(H_2O)_{18}^{9+}$, and $AlO_4Al_{12}(OH)_{24}(H_2O)_{12}^{7+}$. These species are characterized by low degree of polymerization, medium charge density, and ease of polymerization [25-28, 36-38]. In this zone, aluminum ions tend to have an octahedral structure due to the lower pH. The

octahedral structure of aluminum can be polymerized easily by the core-link theory. As a result of this phenomenon, the polymerization of the small and middle-size polymeric Al species occurs in a fast rate [39].

Formation of aluminosilicate in this zone is very complicated. When one assumes that the SO_3^{2-} is consumed quantitatively with aluminum ion (Al^{3+}), the Al/Si ratio would be 2:3. Based on this thinking, when the Al/Si ratio is larger than 0.667, the residual aluminum ions could exist in solution. However, there is another form of aluminosilicate, in the real world, which has a larger number of aluminum atoms than silicon dioxide (silica) in chemical structure, e.g. polyaluminum silicate or polyaluminum silicate chloride.

In this zone, the first group of results from pH 5 in Fig. 4.6 shows negative charge density of SMM, which has a Al/Si ratio that is lower than 0.667. Only this result showed the a negative charge. The negative charge is attributed to the deprotonated silanol group on the surface of sodium aluminosilicate, which is formed due to the excess amount of silicate ion. Other conditions showed positive surface charge. Several solid species are expected to exist; (a) The sodium aluminosilicate, which has silica as its main ingredient and the aluminum ions adsorbed partially inside of primary particle during the condensation and on the surface by condensation reaction with silanol group. The surface charge of the primary particle is slightly negative due to the deprotonated silanol groups. (b) Polyaluminum silicate, which has the aluminum species as a main structural ingredient, in combination with SiO_3^{2-}. The surface of this primary particle has a greater proportion of hydrolyzed aluminum groups due to the acidic conditions and shows a net positive charge, which can be attributed to protonated hydroxyl groups on the aluminum site. (c) Polyaluminum silicate chloride is

expected to form from the reaction between excess $AlCl_3$ and SiO_2 under acidic conditions [41]. (d) Polymerized aluminum species, which are adsorbed on the surface of aluminosilicate by the destabilization and neutralization of the surface charge of aluminosilicate [30, 40]. All expected solid species, with the exception of case (a) have the positive surface charge due to the highly cationic aluminum species in the acidic condition.

(5) Zone V (pH<3.5): Two synthetic conditions exist in this zone (Al/Si=1.00; non-neutralization; pH=3.32 and Al/Si=1.14; non-neutralization; pH=3.27). The main Al species are Al^{3+} and monomeric Al, e.g. $Al(OH)^{2+}$, $Al(OH)_2^{+}$, and aqueous $Al(OH)_3^{0}$. The value of the ratio OH/Al greatly affects the distribution of Al species in the solution of Al^{3+}. The acidity of the initial Al^{3+} solution maintains the free ion or monomeric species, and neutral aqueous $Al(OH)_3$[32]. Silicate ions (SO_3^{2-}) tends to form silicic acid $[SiO_x(OH)_{4-2x}]_n$ in acid condition [45]. The reaction between monomeric aluminum species from aluminum chloride and silicic acid with high salt concentration produces a cluster form of aluminum silicate or aluminum silicate chloride. In this zone, the SMM has a small cluster form of polyaluminum silicate chloride or aluminum chloride with the positive surface charge due to the protonated silanol group on silicate or the cationic charge of aluminum species.

5.2. Charge Densities of SMM Particles and Residual Ionic Materials

The point, at which the residual Al species first become significant and begin to increase (Al/Si =0.667), was very similar with the point where the charge changed from negative to positive, in the case of the SMM synthesized in non-neutralized conditions (Fig 4.4 (a)). As explained in the previous section, the solid forms of SMM suspension are expected to vary, depending on pH changes caused by the variation of Al/Si ratio. However, excess ionic species, e.g. the species of Al^{3+}, SiO_3^{2-}, Na^+, and Cl^-, are expected , based on the reaction equation of ingredients in Section 4.1, and as controlled by Al/Si ratio. Therefore, the charge densities of SMM particles and residual chemicals were measured under the assumptions of:

- When one of the initially dissolved ionic species is in excess, the excess ions can either adsorb onto the precipitated solids or remain in solution.
- The excess ions have strong relationships with the charge of the SMM suspension.

Figure 4.7, which corresponds to some of the data in Fig. 4.4, shows the charge densities based on total solids in SMM suspensions. As explained earlier, neutralization is the main factor that was found to separate the results into two main tendencies, as shown in part (a) of Fig 4.7.

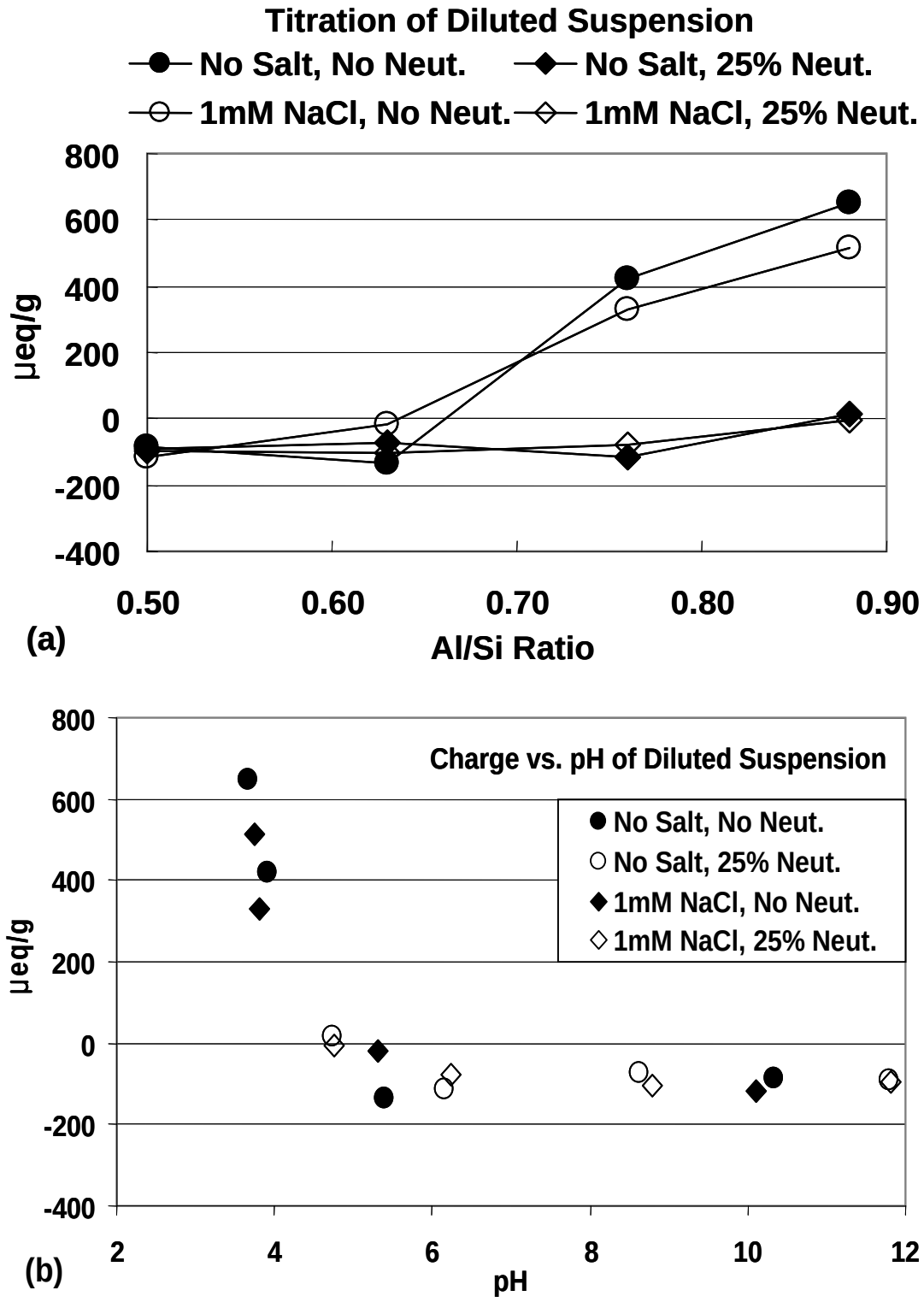

Fig. 4.7. Charge densities of SMM suspensions; (a) *vs.* Al/Si ratio and (b) *vs*. pH.

Fig. 4.8 shows the charge densities of supernatant solutions. These values are attributed to the interactions of the polyelectrolyte titrants with residual ionic species in the supernatant solutions. Only those ionic species that interact strongly with the selected titrants, poly-diallyldimethylammonium chloride and the potassium salt of poly-vinylsulfate (PVSK), can be detected by the procedure used for this analysis. As shown, all of the data lay under, but very near to zero, except for two points corresponding to 0.88 Al/Si, non-neutralized conditions. This means there was no residual cationic species, e.g. aluminum ionic species capable of interacting strongly with PVSK, in SMM suspension synthesized under conditions belong to zone I, II, and III. Based on the finding, all such aluminum species are presumed to have been consumed by condensation reaction with silicate ionic species and aggregation of polyaluminum ionic species onto the surface of aluminum silicate particles.

When the Al/Si ratio increases (with or without partial neutralization of the aluminum solution) until pH falls below 4.5, where the charge properties are reversed from negative to positive, then, the excessive polyaluminum cationic species are expected to exist in aqueous solution or be absorbed on the surface of SMM particles in zone IV.

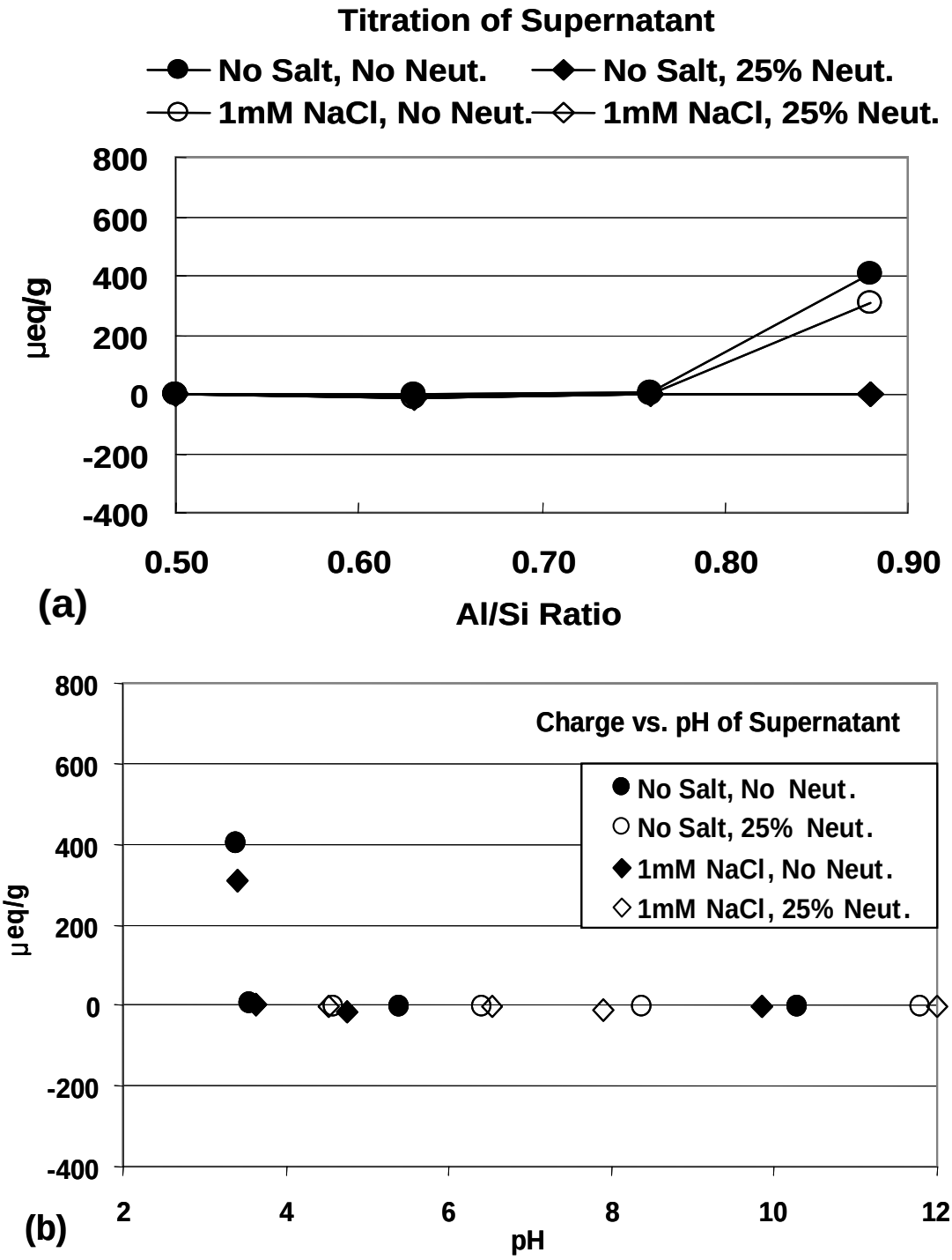

Fig. 4.8. Charge densities of SMM residual ionic species in centrifuged supernatant of SMM suspensions; (a) *vs.* Al/Si ratio and (b) *vs*. pH.

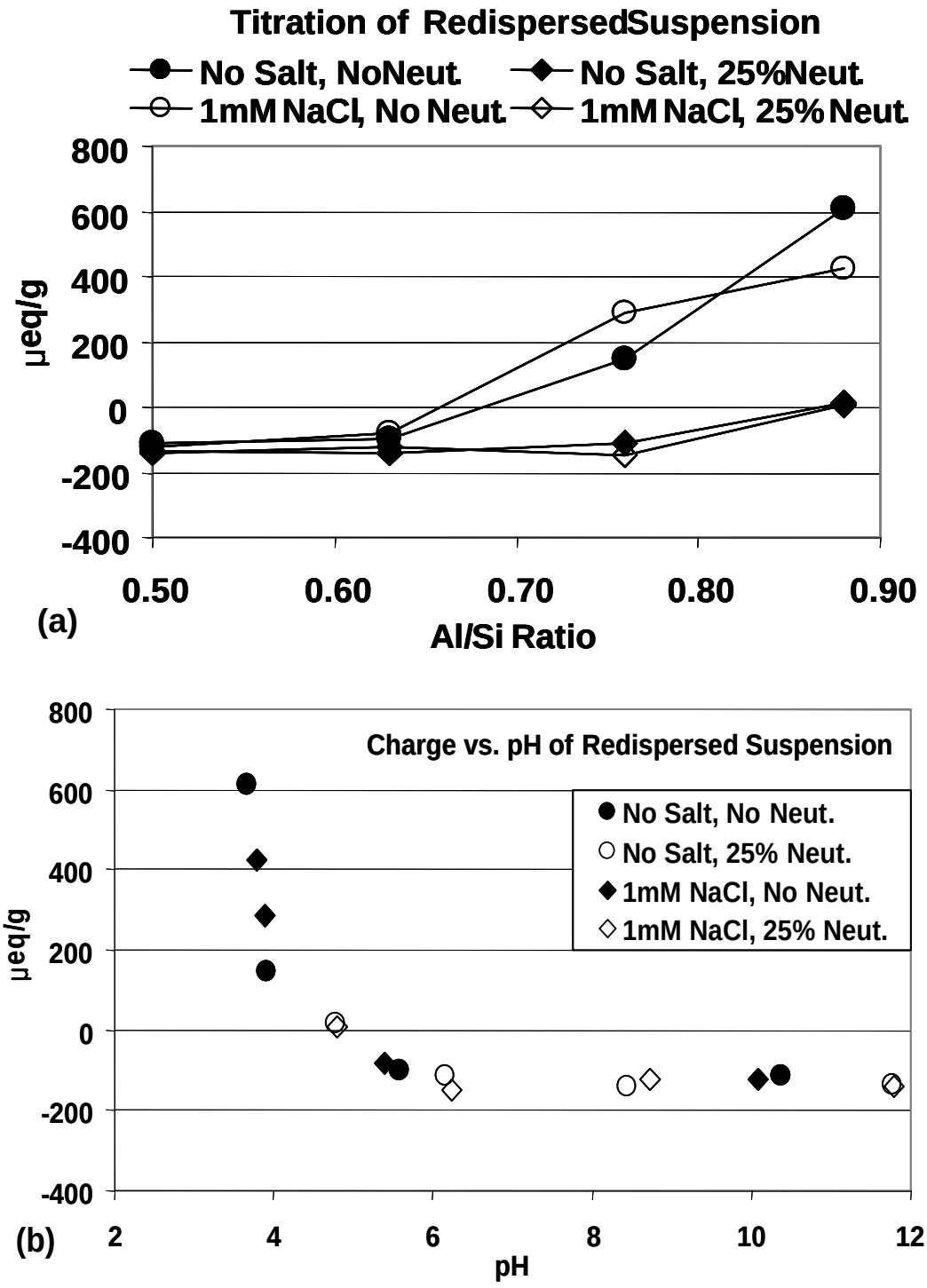

Fig. 4.9. Charge densities of SMM particles; (a) *vs.* Al/Si ratio and (b) *vs*. pH; the ionic species were washed out by centrifuging SMM suspensions and discarding supernatant of SMM suspensions.

Figure 4.9 shows the charge densities of redispersed microparticle suspensions in which the supernatant solution had been replaced by distilled water. By comparing Fig. 4.7 with Fig. 4.9, referring also to Fig. 4.8, it can be concluded that the main factor affecting the charge properties of SMM suspension is not the residual ions in SMM suspension but the surface charges of SMM particles themselves. However, this surface charge of SMM particles can be changed depending on the change of pH and Al/Si ratio. Significant effects of neutralization of $AlCl_3$ during the reaction are clearly evident in Fig. 4.4 (a) and 4.2.1. It is also expected that the increase of Al/Si ratio changes the pH from the basic to the acidic range. It follows that pH is a major factor affecting the change of surface charge properties of SMM microparticles.

An increase in pH promotes aluminum-III hydrolysis and formation of aluminum-based oligomeric ions [26-27]. Hydrolysis also affects charge and surface properties of both silica particles [42-43] and flocculent species [44]. Lartiges *et al.* observed that the same aluminum dosage yields a lower fraction of aluminum, relative to oxygen, in structures formed at pH 8 than at pH 5.5 [30]. Axelos *et al.* and Vigil *et al.* noted the formation of a surface gel layer on precipitated silica at high pH [42-43]. These findings suggest that an enhanced Si/Al reactivity may be responsible for the higher number of aluminosilicate sites found at pH 8 and that deposition of an initial aluminum polymer layer influences the subsequent transfer of other flocculent species to the silica surface. This is explained by a theory of destabilization and neutralization of silica by polymerized aluminum depicted in Fig. 4.10 [30]. Based on this reasoning, the almost neutral flocculent species [44] present at pH = 8 are expected to permit a higher surface coverage of silica particles, giving access to more

reaction sites. Otherwise, the highly charged aluminum polycations [41] repel each other and thus limit aluminum incorporation at pH = 5.

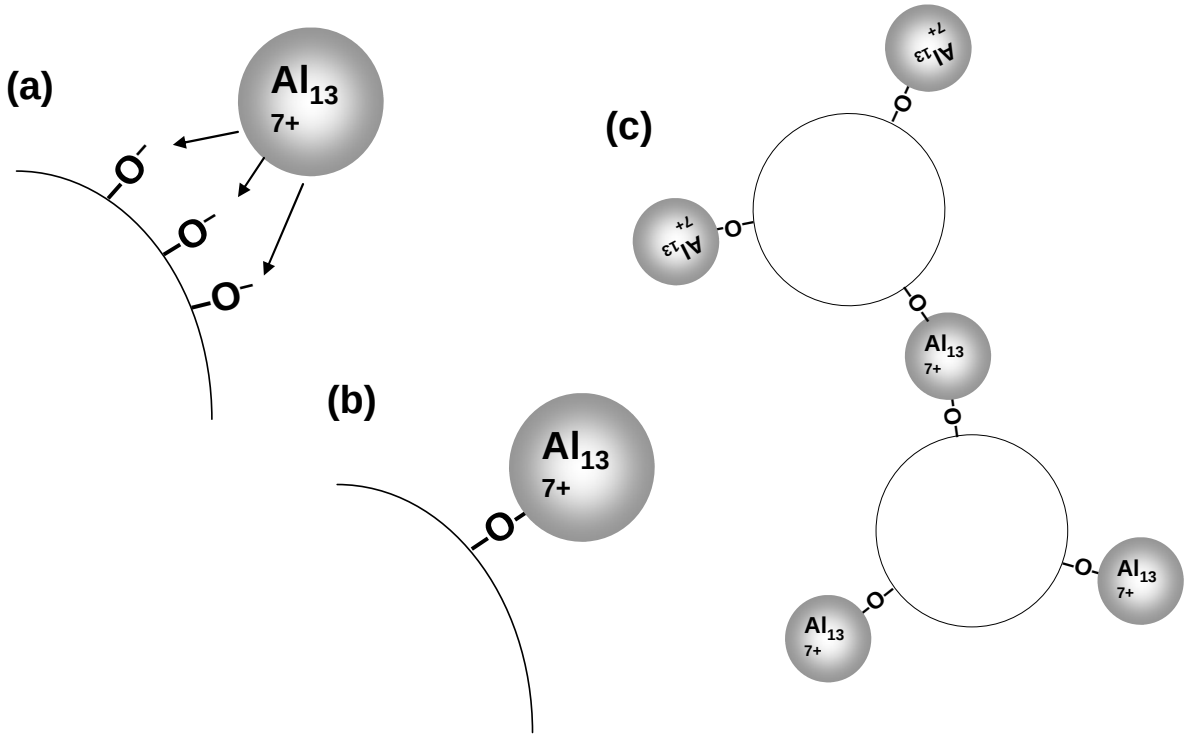

Lartiges, *et al*. *Langmuir 13*(2): 147-152 (1997).

Fig. 4.10. Illustration of the destabilization mechanism of colloidal silica with aluminum polymers: (a) approach of polymeric aluminum cations forms a aluminosilicate site; (b) a negative surface charge is neutralized by cationic charge; (c) residual cationic charge approach and bridge with other silica particles. [30].

These considerations just described help to explain the phenomena in Figs. 4.7, 4.8, and 4.9. Almost neutralized residual aluminum species in the supernatant show slightly negative charges very near to zero at pH values higher than 5. The SMM particles in the redispersed suspension showed lower value of negative charge at higher pH than due to the higher surface coverage of silica particles. There are some critical points where the charges become positive between 4 and 5 in all of Fig. 4.7, 4.8, and 4.9. Increasing Al/Si ratio with the

increase of the amount of $AlCl_3$ solution during synthesis increases the acidity of the SMM suspension system. This acidity is expected to change the charge properties of Al and Si species on the surface of the microparticles.

6. CONCLUSIONS

Streaming current titrations with highly charged polyelectrolytes were used to measure the charge properties of SMM suspensions as a function of the synthetic conditions. The results contribute to a fuller understanding of the interactions among the microparticles, fibers, fiber fines, and cationic polyacrylamide molecules present in papermaking fiber suspension.

Salt addition didn't affect on the charge densities of SMM significantly. This finding is attributed to a sufficient concentration of pre-existing salt, which is produced from the interaction of aluminum chloride and sodium metasilicate during SMM synthesis. Shear rates had a slight effect on the negative change densities of SMM. This effect was tentatively attributed to a breakage of the polymerized flocculation of aluminum ionic species and aluminosilicate at high shear rate (13000 rpm).

The distribution of aluminum ionic species is affected significantly by pH. The change of pH caused by increasing Al/Si ratio with the increase of the amount of $AlCl_3$ solution or by neutralizing Al metal species during synthesis affects the charge properties of SMM particles due to acid-based interactions of Al and Si species on the surface of the microparticles. Furthermore the increased amount of aluminum ionic species with decreasing pH due to the addition of more $AlCl_3$ solution is expected to affect on the formation of ionic site on the

surface of SMM particles. These changes are a consequence of changes in the Al/Si composition ratio in SMM, as well as changes in the surface chemical composition.

7. REFERENCES

1. Hubbe, M. A., "Microparticle Programs for Drainage and Retention", in Rodriguez, Ed., *Micro and Nanoparticles in Papermaking*, Ch. 1, TAPPI Press (2005).

2. Andersson, K., Sandström, A., Ström, K., and Barla, P., "The Use of Cationic Startch and Colloidal Silica to Improve the Drainage Characteristics of Kraft Pulps", *Nordic Pulp and Paper Res. J. 1* (2): 26 (1986).

3. Capozzi, A. M., "Innovations in Microparticle Technology", *PIMA 78* (6): 64 (1996).

4. Drummond, D. K., "Synthetic Mineral Microparticles for Retention Aid Systems", *U.S. Pat. 6,184,258 B1*, Feb. 6. 2001 (filed Feb. 7, 1997).

5. Drummond, D. K., "Synthetic Mineral Microparticles", *U.S. Pat. 5,989,714*, Nov. 23, 1999 (filed May 4, 1998).

6. Drummond, D. K., "Synthetic Mineral Microparticels and Retention Aid and Water Treatment Systems and Methods Using Such Particles", *U.S. Pat. 6,183,650 B1*, Feb. 6, 2001 (filed Oct. 13, 1999).

7. Moffett, R. H., "On-site production of a silica-based microparticulate retention and drainage aid", *TAPPI J. 77* (12): 133-138 (1994).

8. Carroll, S. A., Maxwell, R. S., Bourcier, W., Martin, S., and Hulsey, S., "Evaluation of silica-water surface chemistry using NMR spectroscopy", *Geochimica et Cosmochimica Acta, 66* (6): 913-926 (2002).

9. Milonjić, S.K., "Determination of Surface Ionization and Complexation Constants at Colloidal Silica/Electrolyte Interface", *Colloids and Surface 23*: 301-312 (1987).

10. Parks, G.A., "Isoelectric Points of Solid Oxides, Solid Hydroxides and Aqueous Hydroxo Complex Systems", *Chemical Reviews 65*(2): 177-198 (1965).

11. Bolt, G.H., "Determination of the Charge Density of Silica Sols", *Journal of Physical Chemistry 61*(9): 1166-1169 (1957).

12. Komura, A., Hatsutori K. and Imanaga H., "Acidic and Basic Properties of Silica at Interface with Aqueous-Electrolytes", *Nippon Kagaku Kaishi* (6): 779-784 (1978).

13. Eisenlauer, J. and Killmann, E., "Stability of Colloidal Silica (Aerosil) Hydrolysis: I. Preparation and Characterization of Silica (Aerosil) Hydrolysis", *Journal of Colloid and Interface Science 74*(1): 108-119 (1980).

14. Carroll, S.A., Maxwell, R.S., Bourcier, W., Martin, S. and Hulsey, S., "Evaluation of silica-water surface chemistry using NMR spectroscopy", *Geochimica et Cosmochimica Acta, 66*(6): 913-926 (2002).

15. Sonnefeld, J., Göbel, A. and Vogelsberger, W., "Surface Charge Density on Spherical Silica Particles in Aqueous Alkali Chloride Solutions, Part 1. Experimental Results", *Colloid and Polymer Science 273*(10): 926-931 (1995).

16. Sonnefeld, J., "Surface Charge Density on Spherical Silica Particles in Aqueous Alkali Chloride Solutions, Part 2. Evaluation of the Surface Charge Density Constants", *Colloid and Polymer Science 273*(10): 932-938 (1995).

17. Rodrigues, F.A., Monteiro, P.J.M. and Sposito, G., "The Alkali-Silica Reaction: The Surface Charge Density of Silica and Its Effect on Expansive Pressure", *Cement and Concrete Research 29*: 527-530 (1999).

18. Vogelsberger, W., Löbbus, M., Sonnefeld, J. and Seidel, A., "The Influence of Ionic Strength on the Dissolution Process of Silica", *Colloids and Surfaces A: Physicochemical and Engineering Aspects 159*: 311-319 (1999).

19. Franks, G., "Zeta Potentials and Yield Stresses of Silica Suspensions in Concentrated

Monovalent Electrolytes; Isoelectric Point Shift and Additionsl Attraction", *Journal of Colloid and Interface Science 249*: 44-51 (2002).

20. Cardenas, J.F., "Surface Charge of Silica Determined Using X-ray Photoelectron Spectroscopy", *Colloids and Surfaces A: Physicochem. Eng. Aspects 252*: 213-219 (2005).

21. Haydin, P.L. and Rubin, A.J., "Systematic Investigation of the Hydrolysis and Precipitation of Aluminum(III), in Aqueous-Environmental Chemistry of Metals", *Aqueous-Environmental Chemistry of Metals*, Rubin, A. J., Ed., Ann Arbor Science. Ann Arbor, MI (1976).

22. Akitt, J.W., Greenwood, N.N. and Lester, G.D., "Aluminum-27 Nuclear Magnetic Resonance Studies of Acidic Solutions of Aluminum Salts" *Journal of the Chemical Society A –Inorganic Physical Theoretical*, (5): 803 (1969).

23. Akitt, J.W., Greenwood, W.N., Khandelwal, B.L. and Lester, G.D., "^{27}Al Nuclear Magnetic Resonance Studies of the Hydrolysis and Polymerisation of the Hexa-aquo-aluminium(III) cation. *Journal of the Chemical Society* Dalton: 604-610 (1973).

24. Bottero, J.Y., Porier, J.E. and Fiessinger, F., "Study of Partially Neutralized Aqueous Aluminum Chloride Solutions: Identification of Aluminum Species and Relation between the Composition of the Solutions and Their Efficiency as a Coagulant", *Progress in Water Technology, 1*(1): 601 (1980).

25. Bottero, J.Y. and Fiessinger, F., "Aluminum Chemistry in Aqueous Solution", *Nordic Pulp and Paper Res. J., 4*(2): 81 (1989).

26. Bottero, J. Y., Tchoubar, D., Cases, J. M., Fiessinger F., "Investigation of the Hydrolysis of Aqueous-Solutions of Aluminum-Chloride. 2. Nature and Structure by Small-Angle X-Ray-Scattering", *Journal of Physical Chemistry 86* (18): 3667 (1982).

27. Bottero, J. Y., Cases, J. M., Fiessinger, F., Poirier, J. E., "Studies of Hydrolyzed Aluminum-Chloride Solutions. 1. Nature of Aluminum Species and Composition of

Aqueous-Solutions", *Journal of Physical Chemistry 84* (22): 2933 (1980).

28. Smith, R.W., "Relations among Equilibrium and Nonequilibrium Aqueous Species of Aluminum Hydroxy Complex", *Advances in Chemistry Series, 106*: 250 (1971).

29. Iler, R.K., "The Effect of Surface Aluminosilicate Ions on the Properties of Colloidal Silica", *Journal of Colloid and Interface Science 55*(1): 25-34 (1976).

30. Lartiges, B. S., Bottero, J. Y., Derrendinger, L. S., Humbert, B., Tekely P., and Suty, H., "Flocculation of Colloidal Sililca with Hydrolyzed Aluminum: An ^{27}Al Solid State NMR Investigation", *Langmuir 13* (2): 147-152 (1997).

31. Pinkas, J., "Chemistry of Silicates and Aluminosilicates", *Ceramics-Silikaty 49*(4): 287-298 (2005).

32. Housecroft, C.E. and Sharpe, A.G., *Inorganic Chemistry*, Pearson Education Limited, Essex, England (2001).

33. Bi, S., Wang, C., Cao, Q. and Zhang, C., "Studies on the Mechanism of Hydrolysis and Polymerization of Aluminum Salts in Aqueous Solution: Correlations between the "Core-link" Model and "Cage-like" Keggin-Al_{13} Model", *Coordination Chemistry Reviews 248*: 441-445 (2004).

34. Letterman, R. and Asolekar, S., "Surface-Ionization of Polynuclear Species in Al(III) Hydrolysis – I. Titration Results", *Water Research 24*(8): 931-939 (1990).

35. Letterman, R. and Asolekar, S., "Surface-Ionization of Polynuclear Species in Al(III) Hydrolysis – II. A Conditional Equilibrium-Model", *Water Research 24*(8): 931-939 (1990).

36. Brosset, C., Biedermann, G. and Sillen, L.G., "Studies on the Hydrolysis of Metal Ions. 11. The Aluminum Ion, Al^{3+}", *Acta Chemica Scandinavica 8*(10): 1917-1926 (1954).

37. Mesmer, R.E. and Baes, C.F., "Acidity Measurements at Elevated Temperatures. V.

Aluminum Ion Hydrolysis", *Inorganic Chemistry 10*(10): 2290-2296 (1971).

38. Patterson, J.H. and Tyree, Jr., S.Y., "A Light Scattering Study of the Hydrolytic Polymerization of Aluminum", *Journal of Colloid and Interface Science 43*(2): 389-398 (1973).

39. Stol, R.J., van Helden, A.K. and De Bruyn, P.L., "Hydrolysis-Precipitation Studies of Aluminum(III) Solutions. 2. Kinetic Study and Model", *Journal of Colloid and Interface Science 57*(1): 115-131 (1976).

40. Dentel, S.K., "Application of the Precipitation-Charge Neutralization Model of Coagulation", *Environmental Science and Technology 22*: 825-832 (1988).

41. Zhang, P., Hahn, H.H., Hoffmann, E. and Zeng, G., "Influence of Some Additives to Aluminum Species Distribution in Aluminum Coagulants", *Chemosphere 57*: 1489-1494 (2004).

42. Axelos, M. A. V., Tchoubar, D., Bottero, J. Y., "Small-Angle X-Ray-Scattering Investigation of the Silica Water Interface- Evolution of the Structure with pH", *Langmuir 5* (5): 1186 (1989).

43. Vigil, G., Xu, Z., Steiberg, S., Israelachvili, J., "Interactions of Silica Surfaces", *Journal of Colloid and Interface Science 165* (2): 376 (1994).

44. Furrer, G., Ludwig, C., Schindler, P. W., "On the Chemistry of the Keggin Al^{13} Polymer. 1. Acid-Base Properties", *Journal of Colloid and Interface Science 149* (1): 56 (1992).

45. Iler, R. K., "The Chemistry of Silica – Solubility, Polymerization, Colloid and Surface Properties, and Biochemistry", J. Wiley & Sons, New York (1979).

CHAPTER 5

Net Surface Charge Characteristics of Synthetic Mineral Microparticle Depending on Synthetic Conditions

ABSTRACT

Potentiometric titration was used to analyze the net charge variation of synthetic mineral microparticles (SMM) depending on change of pH in each synthetic condition to predict the charge properties of SMM in the range of pH where paper is produced. Isoelectric pH values, calculated from the data of potentiometric titration, showed high correlation with the pH of synthetic conditions as a power function. In order to understand this relationship, the OH/Al ratio was calculated and compared with the isoelectric pH of SMM. Finally, the relationship between Al/Si ratio and isoelectric pH was estimated through statistical estimation. This procedure permits estimation of the Al/Si ratio values at which the SMM particles can be expected to have a net negative charges, as required for a microparticle system for promotion of retention and dewatering during papermaking.

1. INTRODUCTION

Amorphous aluminosilicate has two kinds of ionic groups on its surface. The first are the surface hydroxyl groups, which are silicate hydr(oxide) [e.g. (≡Si–OH) and (≡Si–O^-)] and aluminum hydroxide groups, [e.g. (≡Al–OH^{2+}) and (≡Al–OH)].

Silicate oxide (≡Si–O^-) in aluminosilicates are not expected to contribute significantly to the surface charge of aluminosilicate under acidic conditions but increase the affect of negative charge source on the surface with increasing pH from 6.8 in alkaline solution at ambient temperature (25℃)[Walther, 1996]. Aluminum oxide tends to have little charge at high pH, where the net charge will be zero. On the other hand, it will have significant positive charge at low pH [Schindler and Stumm, 1987; Huang and Stumm, 1973; Parks, 1965]. As a result of this, Walther assumed that the positive surface charge of an aluminosilicate in a range of acidic pH will be almost completely due to aluminum hydroxide ions (≡Al–OH^{2+}), whereas the negative surface charge at alkaline pH will be on account of the silicate oxide ions (≡Si–O^-) [Walther, 1996].

In 1996, Avena introduced the Si–O–Al group ($SiAlO^-$) as another potential source of negative charge on the surface of amorphous aluminosilicate. This species will be referred to here as the aluminosilicate ion. This group has a negative charge with tetrahedral structure on the surface. As a result of this, proton is bonded to the aluminosilicate ion and it is then available to be exchanged other cations. When sodium ions are present in aqueous solution, the proton starts to be exchanged by these sodium ions with neutralization of the negative charge of aluminosilicate ion (SiAlO-), and the concentration of these exchanged sites increases with increasing pH. After the occurrence of this phenomenon, sodium aluminosilicate oxide (SiAlO-Na+) can not be assessed for cationic exchange [Avena *et al*., 1996]. In addition to these surface charge sources, there is another source of charge, which originates from dissociation of aluminosilicate. Figure 5.1 shows the dissociation of aluminum from aluminosilicate. This dissociation tends to increase with decreasing of pH on

account of high consumption of H_3O^+. This dissolved aluminum ion has a positive charge in aqueous solution, as seen in Fig.5.1.

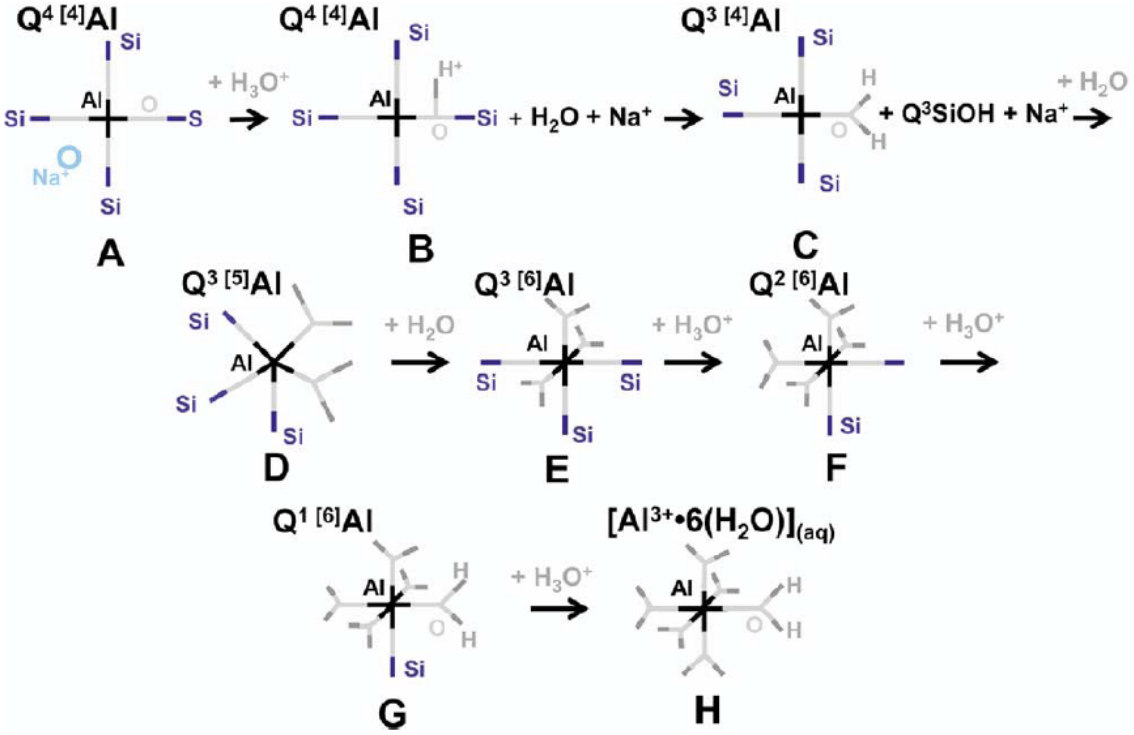

Fig. 5.1. Proposed scheme of dissociation of Al from aluminosilicate; the dissociation tends to increase with decreasing of pH on account of high consumption of H_3O^+ by aluminum containing species [Criscenti *et al.*, 2005].

2. MOTIVATIONS OF PRESENT WORK

As illustrated by the research presented in Chapter 3, synthetic mineral microparticles (SMM), synthesized by adding aluminum chloride as a metal ingredient, showed competent performance as a component of a retention and dewatering program, in comparinson with a system in which bentonite served the role of microparticle. In Chapter 2, the charge densities of SMM, depending on synthetic conditions, were investigated by streaming current measurement. Those results were explained in terms of different pH zones, where different

aluminum species are expected to exist. However, the Al/Si ratio is a much easier factor to control during synthesis of SMM, in comparison to pH, either at a laboratory scale or in a mill application. Additionally, the method of streaming current titration is difficult to apply accurately to the measurement of the charge distribution of SMM with the variation of pH under each synthetic condition. As a result of this thinking, the variations of charge densities of SMM mixtures in each synthetic condition were investigated as a function of pH, within the range 3 to 11, by a potentiometric titration procedure. The relationship between Al/Si ratio and charge density was also analyzed as a control factor for SMM synthesis.

3. EXPERIMENTAL

3.1. Materials

SMM suspensions were synthesized in the manner explained in Chapter 1. The base ingredient was sodium meta-silicate ($Na_2SiO_3 \cdot 5H_2O$) having a molal concentration of 0.445. Aluminum chloride ($AlCl_3$) was used as added metal solution ingredient, using a solution having a 0.566 molal concentration. The synthetic factors constituting this study were as shown in Table 5.1.

Table 5.1. Factors Related to Microparticle Preparation.

Constant	Variables
[Na_2SiO_3]: 0.445 molal solution [$AlCl_3$]: 0.566 molal solution Shear rate: 13,000 rpm.	Al/Si ratios: 0.50, 0.63, 0.76, 0.88, 1.00, 1.14 Neutralization: None *vs*. 25 % with 1 N NaOH

Shear rate and salt content were not varied for this part of the present research, due to the fact that those factors did not significantly affect the charge properties of SMM, as was shown by results of experiments reported in Chapter 4.

3.2. Potentiometric Titration of SMM Suspension

Potentiometric analyses have been used by several scientists in order to titrate the surface charge of colloidal silica, aluminum, and aluminosilicate samples [Bolt, 1957; Escudey *et al*. 1994; Mysen, 2003; Nero, 2004]. After synthesis, SMM suspension was diluted 20 times with water. 50 ml of diluted suspension was placed into a 250 ml beaker. Aliquots of 0.02 ml of 0.1 N NaOH or HCl were added dropwise to the suspension continuously under stirring. Titration was carried out in the range of pH 4 to pH 11. The pH value was recorded at each 0.2 ml drop point. Blank test were performed in same way, with deionized water, to calculate the charge density of SMM.

The charge density (σ) of the SMM suspension at a given pH value was obtained as the difference between the amount of H^+ or OH^- ions added to the suspension, and the amount added to a comparable volume of deionized water using the following equation.

$$\sigma = \frac{1}{S_c}\left(\left[\left[H^+\right]_{blank} - \left[H^+\right]_{consumed}\right] - \left[\left[OH^-\right]_{blank} - \left[OH^-\right]_{consumed}\right]\right) \qquad (1)$$

4. RESULTS AND DICUSSSION

4.1. Potentiometric Titration of SMM Suspension

Fig. 5.2. shows the results of potentiometric titration, based on addition of 0.1N NaOH or HCl to SMM suspensions. There was significant difference between the titration curves for the SMM *vs*. the blank. The differences in the amount of NaOH between the test and the blank are related to the net ionic charge of the SMM, as a function of pH. The differences in consumed NaOH correspond to net positive charge, while differences in consumed HCl amount correspond to net negative charge on the SMM.

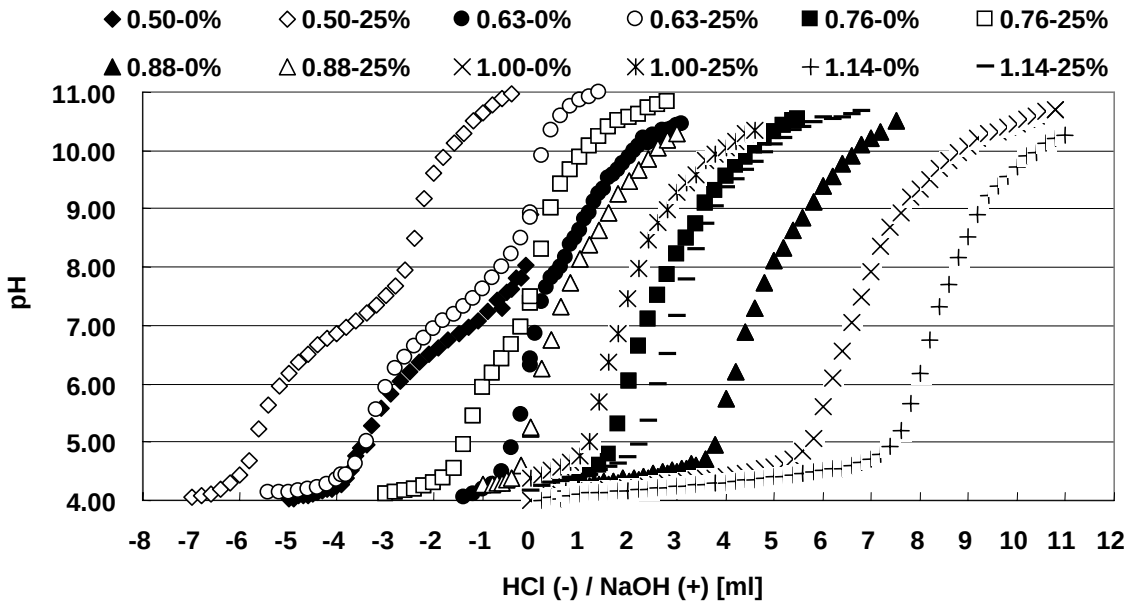

Fig. 5.2. Potentiometric titration of SMM suspensions, based on addition of 0.1N NaOH or HCl; the differences between the titration curves for the SMM *vs*. the blank were used to calculate the net charge densities of SMM suspensions with Eq. (1).

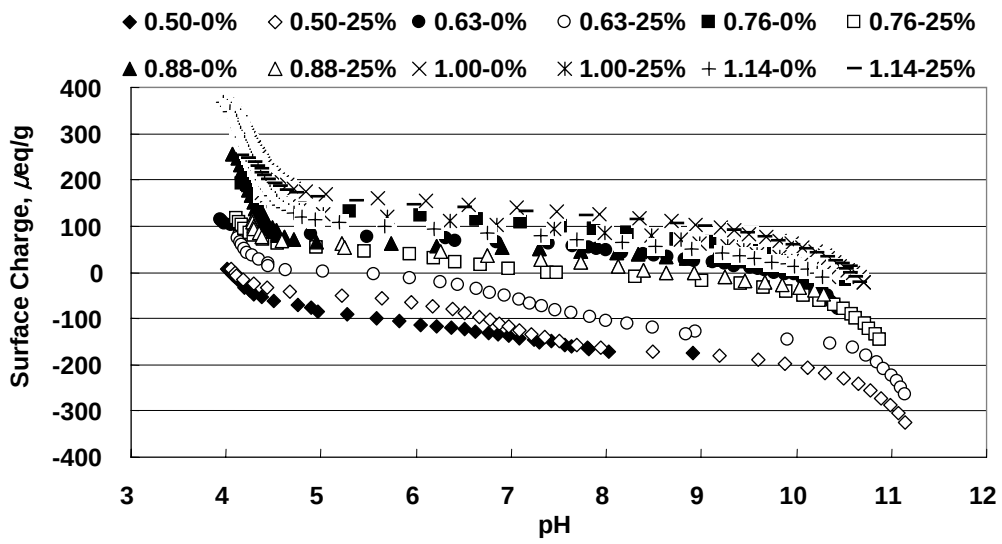

Fig. 5.3. The net charge densities of SMM suspension calculated from the data of potentiometric titration, as depicted in Fig. 5.4.

For the next step in analysis, the differences in amounts of consumed NaOH or HCl for the SMM suspension and blank sample were applied to Equation (1) in order to plot the net charge of the SMM suspension *vs*. pH, as shown in Fig. 5.3. For more detail analysis of data, Fig. 5.3 is divided into Fig. 5.4 and 5.5. As already reviewed in Chapter 4 and the introduction of this chapter, the expected charge sources are silicate oxide ($\equiv SiO^-$), aluminosilicate ion ($SiAlO^-$), aluminum hydroxide ($\equiv Al–OH_2^+$), and aluminum ions, either dissolved from aluminosilicate or remaining associated with solid phases, and capable of reacting with silicate. In case of high pH conditions, charge is expected to originate from silicate oxide groups on the surface of aluminosilicate. However, the charge is expected to come mainly from the surface of aluminosilicate and aluminum ions at lower pH.

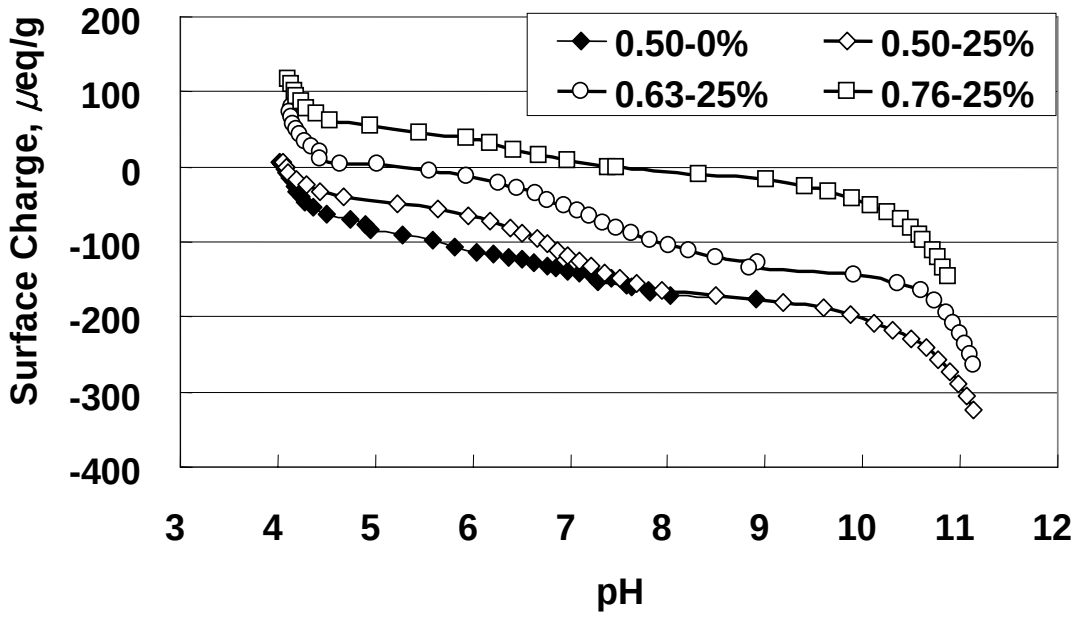

Fig. 5.4. The net charge densities of SMM, synthesized under the conditions in zones I, II, and III, as introduced in Chapter 4.

Fig. 5.4 shows the net charge densities of SMM suspensions, synthesized under the conditions which belong to the zone I, II, and III (5<synthetic pH<12) introduced in Chapter 4. In moderately acidic and alkaline synthetic conditions, SMM suspension showed negative charge, which is expected to originate from silicate oxide (SiO^-) and aluminosilicate oxide ($SiAlO^-$) groups. As assumed in Chapter 4, residual aluminum ions are not expected to exist in SMM suspension under conditions of lower Al/Si ratio (0.50 and 0.63), where the surface charge of SMM suspension also showed highly negative charge densities. In the case of the condition where the Al/Si ratio was 0.76 and aluminum ions were partially neutralized, the observed positive charge, when the value of titration pH is lower than 7.36, is attributed to residual and dissolved aluminum ions as well as aluminum hydroxide ($AlOH_2^+$) on the surface of aluminosilicate.

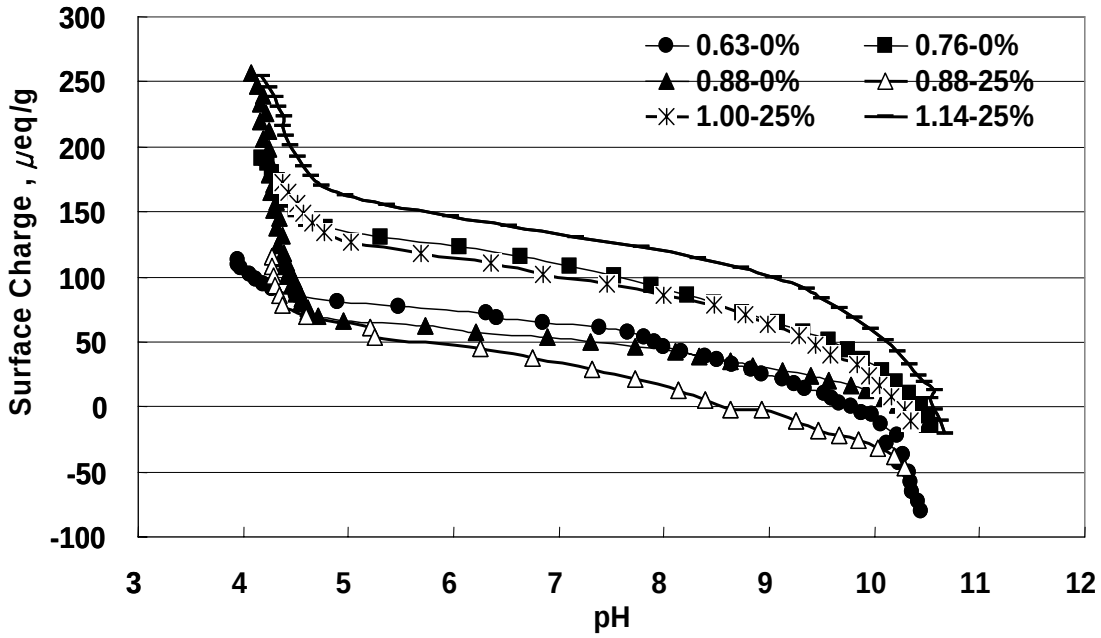

Fig. 5.5. The net charge densities of SMM, synthesized under the conditions in zones IV and V (pH <5), as introduced in Chapter 4.

Fig. 5.5 shows the net charge densities of SMM suspensions that were synthesized under the more acidic conditions (synthetic pH<5). In this region, various aluminum ions, which are mentioned in Chapter 4, are expected to exist within a regime of aqueous conditions under which they can contribute a highly positive charge to SMM suspension. As a comparison of the work of Bi *et al.* [2004] with the NMR results of Bottero *et al.* [1980], this zone should be scrutinized, because different opinions between "Core-link" theory and "Cage-like" theory have been discussed for more than 50 years and not been concluded yet [Bi *et al*., 2004]. Bottero *et al*. [1980] reported that the "Cage-like Keggin-Al_{13}" ($AlO_4Al_{12}(OH)_{24}(H_2O)_{12}^{7+}$), introduced in Chapter 1, was found in the range of pH from 3.5 to 5, by the NMR method. However, Bi *et al.* said that this species was not discovered in aqueous solution with relatively fast rate of reaction during acid titration. Another form, $Al_{13}(OH)_{30}(H_2O)_{18}^{9+}$, which is consistent with the "Core-link" theory, is the main species

during rapid reaction and the "Keggin-Al_{13}" is expected to be the self-assembled form from $Al_{13}(OH)_{30}(H_2O)_{18}^{9+}$ through a long time of aging. As a result of this consideration, this pH zone can be divided into two-pH ranges, from 3.5 to 4.1 and from 4.1 to 5. As was shown in Fig. 4.3 of Chapter 4, two conditions (Al/Si=0.63; non-neutralization; pH=4.9 and Al/Si=0.88; 25 % neutralization; pH=4.5) belong to the later pH range. In this condition, the monomeric aluminum ions start to be polymerized by "Core-link" theory; therefore the total positive charge is decreased by the condensation of aluminum ions. As a result of this, those two conditions showed lower charge densities than others.

4.2. Isoelectric Point *vs*. Al/Si Ratio

Table 5.2 shows the isoelectric point of SMM suspension as a result of the titration. Figure 5.6 shows the relationship between isoelectric point and Al/Si ratio. However, it is difficult to forecast the proper Al/Si ratio that will make it possible to obtain an optimum negative net charge of SMM for retention and drainage, with the isoelectric point as shown in Fig. 5.6.

Table 5.2. pH of synthetic conditions and isoelectric point of SMM measured by potentiometric titration.

Non-Neutralization			25 % Neutralization		
Al/Si ratio	Isoelectric Point, pH	pH of Synthetic Condition	Al/Si ratio	Isoelectric Point, pH	pH of Synthetic Condition
0.50	4.03	9.41	0.50	4.06	11.71
0.63	9.66	4.44	0.63	5.20	7.96
0.76	10.45	3.66	0.76	7.36	5.84
0.88	10.26	3.51	0.88	8.56	4.28
1.00	10.58	3.32	1.00	10.26	3.77
1.14	10.20	3.27	1.14	10.56	3.71

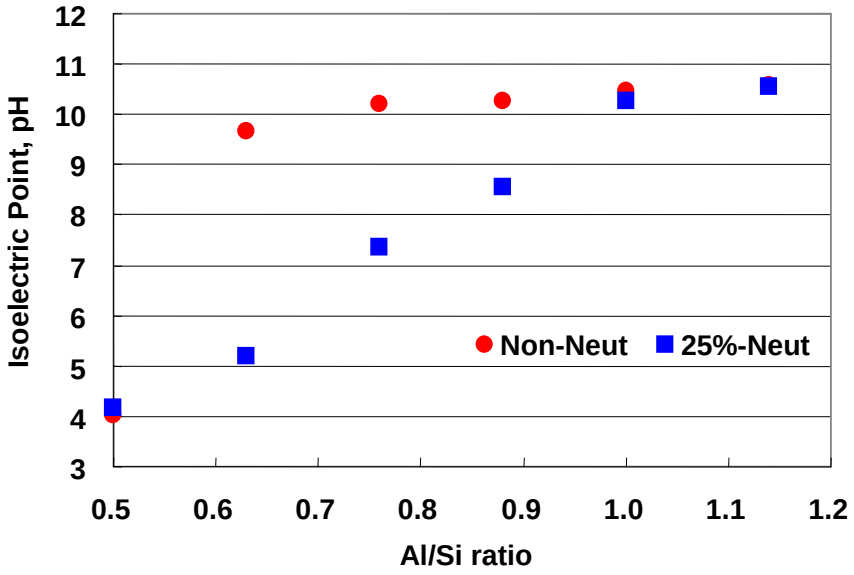

Fig. 5.6. The relationship between isoelectric point of SMM suspension and Al/Si ratio, as depicted in Table 5.2.

In the previous chapter it was concluded that pH can be used as a major factor to control the charge property of SMM particles. Additionally, the behavior of aluminum ionic species has a strong relationship with the ratio of alkalinity and aluminum concentration. As a result of these considerations, the OH/Al ratio was calculated by a simple assumption of following steps in the reaction:

(1) In aluminum chloride solutions, hydrochloric acid is expected by following chemical equation:

$AlCl_3 + 3H_2O \rightarrow Al(OH)_3 + 3HCl$.

With this simple equation, the expected molar concentration of total proton would be $[H+] = 3[AlCl_3]$.

(2) In a solution of sodium metasilicate, sodium hydroxide is expected by following chemical equation:

$Na_2SiO_3 + 5H_2O \rightarrow 2NaOH + Si(OH)_4 + 2\ H_2O$

With this simple equation, the expected molar concentration of total hydroxide ion would be

$[OH^-] = 2[Na_2SiO_3] + 3n\cdot[AlCl_3]$, for the condition of partial-neutralization of Al^{3+} ions, where n is the extent of partial neutralization of Al^{3+} ions. In case of non-neutalization, $n = 0$ and $n = 0.25$ for 25 %..

(3) Therefore, the expected molar concentration of residual alkalinity is

$[OH^-]_{normal} = [OH^-] - [H^+]$

(4) OH/Al ratio = $[OH\ ]_{normal} / [Al^{3+}]$, with the assumption of $[Al^{3+}] = [AlCl_3]$.

in these steps, the term in brackets [ ] means the molar concentration of each chemical component.

The calculated OH/Al ratio was identified with the isoelectric point of SMM suspension in Fig. 5.7. Those two factors showed very strong correlation by statistical linear regression. The relationship between OH/Al ratio and Al/Si ratio can be expressed by following equation.

$$\text{Al/Si ratio} = \frac{2}{\text{OH/Al ratio} - 3(n-1)} \qquad (2)$$

where n is rate of partial neutralization of aluminum ion.

Through the relationship between the Al/Si ratio and OH/Al ratio, the relationship between isoelectric point of SMM suspension and Al/Si ratio was estimated in Fig. 5.8. The conditions belonging to the left-hand area of estimated lines will be expected to produce negatively charged SMM

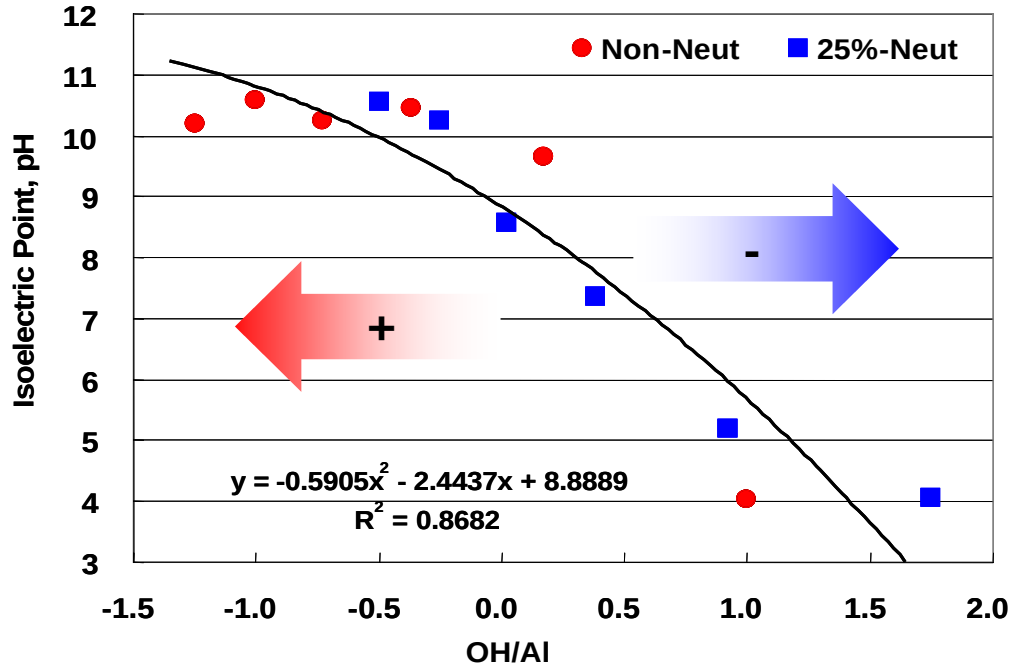

Fig. 5.7. OH/Al ratio *vs*. isoelectric point of SMM suspension; arrows show the expected charged properties of SMM suspensions, synthesized under the conditions belonging to each area, divided by the correlation line.

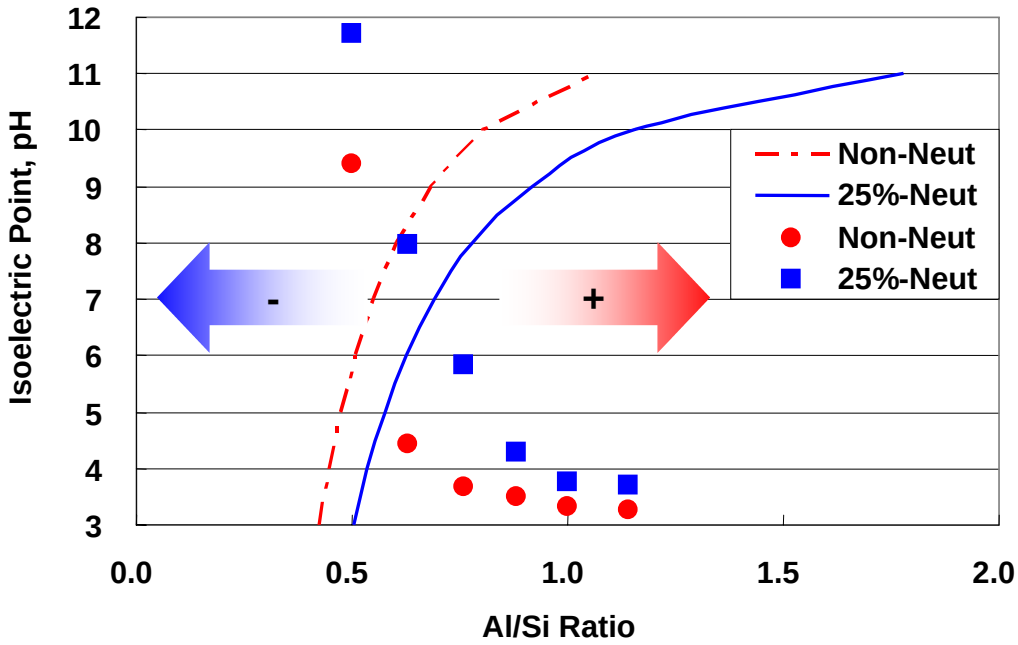

Fig. 5.8. Al/Si ratio *vs*. isoelectric point calculated from OH/Al ratio, depending on condition of neutralization: line - estimated isoelectric point depending on Al/Si ratio; squares and circles - the pH values of synthetic conditions *vs*. Al/Si ratio.

5. CONCLUSIONS

The net charge properties of SMM were investigated by potentiometric titration, in order to understand the relationship between the surface charge behavior and the ionic species that are expected to be on the surface of SMM particles, as discussed in Chapter 4.

Through the concept of pH zone division, the charge behavior was explained. SMM suspensions, synthesized under the alkaline and moderately acidic conditions with low Al/Si ratio (0.50 and 0.63), showed strong negative net charge, due to the silicate oxide ions and aluminosilicate ions on the surface of SMM particles. The strong acid condition with high Al/Si ratio produced SMM suspensions that showed strong positive charge, due to the residual and dissolved aluminum ions. The positive charge of SMM suspension was expected to decrease through the polymerization of aluminum ions following Core-link phenomena.

For the measurement of the isoelectric point of SMM suspensions, a concept based on the OH/Al ratio with neutralization constant *n*, was introduced to reanalyze the Al/Si ratio as a control factor for synthesis of negatively charged SMM particles.

6. REFERENCES

Avena, M.J., and De Pauli, C.P. (1996). "Modeling the Interfacial Properties of an Amorphous Aluminosilicate Dispersed in Aqueous NaCl Solution", *Colloids and Surfaces A: Physicochemical and Engineering Aspects 118*: 75-87

Bi, S., Wang, C., Cao, Q. and Zhang, C. (2004). "Studies on the Mechanism of Hydrolysis and Polymerization of Aluminum Salts in Aqueous Solution: Correlations between the "Core-link" Model and "Cage-like" Keggin-Al_{13} Model", *Coordination Chemistry Reviews 248*: 441-445.

Bolt, G.H. (1957). "Determination of the Charge Density of Silica Sols", *Journal of Physical Chemistry 61* (9): 1166-1169.

Bottero, J.Y., Porier, J.E. and Fiessinger, F. (1980). "Study of Partially Neutralized Aqueous Aluminum Chloride Solutions: Identification of Aluminum Species and Relation between the Composition of the Solutions and Their Efficiency as a Coagulant", *Progress in Water Technology, 1*(1): 601.

Criscenti, L.J., Brantley, S.L., Mueller, K.T., Tsomata, N., and Kubicki, J.D. (2005). "Theoretical and ^{27}Al CPMAS NMR Investigation of Aluminum Coordination Change during Aluminosilicate Dissolution", *Geochimica et Cosmochimica Acta 69* (9): 2205-2220

Escudey, M. and Galindo, G. (1994). "Net Surface Charge Characteristics of Allophane and Synthetic Aluminosilicates", *BOLETIN DE LA SOCIEDAD CHILENA DE QUIMICA 39* (1): 63-70.

Huang, C.P., and Stumm, W. (1973). "Specific Adsorption of Cations on Hydrous α-Al_2O_3", *Journal of Colloid and Interface Science 22*: 231-259.

Mysen, B. (2003). “Physics and Chemistry of Silicate Glasses and Melts”, *European Journal of Mineralogy 15* (5): 781-802.

Nero, M.D., Assada, A., Madé, B., Barillon, R., and Duplâtre, G. (2004). “Surface Charge and Np(V) Sorption on Amorphous Al and Fe silicates”, *Chemical Geology 211*: 15-45.

Parks, G.A. (1965). “The Isoelectric Points of Solids, Solid Hydroxides, and Aqueous Hydroxo Complex Systems”, *Chemical Review 65* : 117-198.

Schindler P.W., and Stumm, W. (1987). “The Surface Chemistry of Oxides, Hydroxides and Oxide Minerals”, in Stumm, W., editor, *Aquatic Chemical Kinetics*, New York, John Wiley & Sons: 83-110.

Tsuchida, H., Ooi, S., Nakaishi, K. and Adachi, Y. (2005). “Effects of pH and ionic strength on electrokinetic properties of imogolite”, *Colloid and Surface A: Physicochem. Eng. Aspects 265*: 131-134.

Walther, J. (1996). “Relation between Rates of Aluminosilicate Mineral Dissolution, pH, Temperature, and Surface Charge”, *American Journal of Science 296*: 693-718.

Yokoyama, T., Ueda, A., Kato, K., Mogi, K., and Matsuo, S. (2002). “A Study of the Alumina-Silica Gel Adsorbent for the Removal of Silicic Acid from Geothermal Water: Increase in Adsorption Capacity of the Adsorbed due to Formation of Amorphous Aluminosilicate by Adsorption of Silicic Acid”, *Journal of Colloid and Interface Science 252*: 1-5.

CHAPTER 6

Morphologies of Synthetic Mineral Microparticles for Papermaking as a Function of Synthetic Conditions

ABSTRACT

As was introduced in Chapter 1, the gel form of a microparticle additive, as depicted in Fig. 1.1, performed better than sol form, in terms of fine-particle retention during papermaking. For this reason it was of interest to investigate the morphological behavior of synthetic mineral microparticles (SMM) as a function of the conditions of synthesis. BET nitrogen adsorption was used to measure the surface area of SMM. The distribution of SMM particle size was investigated in the aqueous state, using a patented light-scattering technique. The coagulation behavior and morphology of SMM were analyzed using scanning electron microscopy (SEM). It was found that the structural characteristics of SMM particles could be explained in terms of the effects of ionic charges on colloidal stability of primary particles during formation of the SMM.

1. INTRODUCTION

1.1. Coagulation

When mineral particles are dispersed in aqueous solution, electrostatic repulsion often is the major force to stabilize the system against coagulation. If the particles have a sufficiently high density of electrical charge at the surface, which may be either negative or positive, the

electrostatic force can overcome the attraction of van der Waals' forces and prevent aggregation [Jiang *et al*., 1998].

On the other hand, a positively charged ion, e.g. an aluminum or ferric ion, can neutralize the negatively charged surface of colloidal particle and make the particles aggregate as flocs. The effectiveness of ions as coagulants of oppositely charged particles in suspension is know to increase with increasing valence. There is critical coagulation concentration (CCC) which refers the lowest concentration of a certain ion coagulating a suspended colloidal particle which has an opposite net charge [Tezak *et al.* 1951].

1.2. Coagulation with Aluminum Ions

There are two major factors that affect to the coagulation rate of a suspension of negatively charged particles in the presence of aluminum ions, i.e. coagulant dosage and the pH. It is believed that increasing the dosage of aluminum ionic coagulant leads to the increase of coagulation, due to neutralizing the surface charges of coagulated particles [Matijević, *et al.* 1961; Jiang *et al.*,1998]. This phenomenon can be restated by the destabilization mechanism [Latiges *et al.* 1997]. As depicted in Fig, 4.10, Chapter 4, the adsorption of polymeric aluminum cations on the surface of colloidal silica forms an aluminosilicate site at which a negative surface charge is neutralized by the cationic charge of the coagulant. Then, the residual cationic charge of this adsorbed polymeric aluminum cation is able to form a complex involving an aluminum cation and silica anions adsorbed onto the negatively charged surface of other silica particles.

Matijević, *et al.* [1961] demonstrated the restabilization of a coagulated suspension, as a function of increasing dosage of an aluminum coagulant. They observed that the turbidity of the sol reached to a maximum and then dropped dramatically with increasing the dosage of aluminum coagulant. At first, the adsorption of counter-ions, such as sodium ions, onto the surface of silica and stabilizes the surface charge with a slight degree of coagulation, which increases the effective size of suspended particles, reaching a size of maximum effectiveness for the scattering of light, and resulting in a high turbidity number. Then, increasing the amount of aluminum coagulant neutralizes the surface charge of the particles of colloidal silica, bringing about extensive coagulation, and decreasing the efficiency of light scattering. Further adsorption of aluminum ions is expected to reverse the surface charge of silica particles, and then restabilize colloidal silica particles with opposite charge.

Dentel [1988] assumed that the total charge of counter-ions in the diffuse layer about a coagulated particle is the sum of two component diffuse layer charges. Based on this assumption, they calculated "Zero-Electrophoretic Mobility" lines, based on the assumption that there are two idealized ways in which aluminum hydroxide species can deposit onto colloidal particles. On the one hand, the size of aluminum hydroxide species or particles may be much larger than the dimension of the electric double layer of a colloidal particle. On the other hand, the aluminum species may be much smaller than the dimensions of the electric double layer. Based on these considerations, they presented a coagulation map of $Al(NO_3)_3$ and some kinds of commercial colloidal silica suspensions, as depicted in Fig. 6.1. This result matched well with their calculated "Zero-Electrophoretic Mobility" and the previous work done by Brace *et al.* [1977].

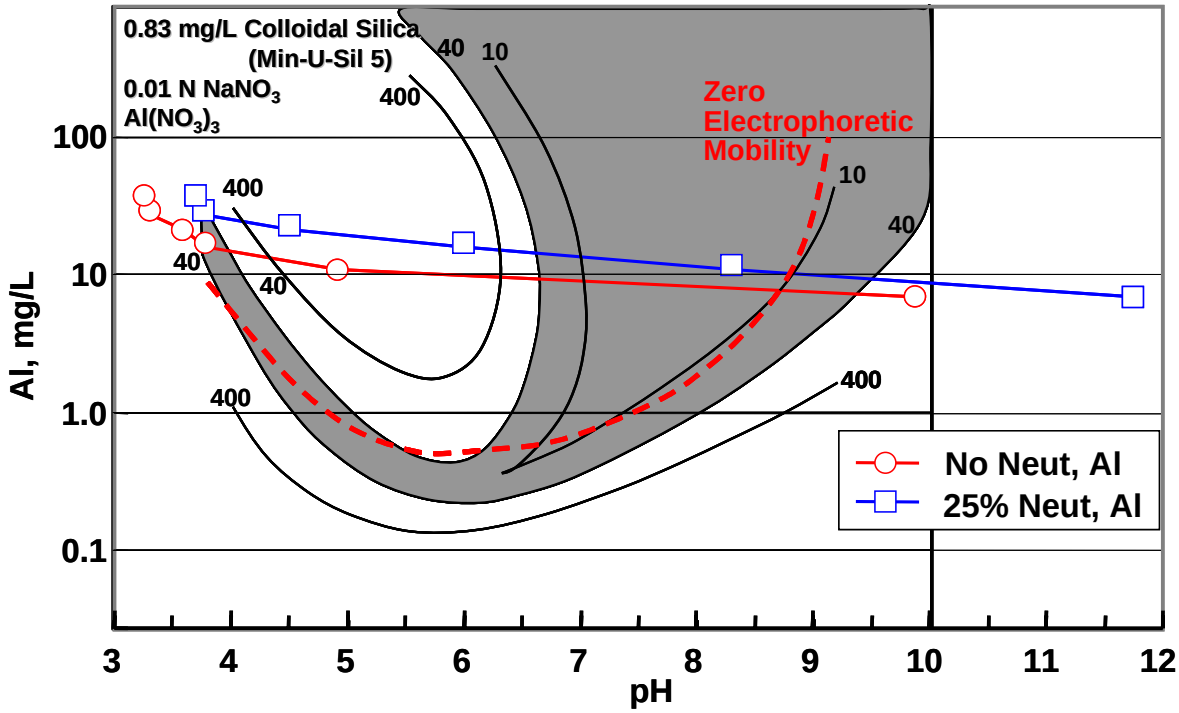

Dentel, *Envionmental Science and Technolgy 22* : 825-832 (1998)

Fig. 6.1. A scheme of precipitation and charge neutralization model; Numbers of each lines show the result of turbidity test. Gray area is where the coagulation occurred on account of "Zero Electrophoretic Mobility", caused by the charge neutralization between residual or dissolved aluminum ions and still negatively charged silanol group. Blank squares and circles were drawn by Lee. S.Y. to compare with the SMM synthetic conditions of Al amounts and pH.

Katsanis *et al*. [1983] presented evidence suggesting that the effectiveness of HNO_3 with respect to aggregation and precipitation of aluminum from aluminosilicate is similar with HCl. This statement can be used as justification to employ Dentel's figure [1988] to the case of $AlCl_3$. They also said that, within a pH range from 2.2 to 2.8, aluminum ions were dissolved from the surface of aluminosilicate. The electric mobility of aluminum hydroxide was positive at very low pH (2.83) and increased with increasing pH to 4.32 in case of HNO_3.

2. MOTIVATIONS OF PRESENT WORK

As discussed in Section 1.6, Chapter 1, the effectiveness of a microparticle in a term of fine-particle retention depends on it's structure. As shown in Fig. 1.8, the highly structured gel form of colloidal silica, as depicted in Fig. 1.8, performed better than the sol form. Due to the wide variation of aluminum ionic species, depending on pH, a variety of morphological properties of SMM can be expected. Variables that control the morphology are expected to include the Al/Si ratio, the pH, and the OH/Al ratio. For this reason, the morphological behavior of synthetic mineral microparticles (SMM) was investigated to find the optimum synthetic conditions for high performance as part of a microparticle retention aid system.

3. EXPERIMENTAL

3.1. Materials

SMM suspensions were synthesized in a manner consistent with the patents [Drummond, 1999, 2001a,b]. Sodium meta-silicate ($Na_2SiO_3 \cdot 5H_2O$) was used as the base ingredient, with 0.445 molal concentration. The added metal solution ingredient was 0.566 molal aluminum chloride ($AlCl_3$). The synthetic factors constituting this study were as shown in Table 6.1. The percent neutralization was defined as the ratio of added NaOH to $AlCl_3$, on a molar equivalent basis, noting that aluminum is tri-valent and the hydroxyl ion is monovalent.

Table 6.1. Factors Related to Microparticle Preparation.

Constant	Variables
[Na_2SiO_3]: 0.445 molal solution [$AlCl_3$]: 0.566 molal solution Shear rate: 13,000 rpm.	Al/Si ratios: 0.50, 0.63, 0.76, 0.88, 1.00 Neutralization: None *vs*. 25 % with 1 N NaOH

3.2. Specific Surface Area of SMM

Prepared SMM samples were diluted 10 times based on mass and freeze-dried in order to prevent the collapse of pore structure of SMM. After that, the freeze-dried samples were placed in U-shape tubes of the type used for measurement of surface area by BET nitrogen adsorption. The tubes were placed in an oven over night to dry out the moisture more completely, and then transferred into a desiccator. Both ends of the U-tube were clamped into the clipping cell. The tube was placed into the external tube of nitrogen, with preheating at 110 °C for 15 min. The preheated tube was connected in the circulation of nitrogen gas to measure the specific surface area (m^2/g).

3.3. Particle Size Distribution of SMM with Laser Scattering Technique

Each prepared sample was directly added to the water chamber of a Beckman Coulter LS230 laser diffraction analyzer, using the patented PIDS technology. The sample was added gradually until the PIDS obscuration became within the range from 45 to 55 %, at which point the analysis was carried out.

3.4. Morphology of Microparticles by Means of Scanning Electron Microscopy

Synthesized microparticle suspensions were diluted 50 times with deionized water to investigate the morphology of aggregated structures under conditions more similar to real usage. Diluted suspensions were dropped onto the surface of mica and dried in a vacuum dryer overnight. Finally, the top surface was coated with gold and placed in a field emission scanning electron microscope (FE-SEM: JEOL 6400F Field Emission SEM). Resulting micrographs are provided in the Appendix.

4. RESULTS AND DISCUSSION

It is known that the mechanism of formation of crystalline aluminosilicate species, as depicted in Fig. 6.2, requires an aluminosilicate gel structure with the ratio Al/Si < 0.5 [Davidovits, 1991]. As a result of this, an amorphous sodium aluminosilicate gel structure, as depicted in Fig. 6.3, is expected to exist in SMM suspension at ambient temperature. As shown in Fig 6.3, captured water of hydration is expected to accompany the sodium ion within the amorphous structure [Hos *et al.*, 2002]

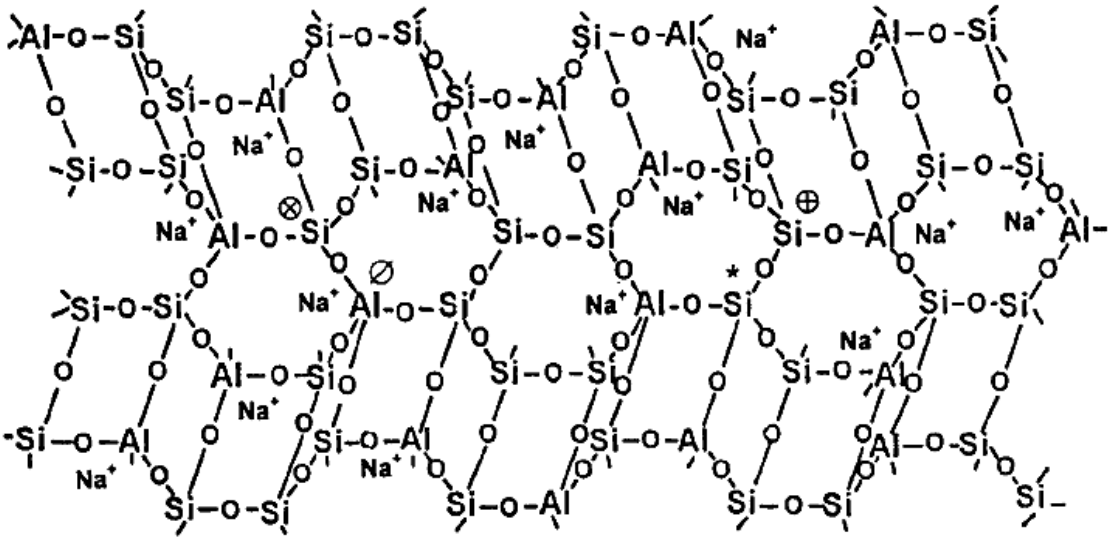

Fig. 6.2. Scheme of 3-dimensional framework structure having crystalline, based on a suggested model for K-polysialate polymer: ⊗, Si-3Al; *, Si-2Al; ⊕, Si-Al; ⊘, Al-4Si [Davi dovits, 1991].

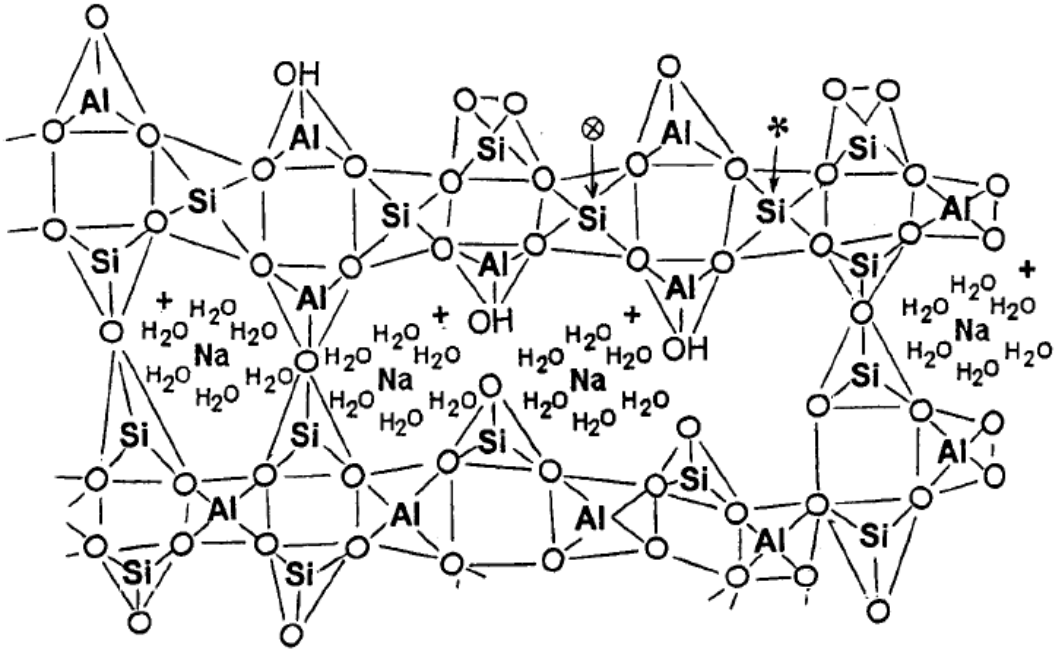

Fig. 6.3. Scheme of amorphous structure for sodium-aluminosilicate polymer; sodium ions are expected to exist with the captured water within the amorphous structure: ⊗, Si-3Al; *, Si-2Al; ⊕, Si-Al; ⊘, Al-4Si [Barbosa, 2000].

4.1. Surface Area of SMM

Figure 6.4 shows the relationship between the surface area of SMM and the Al/Si ratio. As was explained in Chapter 5, two key variables that are expected to affect SMM charge properties are the OH/Al ratio and the pH. These two variables are expected to govern the speciation and behavior of aluminum ions, highly depending on pH and the amount of added alkalinity. However, it is inherently difficult to explain the correlation between these factors and the resulting morphology of SMM products.

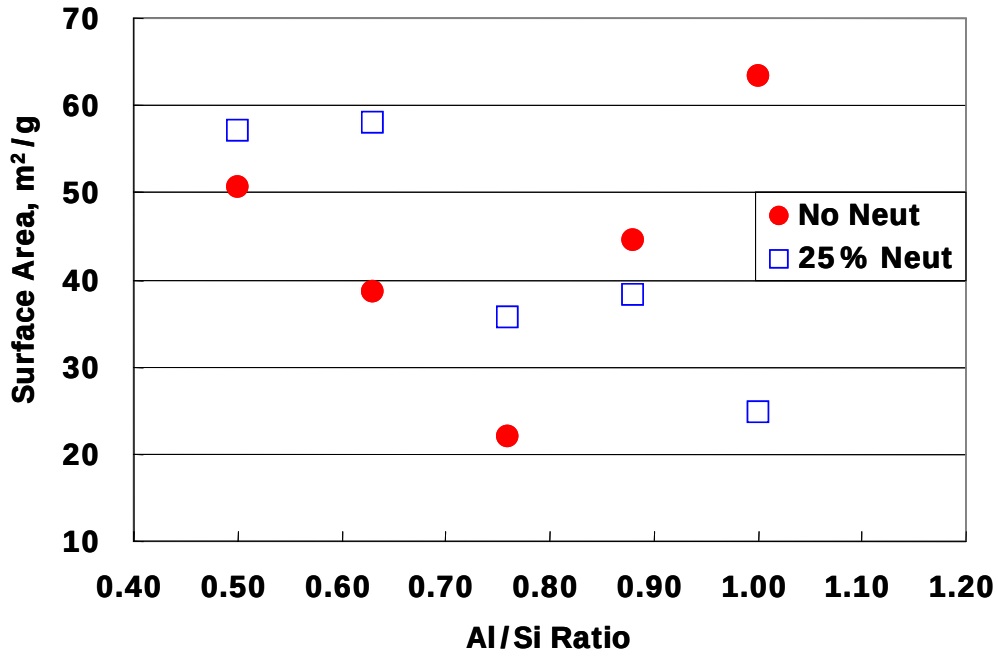

Fig. 6.4. The relationship between the surface area and the Al/Si ratio.

The data for surface area were replotted as a function of pH and OH/Al ratio, as depicted in Fig. 6.5. The results plotted in this manner showed a strong relationship. As already

mentioned at the beginning of this discussion, SMM particles are expected to have an amorphous polymeric structure. Under alkaline synthetic conditions, the base ingredient, SiO_3^{2-} is easily converted to $Si(OH)_4$ and starts to condense with silica oxide ($\equiv$Si-O$^-$) or aluminum hydroxide ($Al(OH)_3$).

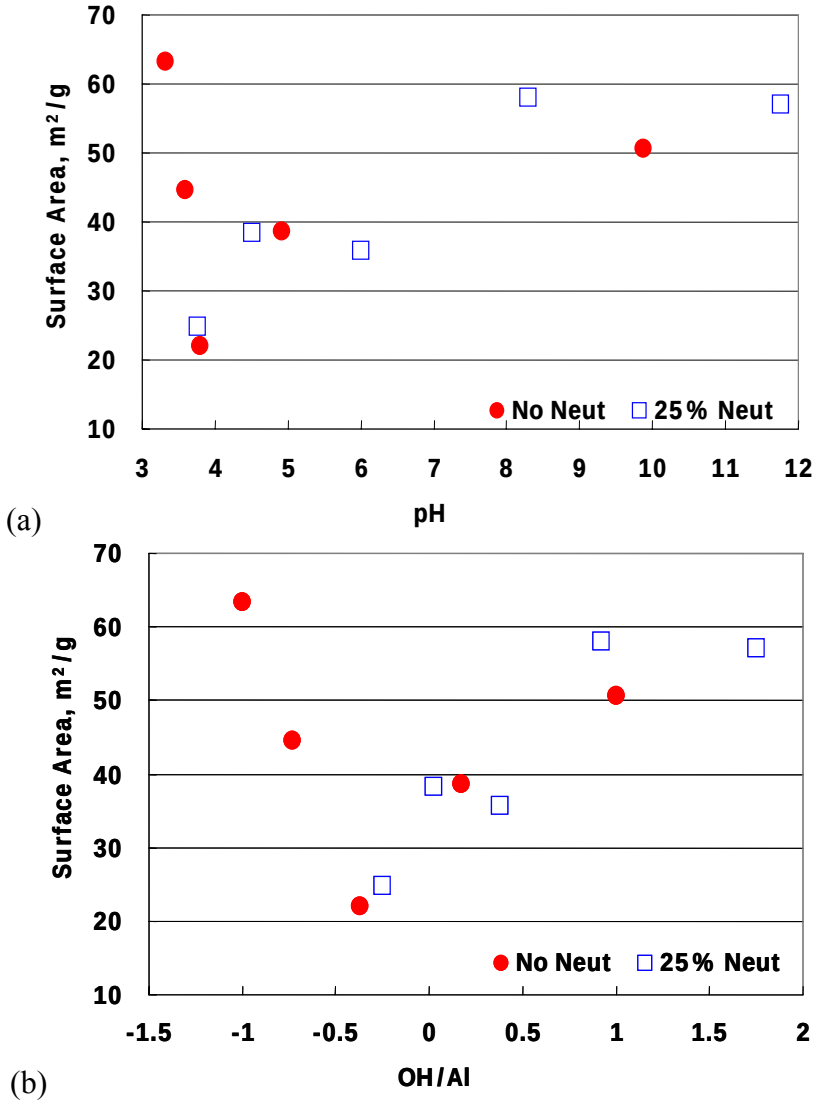

Fig. 6.5. Surface Area of SMM particles *vs*. (a) pH and (b) OH/Al; as discussed in Chapter 5, these two variables showed strong relationships with SMM charge properties and showed also very strong relationships with surface area of SMM particles.

During this condensation reaction, the amorphous aluminosilicate is expected to have a nano-porous structure, as shown in Figs. A.5, A.8, and A.19 in the Appendix. This explains why the SMM that was synthesized under conditions of low Al/Si ratio and alkaline pH had a high value of surface area.

In a range of 3<pH<5, there are several things that deserve to be pointed out, as already discussed in Chapters 4 and 5. First, several aluminum ionic species are expected to exist as a monomeric or lowly polymerized form at pH lower than 3.5. These aluminum ions are either a residual from the synthetic reaction of SMM or they are dissolved from amorphous aluminosilicate due to the highly acidic conditions. Additionally, these ions have highly positive charge. Silicate oxide ions are expected still to have a slight negative charge, but it is near to neutral because of proximity to the isoelectric point of silica. As a result of this, the net charge of the SMM suspension showed highly positive character, as already witnessed in Chapters 4 and 5. This means that the particles in this pH range tend to become disperses in suspension. In addition, the condensation between $Si(OH)_4$ and aluminum hydroxide ions is weaker than one of high pH condition. Thereby, the condensated primary particles are expected to be small. Considering these factors explained the high surface area.

In the case of pH conditions higher than 3.5, highly polynuclear aluminum ionic species exist with lower positive charge. The isoelectric point of SMM particles in suspension is expected to be between 4 and 5, based on the results of streaming current titrations reported in Chapter 4. Additionally, the positive polynuclear aluminum ions are expected to approach and destabilize the surface negative charge of aluminosilicate, as already explained in the destabilization and neutralization model in Chapter 5. As a result of these considerations,

coagulation of the system by aluminum ions is expected to occur in this pH range. Furthermore, the residual or dissolved aluminum ions can be polymerized, according to the "core-link" theory. These aluminum ionic polymers are expected to have a denser structure, in comparison to amorphous aluminosilicate. This phenomenon was confirmed by comparing Figs. A.5, A.8, A.19, A.20, A.24, A.30, A.37, and A40 in the Appendix.

4.2. Particle Size Distribution of SMM

Laser scattering measurements of particle size distributions give information of three types: volume fraction, number fraction, and surface area fraction. As shown in Fig. 6.6, the volume fraction tends to exaggerate the contribution of large particles in the size distribution. Likewise, the number fraction tends to exaggerate the contribution of the small particles to the size distribution. Because the present study involves interactions at surfaces, the surface area fraction will be emphasized in the discussion that follows.

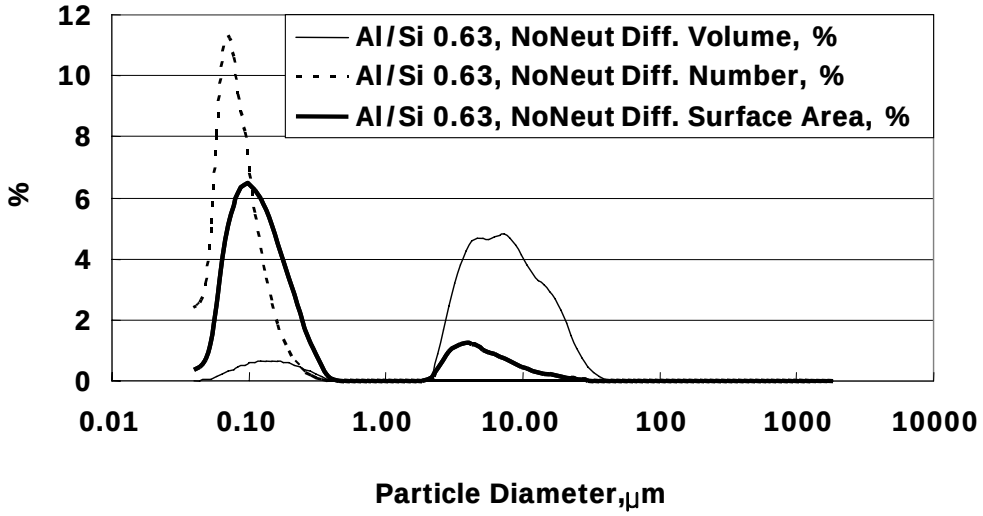

Fig. 6.6. Differences among the three fractions; volume, number and surface area %.

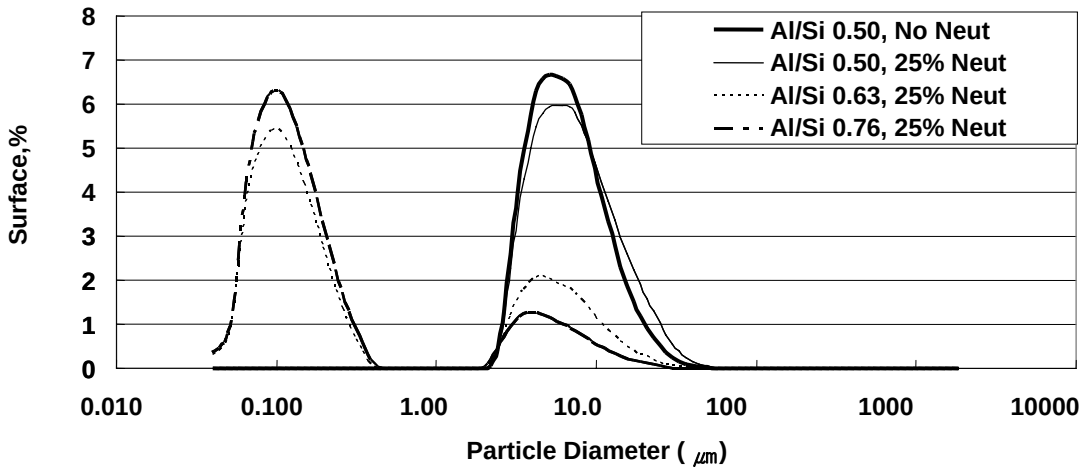

Fig. 6.7. Particle size distributions of SMM synthesized under the conditions in zones I, II, and III, as described in Chapter 4.

In Fig. 6.7, the first two conditions showed that neutralization tends to increase the polymerization of aluminosilicate. In the conditions which have Al/Si =0.50, no residual aluminum ions are expected. Adding sodium hydroxide increases the activity of Na^+ and promotes the condensation reaction between silicate and aluminum hydroxide anions, which resulted in highly polymerized amorphous aluminosilicate. Referring to the two sets of results corresponding to a neutralized condition at Al/Si=0.50, the contribution of larger particles, having a modal size between 10 micron to 100 micron, was increased.

When the Al/Si ratio increased from 0.50 to 7.6 under the same 25 % neutralized conditions, the proportion of large polymerized particles decreased, with an increase of small particles. Under these conditions, the increased amount of aluminum species is consumed for the condensation reaction. As a results of this, more of the aluminosilicate oxide anion, $(Si\text{-}O\text{-}Al)^-$ is expected to exist in amorphous aluminosilicate particles. Under alkaline conditions,

the sodium ion tends to adsorb on this aluminosilicate oxide ion, bringing along its water of hydration. As a result of this, this site tends to become less accessible for the condensation to take place. Therefore, the polymerization rate is decreased. This consideration explains why the high Al/Si conditions produced smaller particles in zone II and III (5<pH<10).

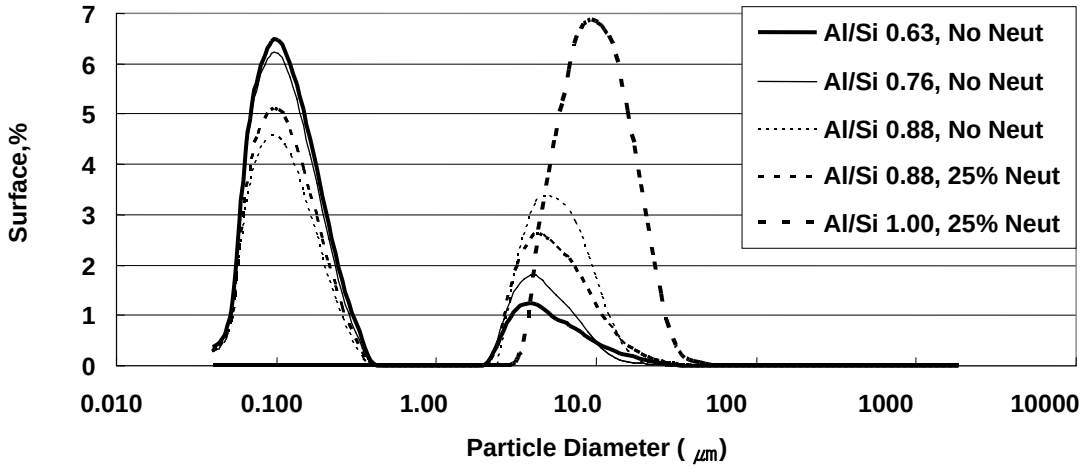

Fig. 6.8. Particle size distributions of SMM synthesized under the conditions in zone IV, as described in Chapter 4.

With increasing Al/Si ratio, a higher concentration of aluminum ionic species is expected to occur in the aqueous phase of SMM suspension. These ionic species can start to act as a coagulant as already explained in the previous section. This explains why the large floc distribution increased again according to the increase of Al/Si ration in zone IV and V as depicted is Fig. 6.8. At some point, where the net charge reaches zero, *i.e.* the point of zero electrophoretic mobility, very large flocs are formed. After this point, the distribution of large floc decreased again, as shown in Fig. 6.9.

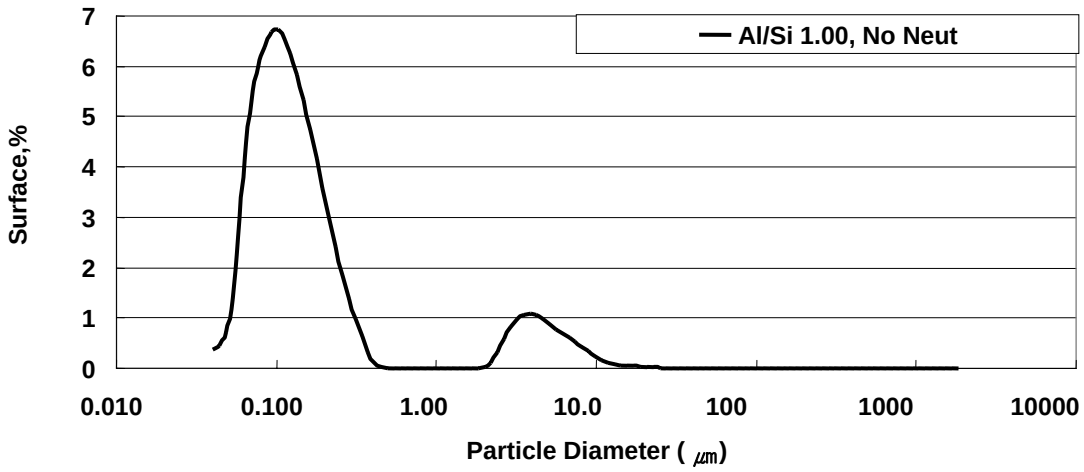

Fig. 6.9. Particle size distributions of SMM synthesized under the conditions in zone V, as described in Chapter 4.

5. CONCLUSIONS

It is necessary to consider several factors, taken together, in order to account for the surface areas and distribution of particle sizes of SMM products. The coagulation map for aluminum chloride and silica is complicated, having a multi-dimensional structure. Under neutral to slightly alkaline conditions, most of the morphological effects appear to be controlled by the Al/Si ratio, together with the amount of Si, and the salt concentration caused by neutralization.

From neutral pH to a moderately acidic pH, the Al/Si ratio appears to be a controlling variable, because of the occurrence of positively charged polymerized aluminum ions. In the very acidic range, monomeric and low-polymerized aluminum species need to be considered, together with destabilization and neutralization concepts, including conditions leading to coagulation.

6. REFERENCES

Barbosa, V.F.F., MacKenzie, K.J.D., and Thaumaturgo, C. (2000). "Synthesis and Characterization of Material Based on Inorganic Polymers of Alumina and Silica: Sodium Polysialate Polymers", *International Journal of Inorganic Materials 2* : 309-317.

Brace, R., and Matijević, E. (1977). "Coprecipitation of Silica with Aluminum Hydroxide", *Colloid and Polymer Science 255* : 153-160.

Criscenti, L.J., Brantley, S.L., Mueller, K.T., Tsomaia, N., and Kubicki, J.D. (2005). "Theoretical and ^{27}Al CPMAS NMR Investigation of Aluminum Coordination Charges during Aluminosilicate Dissolution", *Geochimica et Cosmochimica Acta 69* (9): 2205-2220.

Davidovits, J. (1989). "Geopolyers and Geopolymeric Materials", *Journal of Thermal Analysis 35*: 429-441.

Davidovits, J. (1991). "GEOPOLYMERS – Inorganic Polymeric New Materials", *Journal of Thermal Analysis 37*: 1633-1656.

Dentel S.K. (1988). "Application of the Precipitation-Charge Neutralization Model of Coagulation", *Environmental Science and Technology 22* : 825-832.

Drummond, D. K. (2001a). "Synthetic Mineral Microparticles for Retention Aid Systems", *U.S. Pat. 6,184,258 B1*, (filed Feb. 7, 1997).

Drummond, D. K. (1999). "Synthetic Mineral Microparticles", *U.S. Pat. 5,989,714*, (filed May 4, 1998).

Drummond, D. K. (2001b). "Synthetic Mineral Microparticels and Retention Aid and Water Treatment Systems and Methods Using Such Particles", *U.S. Pat. 6,183,650 B1*, (filed Oct. 13, 1999).

Gao, B., Yue, Q., and Wang, B. (2004). "Coagulation Efficiency and Residual Aluminum Content of Polyaluminum Silicate Chloride in Water Treatment", *Acta Hydrochimica et Hydrobiologica 32* (2): 125-130.

Gao, B.Y., Yue, Q.Y., Wang, B.J., and Chu, Y.B. (2003). "Poly-Aluminum-Silicate-Chloride (PASiC) – A New Type of Composite Inorganic Polymer Coagulant", *Colloids and Surfaces A: Physicochem. Eng. Aspects 229*: 121-127.

Hos, J.P., McCormick, P.G., and Byrne, L.T. (2002). "Investigation of a Synthetic Aluminosilicate Inorganic Polymer", *Journal of Materials Science 37*: 2311-2316.

Hubbe, M. A., "Microparticle Programs for Drainage and Retention", in Rodriguez, Ed., *Micro and Nanoparticles in Papermaking*, Ch. 1, TAPPI Press (2005).

Iler, R. K., "The Chemistry of Silica – Solubility, Polymerization, Colloid and Surface Properties, and Biochemistry", J. Wiley & Sons, New York (1979).

Jiang, J.-Q., and Graham, N. (1998). "Clearly Cleaner", *Chemistry in Britain 34* (3): 38-

Katsanis, E.P., and Matijević, E. (1983) "Properties of Aluminated Silica Sols[1]", *Colloid & Polymer Science 261*: 255-264.

Matijević, E., Mathai, K.G., Ottewill, R.H., and Kerker, M. (1961). "Detection of Metal Ion Hydrolysis by Coagulation. III Aluminum", *Journal of Physical Chemisty 65* (5): 826-830.

Provatas, A., and Matisons, J.G. (1997). "Silsesquioxanes: Synthesis and Applications", *Trends in Polymer Science 5* (10): 327-332.

Tezak, B., Matijević, E.J., and Schulz, K. (1951). "Coagulation of Hydrphobic Sols in-Statu-Nascendi 2. Effect of Concentration of the Sol and of the Stabilizing Ion on the Coagulation of Silver Chloride, Silver Bromide, and Silver Iodide", *Journal of Physical and Colloidal Chemistry 55* (9): 1567-1576

Yokoyama, T., Ueda, A., Kato, K., Mogi, K., and Matsuo, S. (2002). “A Study of the Alumina-Silica Gel Adsorbent for the Removal of Silicic Acid from Geothermal Water: Increase in Adsorption Capacity of the Adsorbent due to Formation of Amorphous Aluminosilicate by Adsorption of Silicic Acid”, *Journal of Colloidal and Interface Science 252*: 1-5.

CHAPTER 7

Summary of Conclusions

In summary, this thesis research has documented how various synthetic factors affect the properties of synthetic mineral microparticles (SMM) as a retention and drainage system. The primary focus was on the analysis of charge properties of SMM, using streaming current and potentiometric titration. Other methods were used to provide the information related to the morphological properties of SMM. The relationship between charge properties of SMM and controlling factors, such as the Al/Si ratio, partial neutralization of metallic ingredients, shear rate, and salt were analyzed. The isoelectric point of SMM suspension was evaluated, in conjunction with potentiometric titration. The relationship between the isoelectric points of SMM suspensions and the Al/Si ratio was estimated by statistical regression. Morphological properties of SMM were investigated to understand the relationship between physical properties and the performance of SMM in terms of retention and drainage.

In order to confirm the efficacy of synthetic mineral microparticles (SMM) when used in combination with a cationic polyacrylamide treatment of papermaking furnish, turbidity and gravity drainage time were measured, using a Britt-Jar test with representative SMM formulations, covering a wide range of compositions. An iron silicate showed the highest retention performance, as well as suitably fast drainage time relative to other metal silicate versions of SMM, as well as bentonite. Zinc silicate improved retention and drainage. SMM synthesized from aluminum sulfate ($Al_2(SO_4)_3$) did not show favorable benefits in retention and drainage, relative to bentonite. SMM synthesized from aluminum chloride ($AlCl_3$)

performed better in drainage and retention than bentonite when the Al/Si ratios were 0.76 and 1.00. However, zinc chloride, ferric chloride, and aluminum sulfate have SO_4^{2+}, Zn^{2+}, and Fe^{3+}, which are not welcomed by papermakers, due to environmental concerns. For these reasons, $AlCl_3$ was selected for the next series of studies as the major metal species to synthesize SMM suspensions. However, it was found that when the Al/Si ratio and neutralization are considered, the results of turbidity measurement and dewatering speed varied significantly. Therefore, pH variation due to the change of Al/Si ratio was expected to be a key factor to control the efficacy of SMM by changing the size of primary metal silicate particles and the degree of coagulation of the primary particles.

In order to understand the interactions among the microparticles, fibers, fiber fines, and cationic polyacrylamide molecules present in papermaking fiber suspension, streaming current titration and potentiometric titration method were employed.

Streaming current titrations with highly charged polyelectrolytes were used to measure the charge properties of SMM suspensions, SMM particles, and residual ionic species in SMM suspensions, as a function of the synthetic conditions. Salt addition didn't affect on the charge densities of SMM significantly. This finding was attributed to the presense of pre-existing salt, which is produced from the interaction of aluminum chloride and sodium metasilicate during SMM synthesis. Shear rates had a slight effect on the negative change densities of SMM.

The distribution of aluminum ionic species is affected significantly by pH, especially at within a lower range ($3<pH<5$). The change of pH caused by increasing Al/Si ratio or by

neutralizing Al metal species prior to synthesis, affects the charge properties of SMM particles due to acid-based interactions of Al and Si species on the surface of the microparticles. In order to understand this interaction, pH was divided into five different pH zones. In zones I and II, relatively high amounts of Si species gave a negative charge on SMM suspensions under high pH conditions. From zone III to V, the increased amount of aluminum ionic species with decreasing pH, due to the increase of Al/Si ratio, is expected to produce cationic sites on the surface of SMM particles. As a result of this, highly positive charge was observed in SMM suspensions as well as on the surfaces of SMM particles.

The net charge properties of SMM were investigated by potentiometric titration, in order to understand the relationship between the net charge behavior and the ionic species that were expected to be on the surface of SMM particles by streaming current method. Through the concept of pH zone division, the charge behavior was explained. SMM suspensions, synthesized under the alkaline and moderately acidic conditions with low Al/Si ratio (0.50 and 0.63), showed strongly negative net charge, due to the silicate oxide ions and aluminosilicate ions on the surface of SMM particles. The strong acid condition with high Al/Si ratio produced SMM suspensions that showed strong positive charge, due to the residual and dissolved aluminum ions. The positive charge of SMM suspension was expected to decrease through the polymerization of aluminum ions following “core-link” phenomena.

For the measurement of the isoelectric point of SMM suspensions, a concept based on the OH/Al ratio with neutralization constant *n*, was introduced to reanalyze the Al/Si ratio as a control factor for synthesis of negatively charged SMM particles.

Based on the usual understanding that the gel form of a microparticle additive performs better than sol form, in terms of fine-particle retention during papermaking, the morphological behavior of SMM was investigated as a function of the conditions of synthesis. BET nitrogen adsorption was used to measure the surface area of SMM. The distribution of SMM particle size was investigated in the aqueous state, using a patented light-scattering technique. The coagulation behavior and morphology of SMM were analyzed using scanning electron microscopy (SEM).

In order to account for the surface areas and distribution of particle sizes of SMM products, several factors were considered together. Under neutral to slightly alkaline conditions, most of the morphological effects appear to be controlled by the Al/Si ratio, together with the amount of Si, and the salt concentration caused by neutralization. In particular, the SMM that was synthesized at a ratio of Al/Si = 0.50 showed high relative surface area, in spite of large particle size, owing to the expected nano-porous structure in amorphous aluminosilicate. From neutral pH to a moderately acidic pH, the Al/Si ratio appears to be a controlling variable, because of the occurrence of positively charged polymerized aluminum ions. In the very acidic range, monomeric and low-polymerized aluminum species need to be considered, together with destabilization and neutralization concepts, including conditions leading to coagulation.

Finally, a series of conditions, which were Al/Si=0.63, 0.76, 0.88, with 25 % neutralization of the aluminum ion and Al/Si=0.63 with non-neutralization of aluminum ions, could be expected as the most optimal conditions to synthesize SMM in this study. Criteria for judging optimum performance factors of microparticles as a retention and drainage system

during papermaking included negatively charged surface, small particle size, and large surface area. These factors make sense in terms of the proposed molecular mechanisms. For the more general SMM synthesis, moderate pH condition (from 5 to 8), relatively low Al/Si ratio (from 0.63 to 0.88), and partial neutralization of Al species into the range of OH/Al ratio between 0 to 1 are suggested.

CHAPTER 8

Proposed Future Research

This dissertation focused on various synthetic conditional factors affecting the charge and morphology of synthetic mineral microparticles (SMM). Some unique findings of the present study appear to be prime areas of future research. There are both practical and theoretical aspects that are worth of further investigation.

Practical Aspects:

Many of the results from the present work have potential to be applied in practical situations, such as a system to promote retention and drainage rate during papermaking, or as a coagulant system to treat recycled water. However, the aqueous environments found in the common practice of several industries may be much more complicated in terms of the presence of varieties of inorganic ions and polymeric materials. The present work mainly concentrated on the charge and morphology of the synthesized particles. Therefore, a series of research is necessary to apply SMM products under realistic conditions of papermaking. In order to applySMM as a retention and drainage aid, it is proposed to investigate the reaction between cationic polyelectrolyte and SMM synthesized under the conditions suggested in the Conclusion section. Also, the positively charged SMM products, which were synthesized at high Al/Si ratio, can be considered as a coagulant system for water treatment, as well as for partical blocking adsorption sites, during optimization of a high-mass cationic retention aid in papermaking.

Theoretical Aspects:

The variation of aluminum ionic species and different behaviors of silica ions are elucidated in this work. However, the chemical composition of SMM solids, depending on synthetic conditions, was not investigated. As already introduced, nuclear magnetic resonance (NMR) and X-ray photoelectron spectroscopy have been widely used to elucidate the chemical composition of aluminosilicate, with high potential for accurate determination of both bulk and surface characteristics. It is proposed to use these techniques to elucidate the relationship between the chemical composition of SMM and synthetic conditions. The results of this proposed work can be used to model the charge properties and coagulation behavior of SMM under a certain condition.

SMM products are expected to be affected by aging, because the amorphous aluminosilicate tends to crystallized by aging, depending on changes of temperature. The expected residual aluminum species also have a various polymerization routes, depending on aging and pH conditions. Therefore, it is also proposed to investigate the morphological behavior and the change of charge properties of SMM depending on aging time.

APPENDIX

A. Pictures by Field Emission Scanning Electron Microscopy

SMM particels are synthesized in a manner of synthesizing method, dectated in Chapter 1.

Synthetic Condition Factors: Al/Si ratio / Neutralization / Shear Rate / Status of Sample

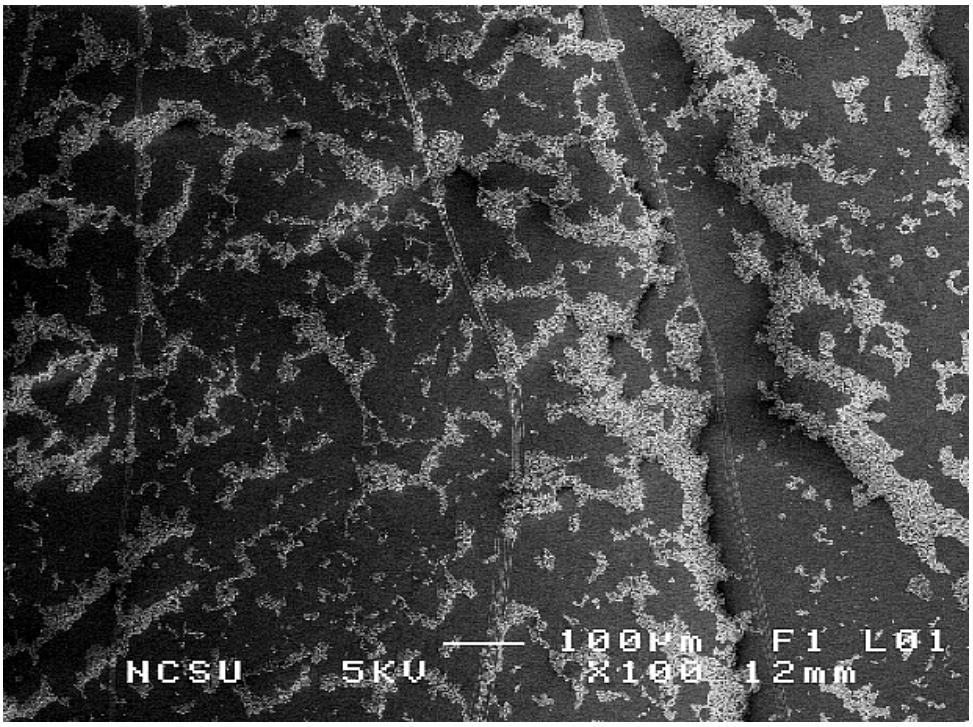

Fig.A.1. 0.50 / non / 13000 rpm / 50 times diluted.

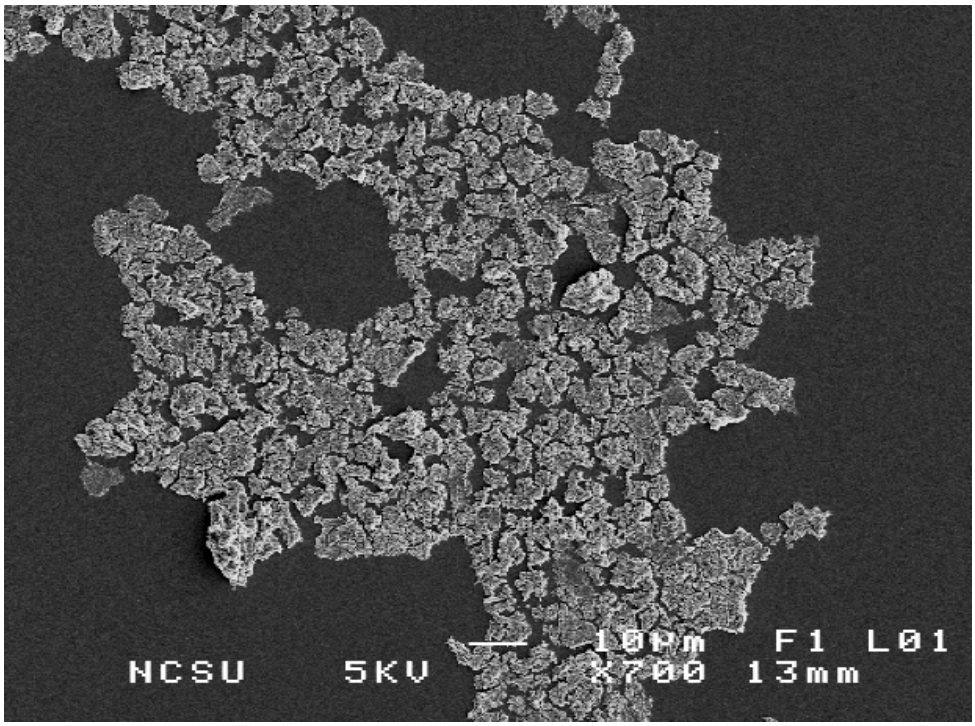

Fig.A.2. 0.50 / non / 13000 rpm / 50 times diluted.

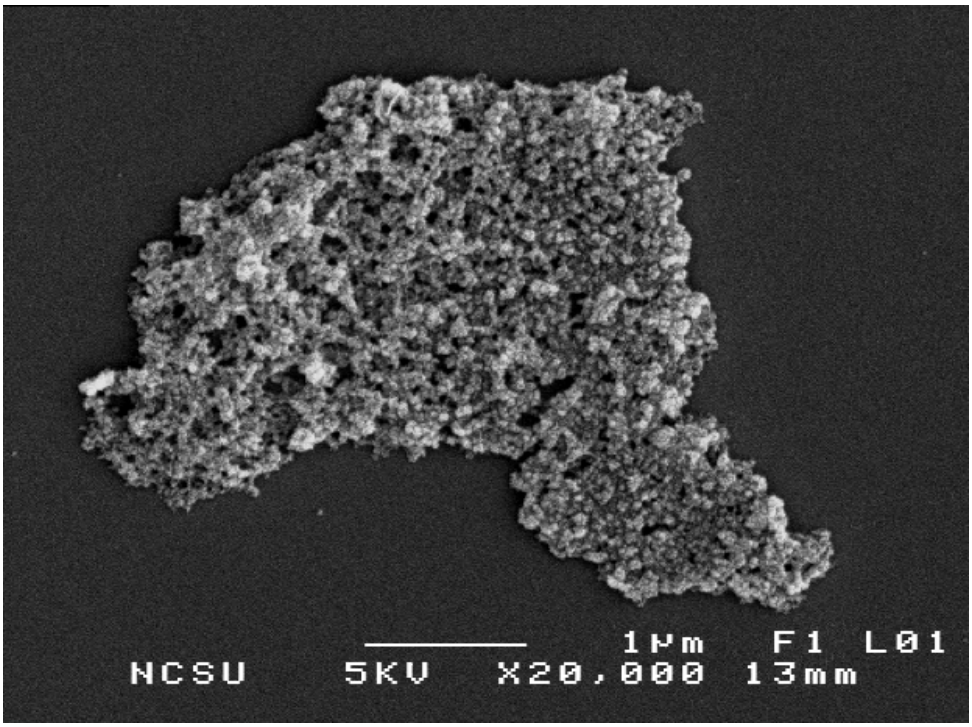

Fig.A.3. 0.50 / non / 13000 rpm / 50 times diluted.

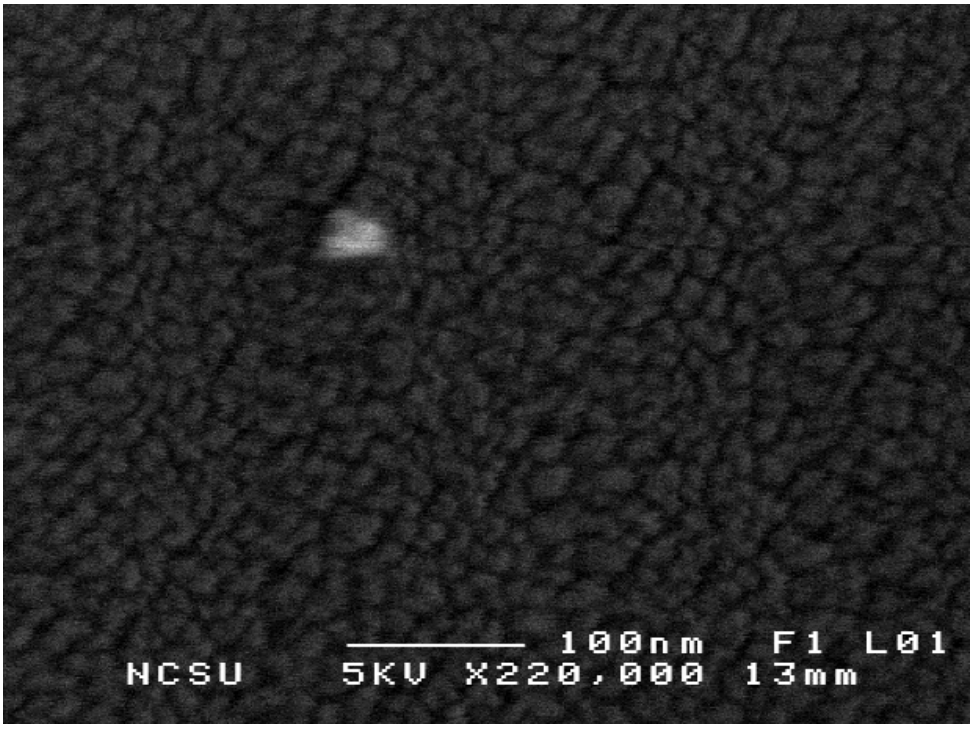

Fig.A.4. 0.50 / non / 13000 rpm / 50 times diluted.

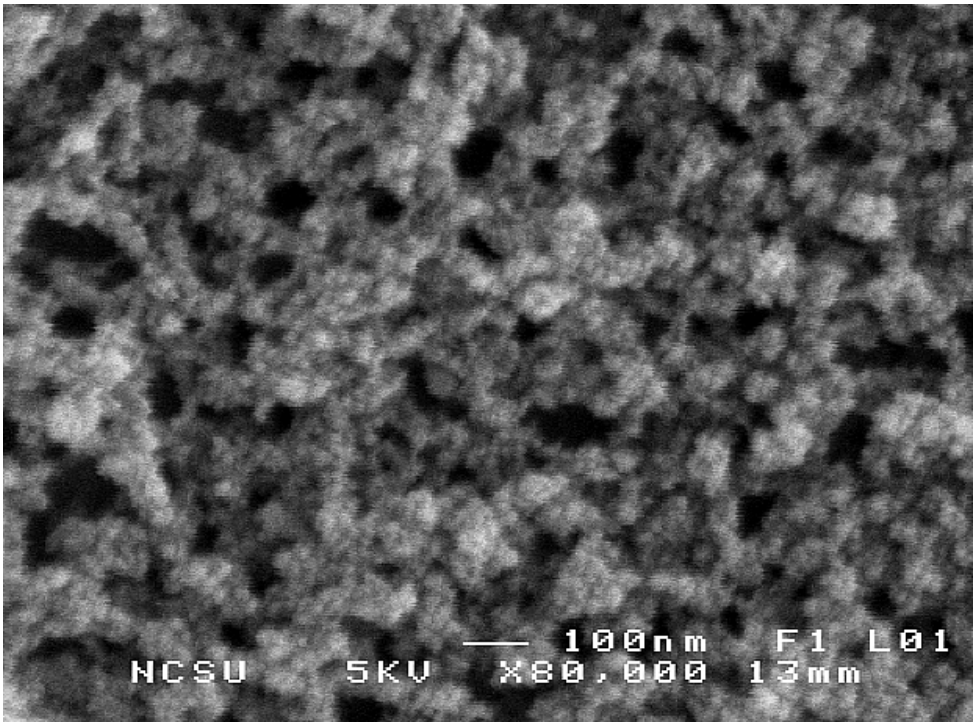

Fig.A.5. 0.50 / non / 13000 rpm / 50 times diluted.

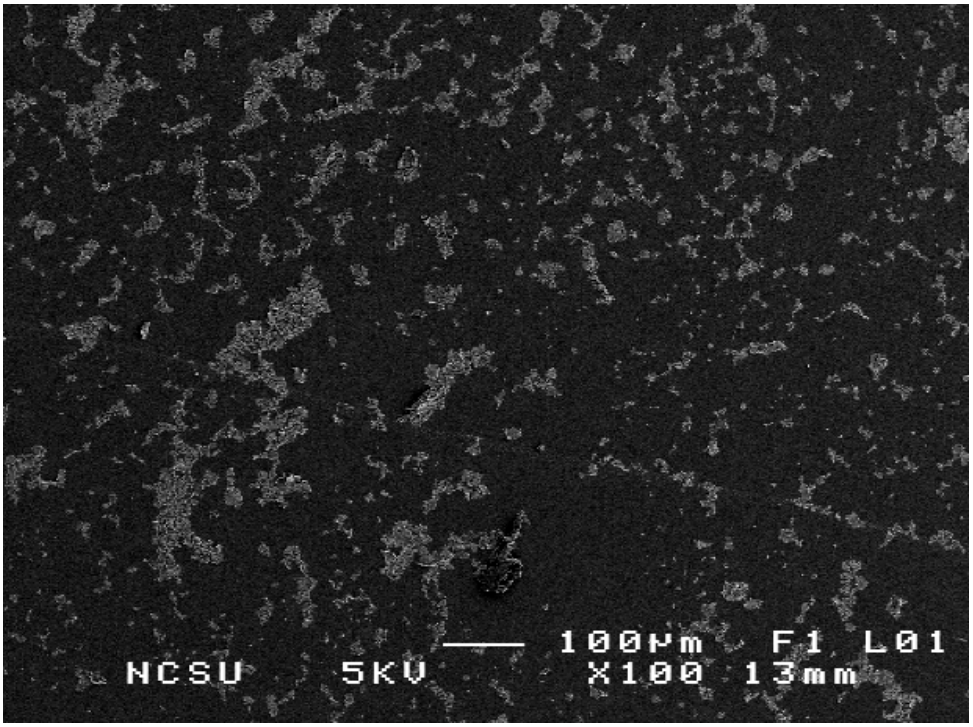

Fig.A.6. 0.50 / 25% / 13000 rpm / 50 times diluted.

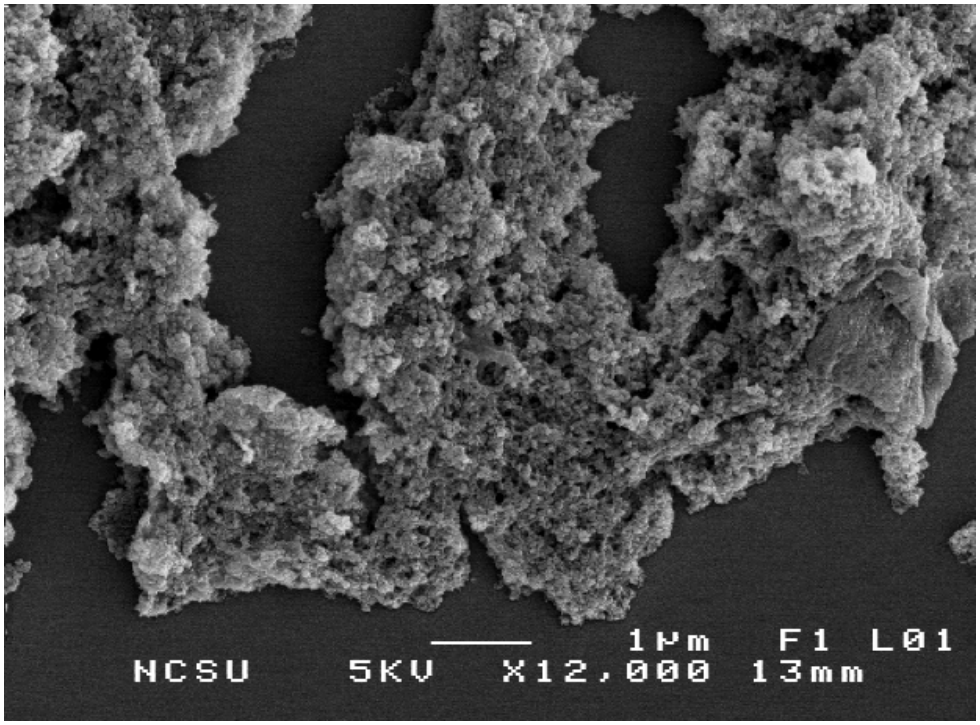

Fig.A.7. 0.50 / 25% / 13000 rpm / 50 times diluted.

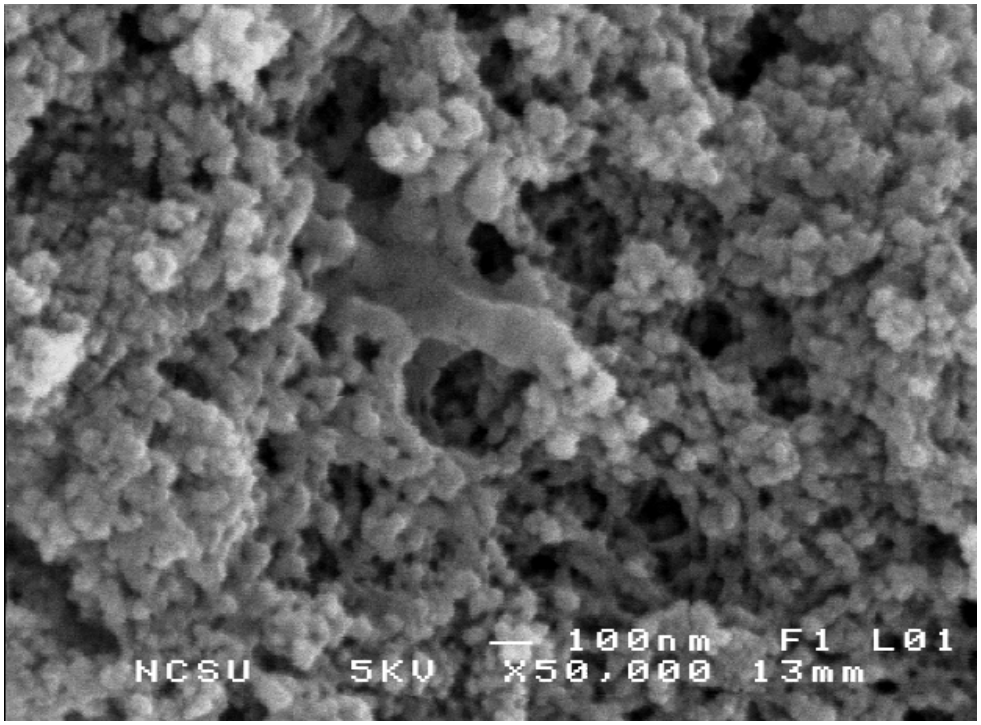

Fig.A.8. 0.50 / 25% / 13000 rpm / 50 times diluted.

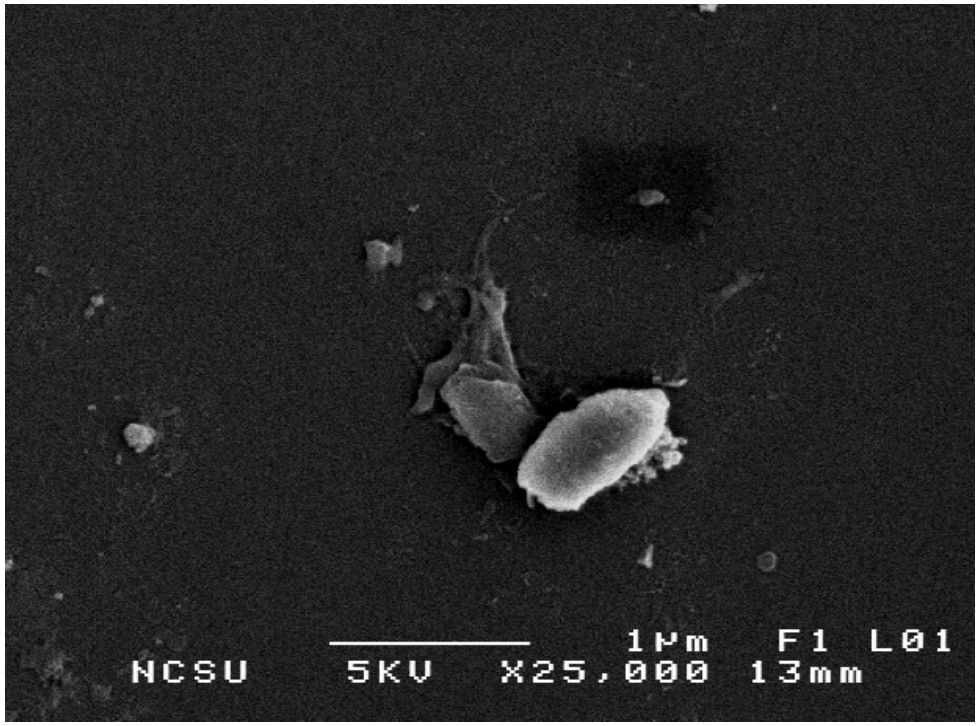

Fig.A.9. 0.50 / 25% / 13000 rpm / 50 times diluted.

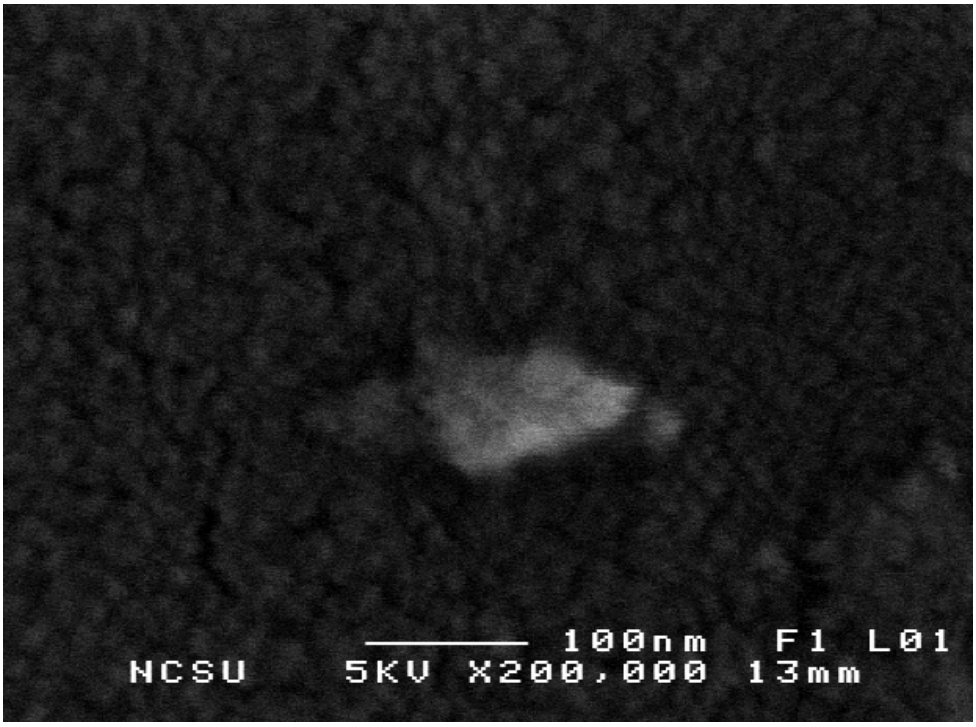

Fig.A.10. 0.50 / 25% / 13000 rpm / 50 times diluted.

Fig.A.11. 0.50 / 25% / 13000 rpm / 50 times diluted.

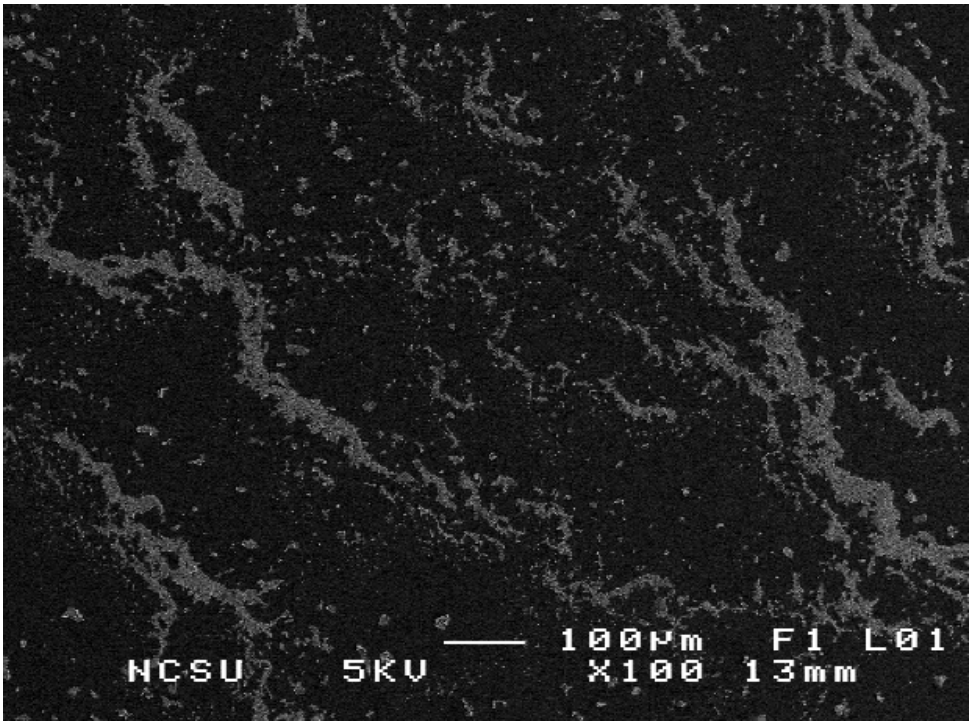

Fig.A.12. 0.63 / non / 13000 rpm / 50 times diluted.

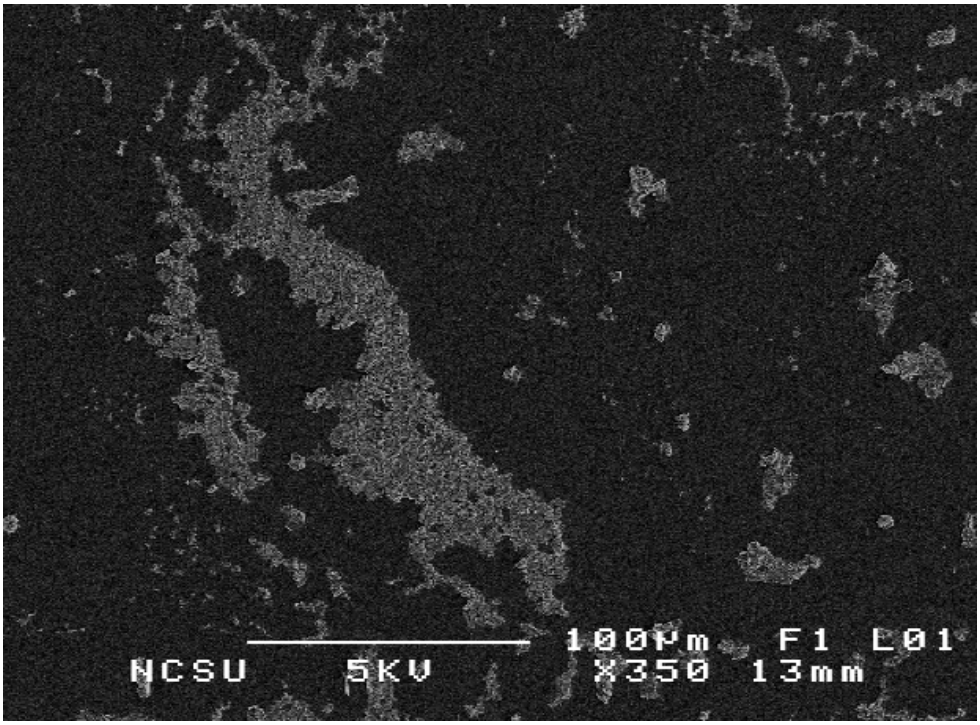

Fig.A.13. 0.63 / non / 13000 rpm / 50 times diluted.

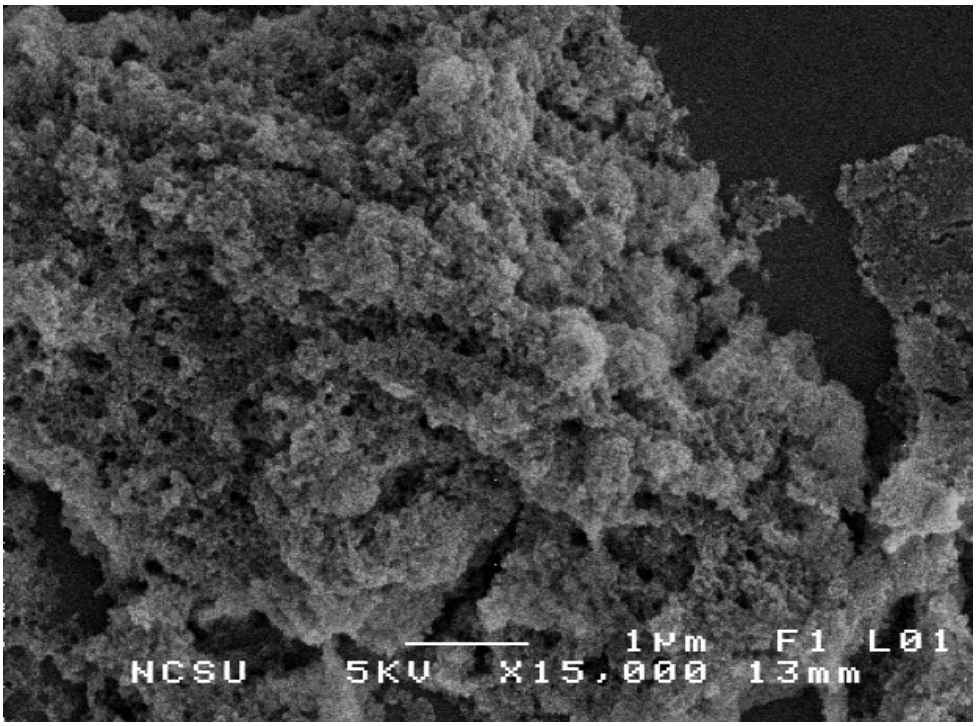

Fig.A.14. 0.63 / non / 13000 rpm / 50 times diluted.

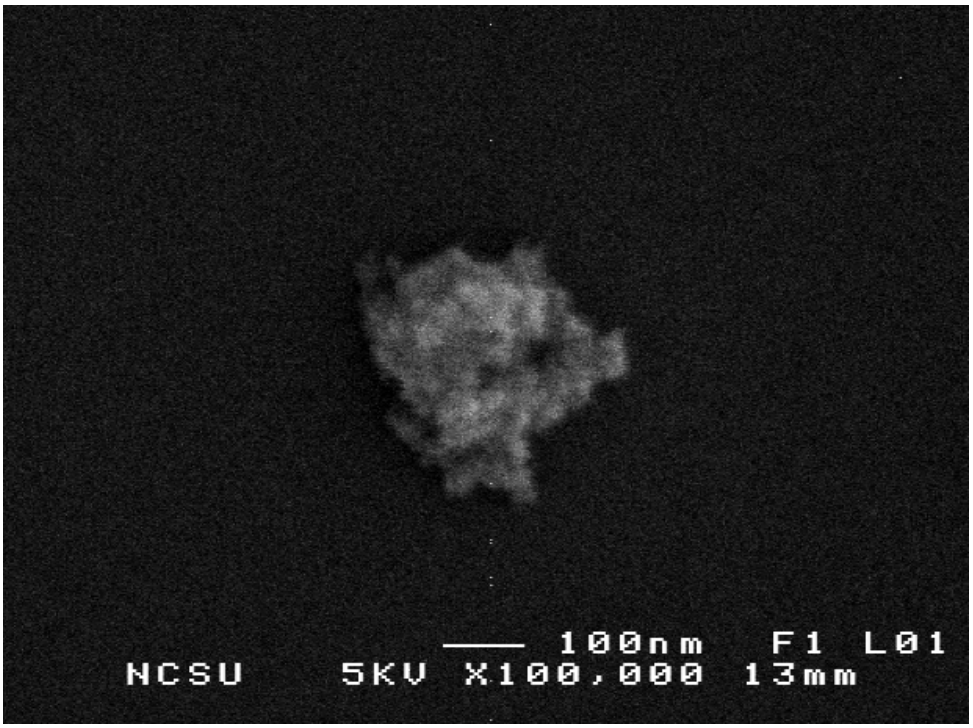

Fig.A.15. 0.63 / non / 13000 rpm / 50 times diluted.

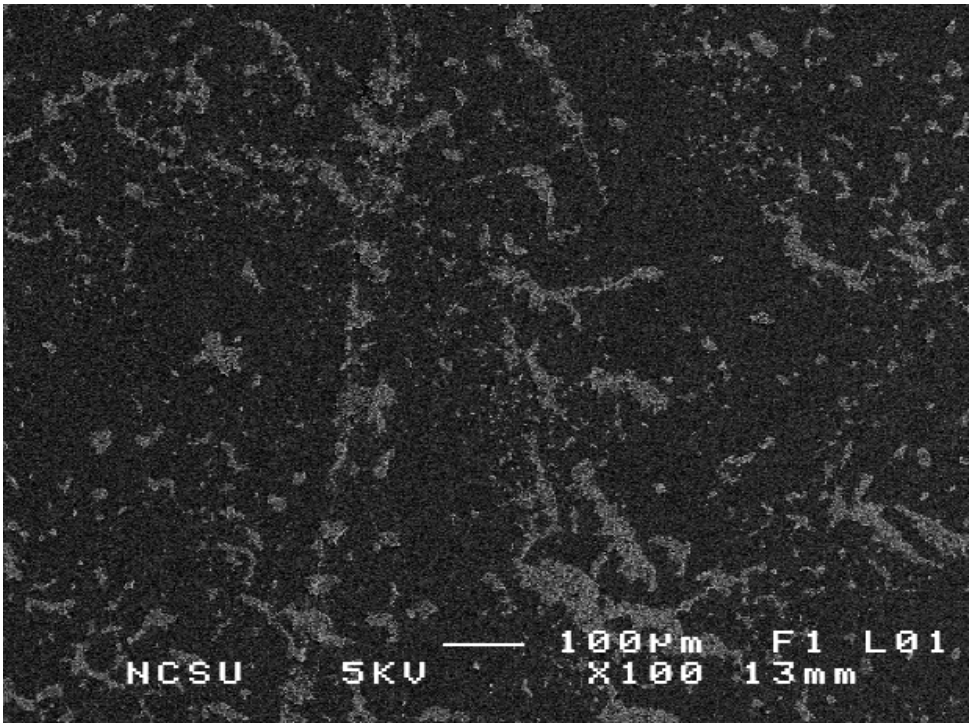

Fig.A.16. 0.63 / 25% / 13000 rpm / 50 times diluted.

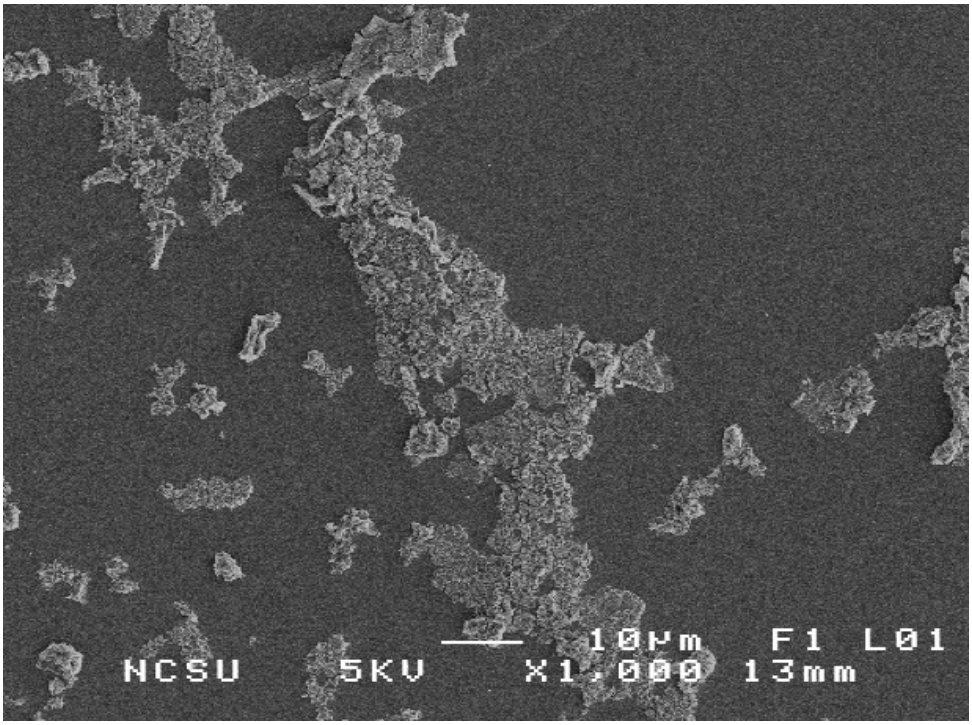

Fig.A.17. 0.63 / 25% / 13000 rpm / 50 times diluted.

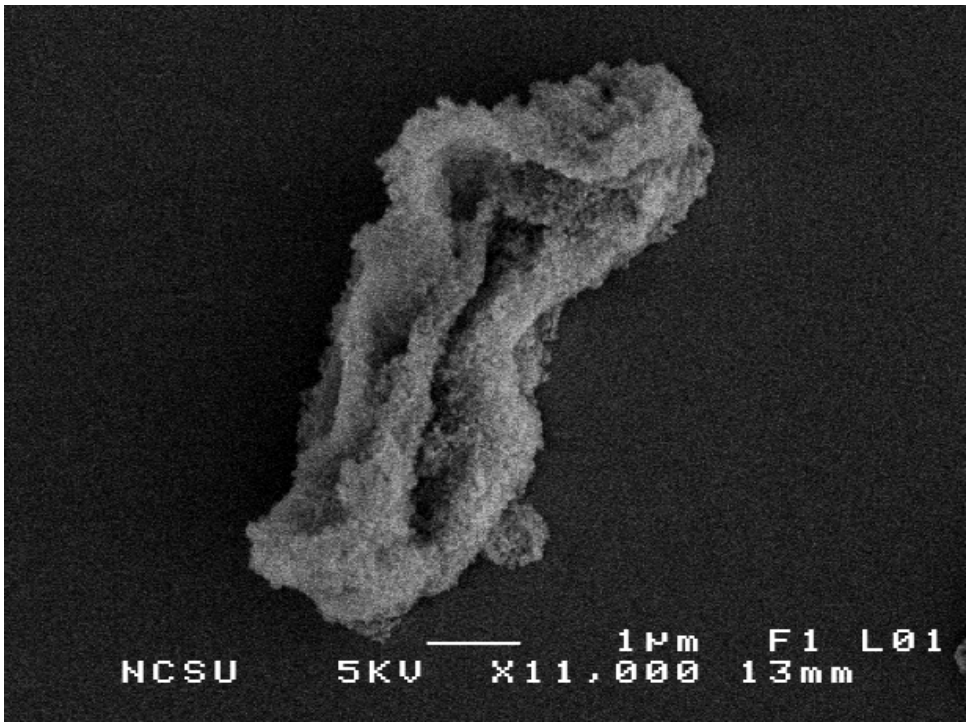

Fig.A.18. 0.63 / 25% / 13000 rpm / 50 times diluted.

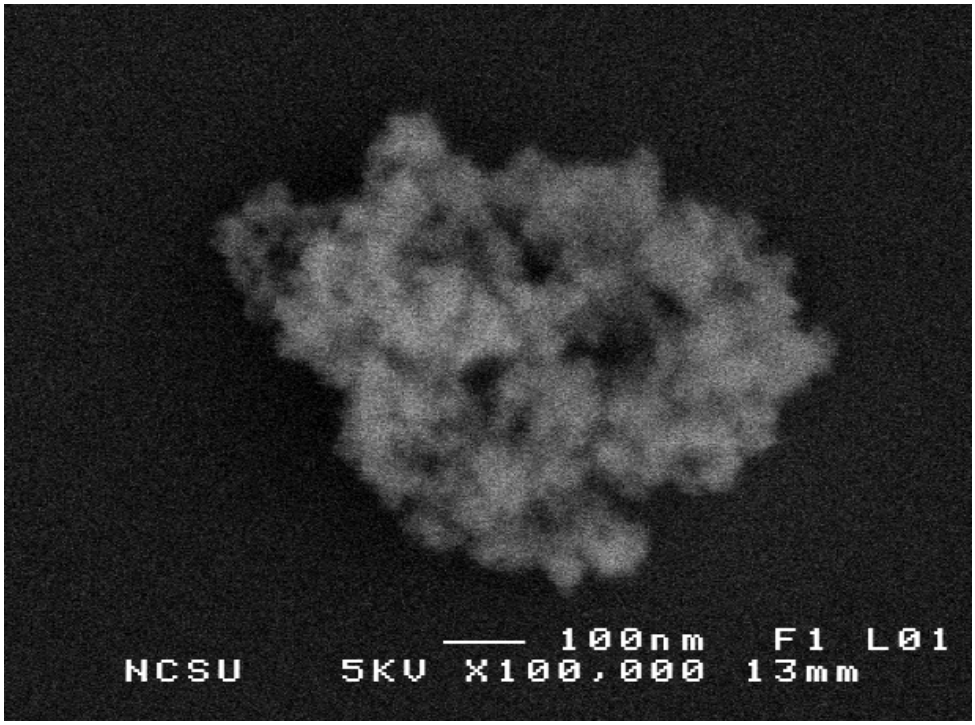

Fig.A.19. 0.63 / 25% / 13000 rpm / 50 times diluted.

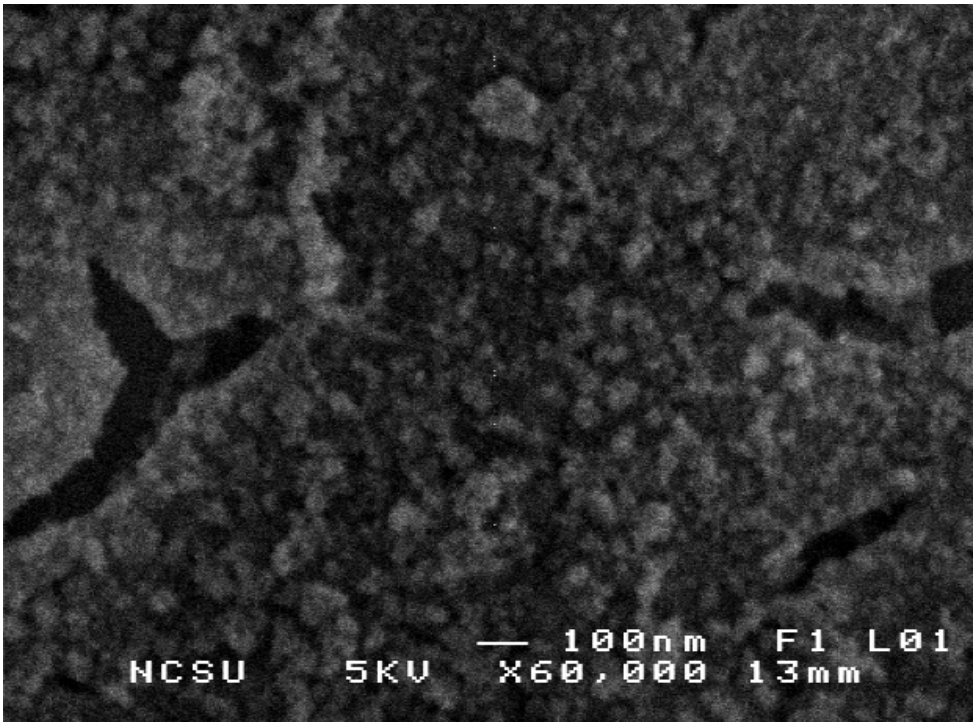

Fig.A.20. 0.63 / 25% / 13000 rpm / 50 times diluted.

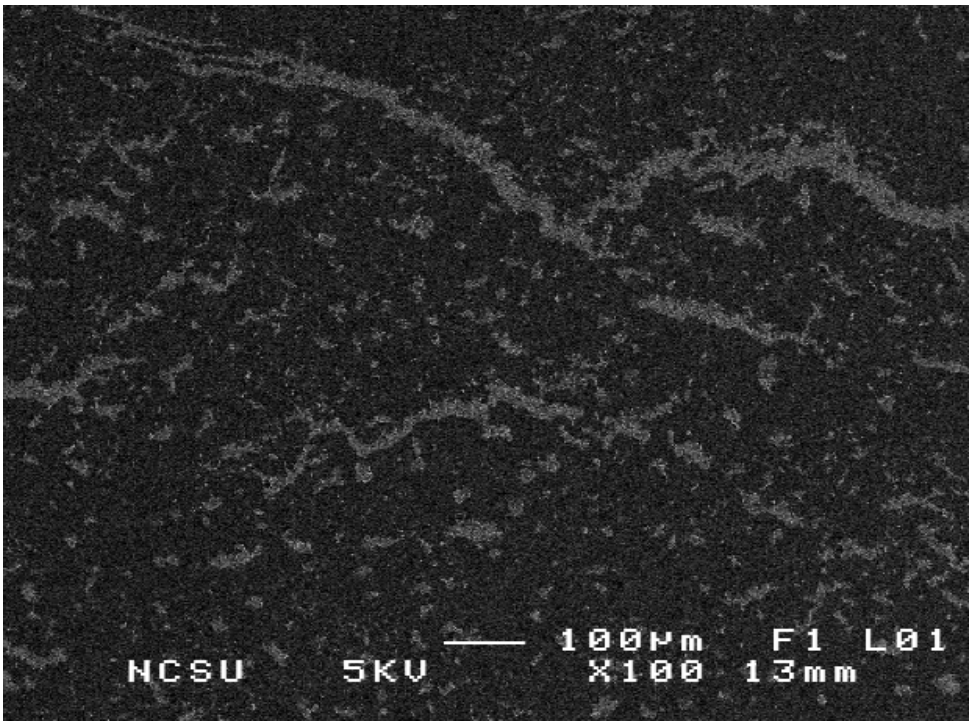

Fig.A.21. 0.88 / non / 13000 rpm / 50 times diluted.

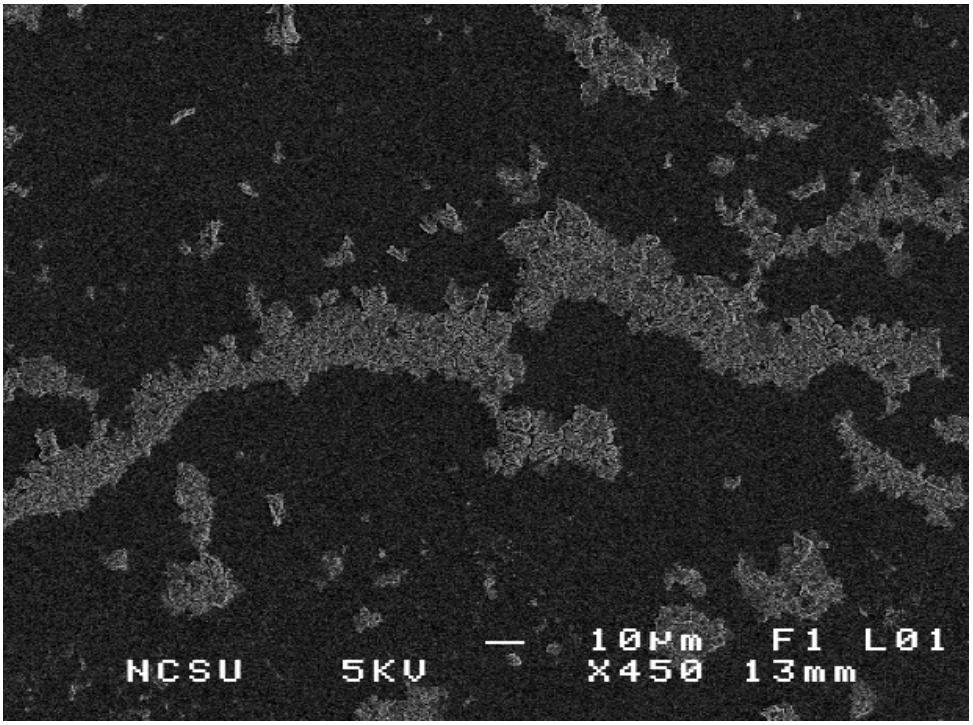

Fig.A.22. 0.88 / non / 13000 rpm / 50 times diluted.

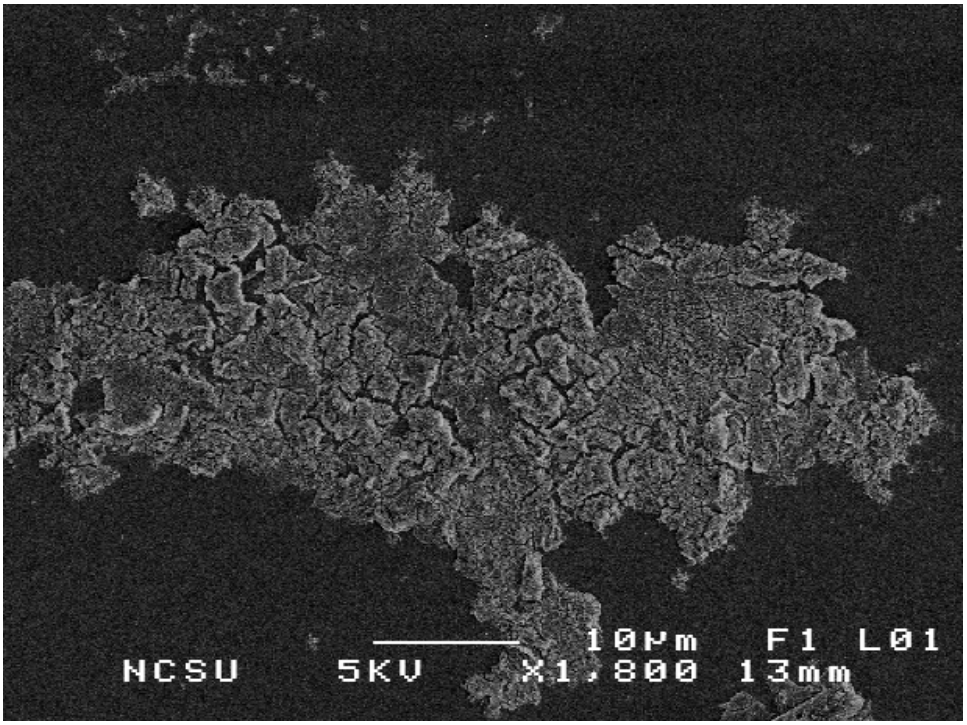

Fig.A.23. 0.88 / non / 13000 rpm / 50 times diluted.

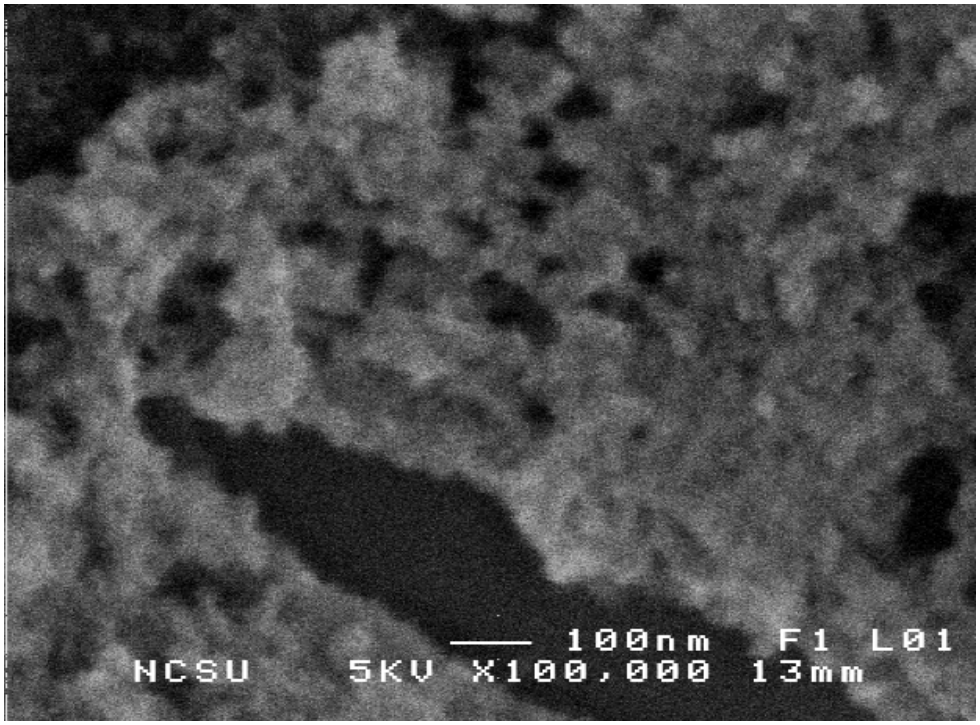

Fig.A.24. 0.88 / non / 13000 rpm / 50 times diluted.

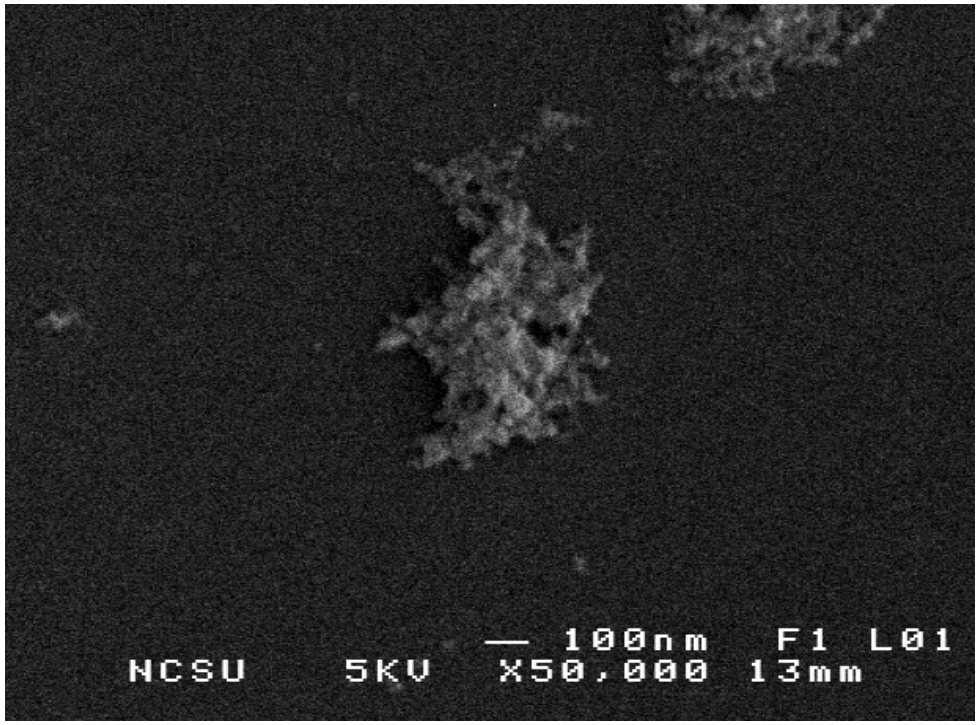

Fig.A.25. 0.88 / non / 13000 rpm / 50 times diluted.

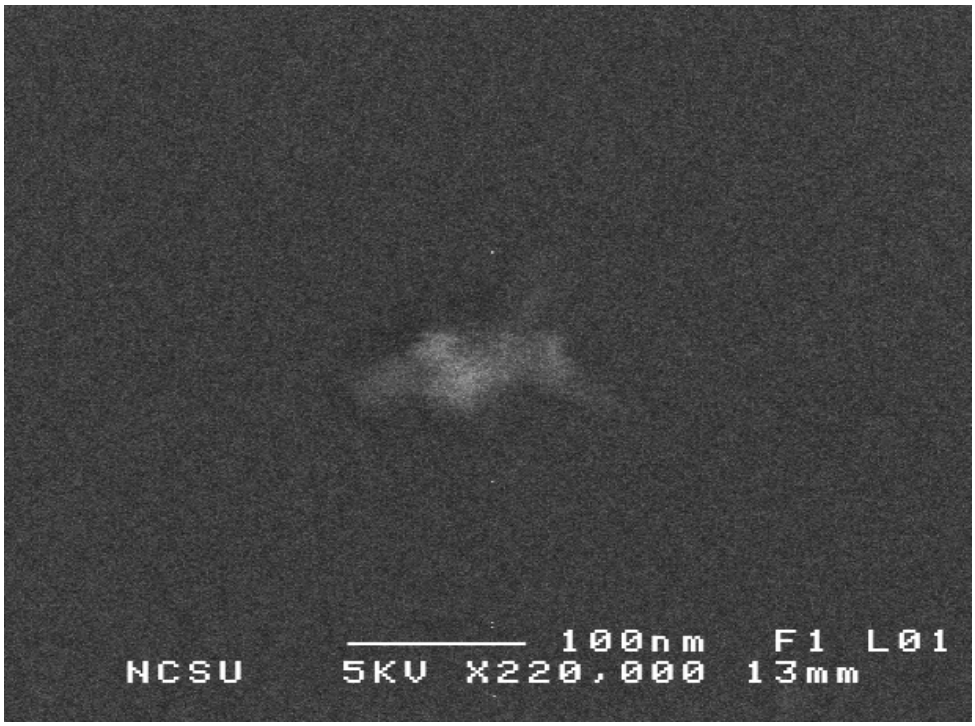

Fig.A.26. 0.88 / non / 13000 rpm / 50 times diluted.

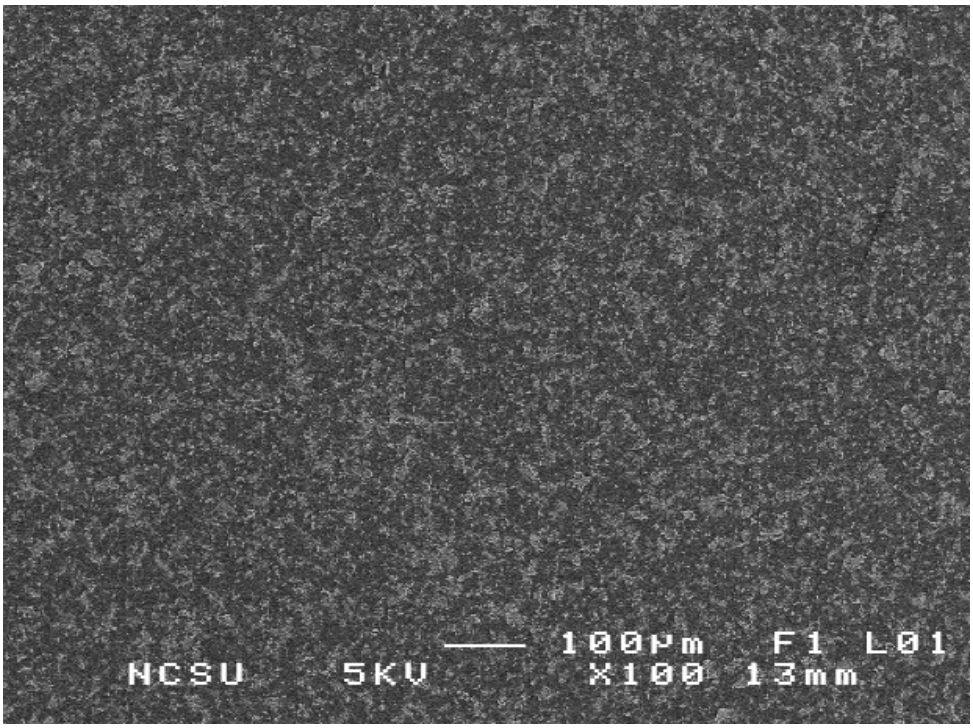

Fig.A.27. 0.88 / 25% / 13000 rpm / 50 times diluted.

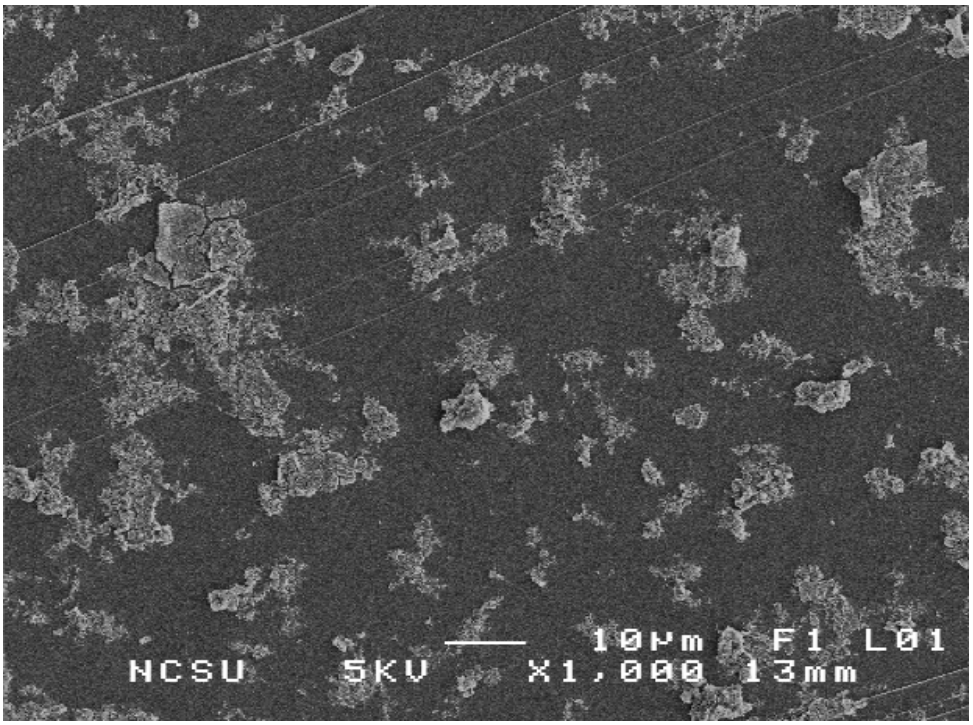

Fig.A.28. 0.88 / 25% / 13000 rpm / 50 times diluted.

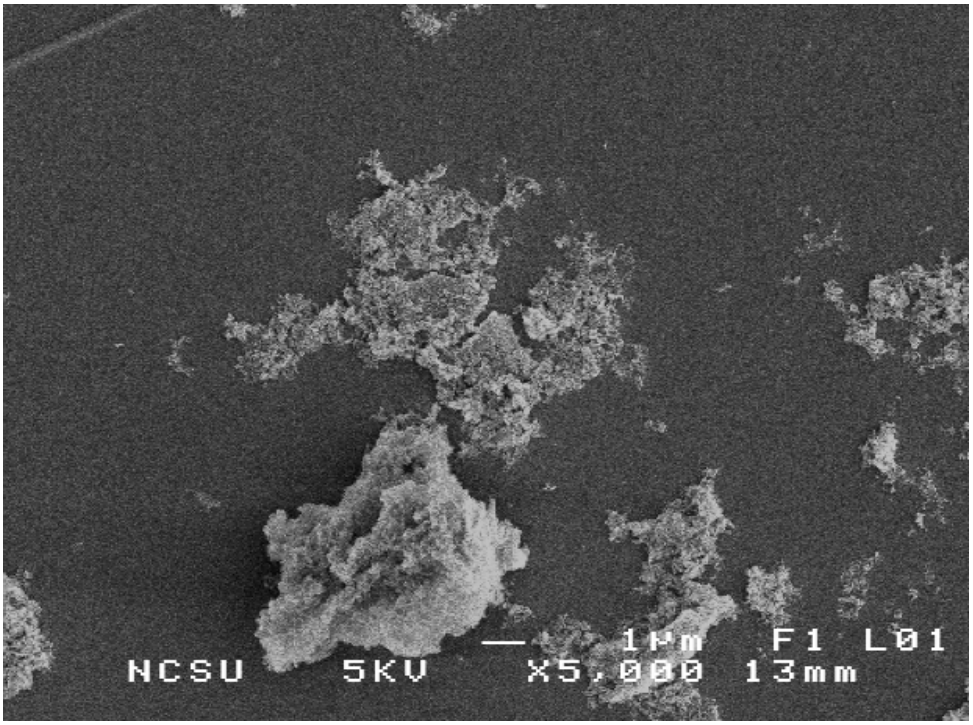

Fig.A.29. 0.88 / 25% / 13000 rpm / 50 times diluted.

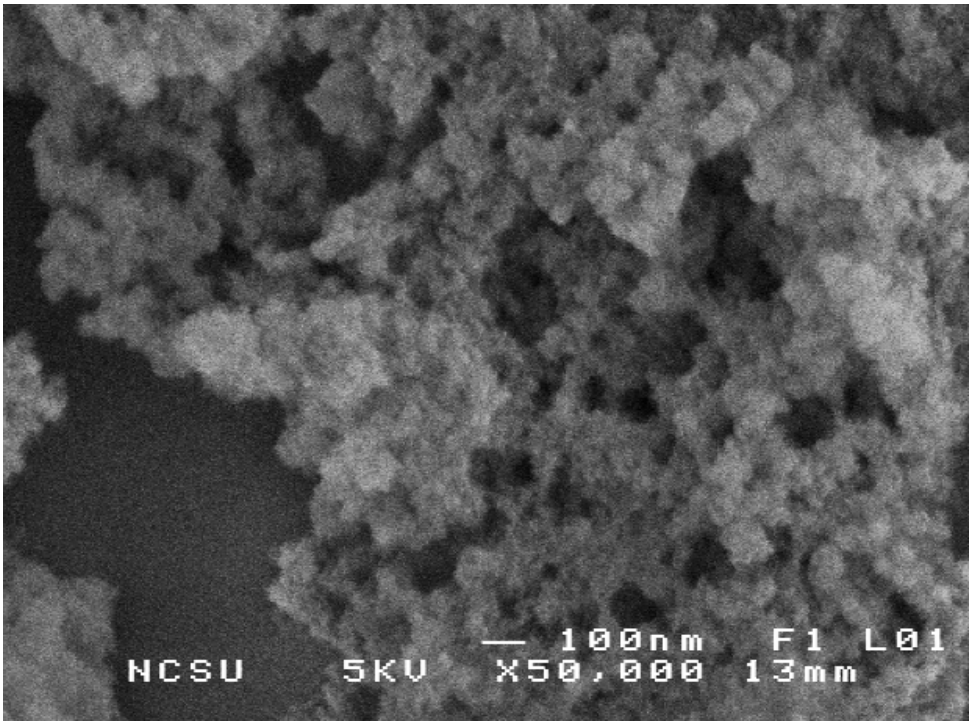

Fig.A.30. 0.88 / 25% / 13000 rpm / 50 times diluted.

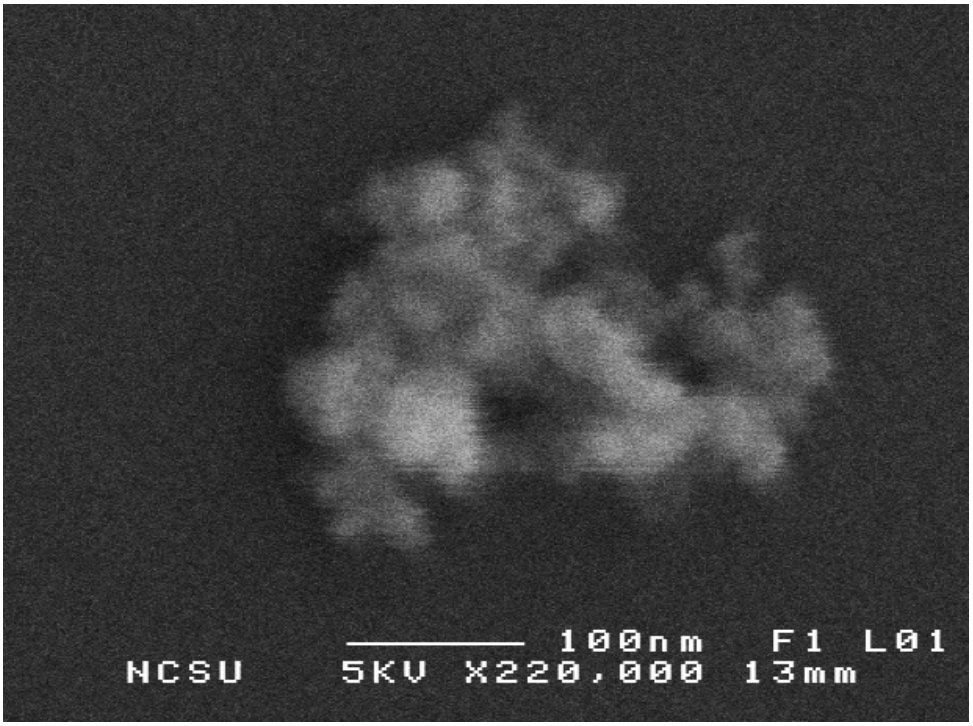

Fig.A.31. 0.88 / 25% / 13000 rpm / 50 times diluted.

Fig.A.32. 0.88 / 25% / 13000 rpm / 50 times diluted.

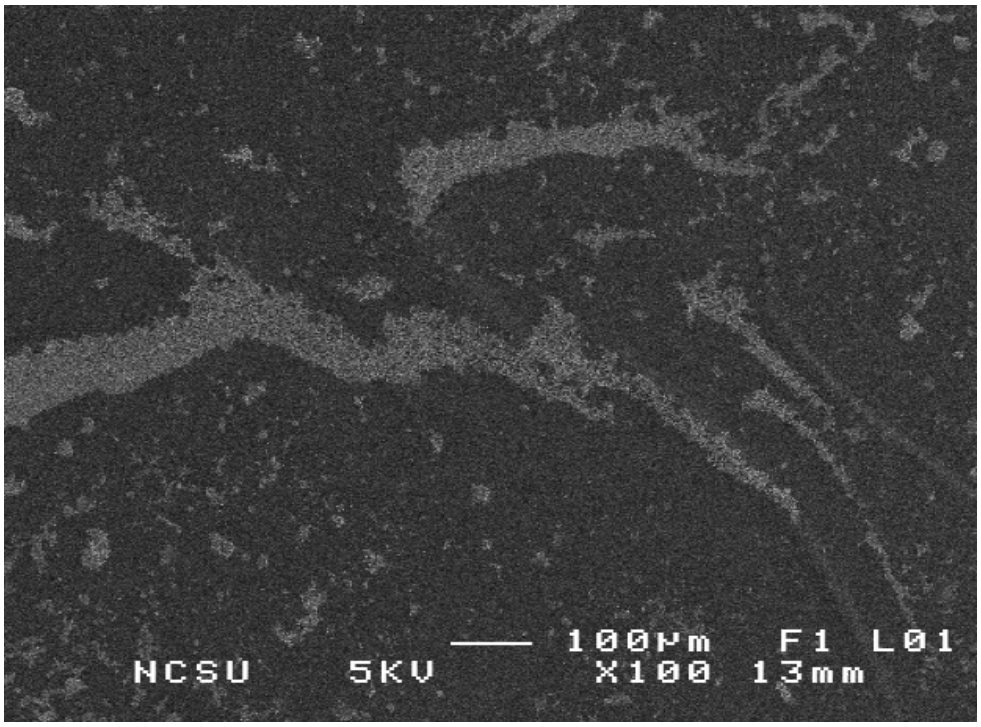

Fig.A.33. 1.00 / non / 13000 rpm / 50 times diluted.

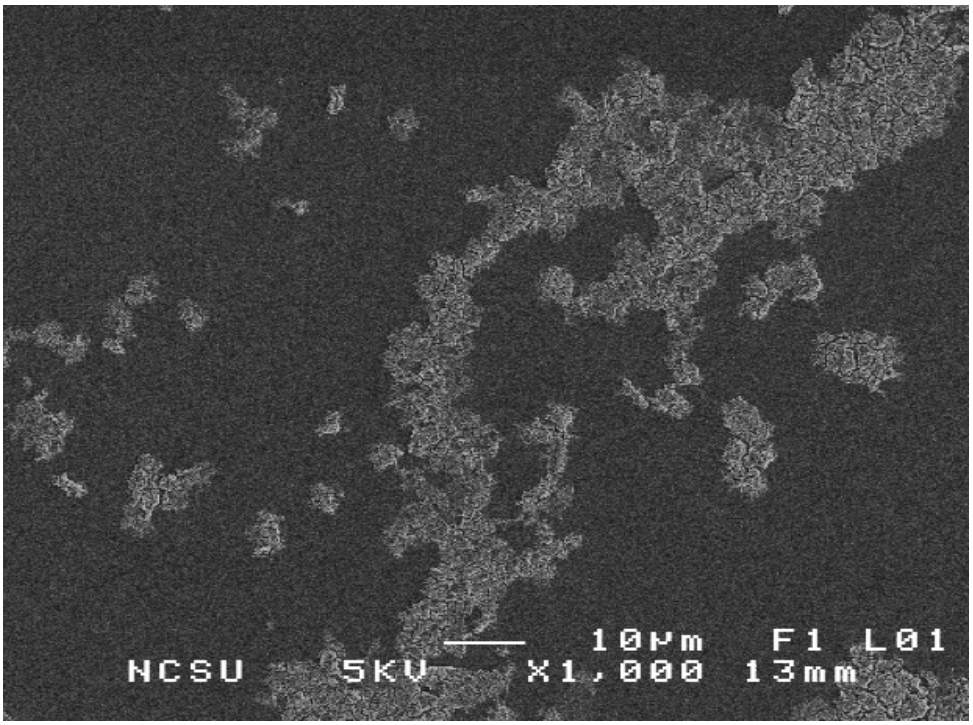

Fig.A.34. 1.00 / non / 13000 rpm / 50 times diluted.

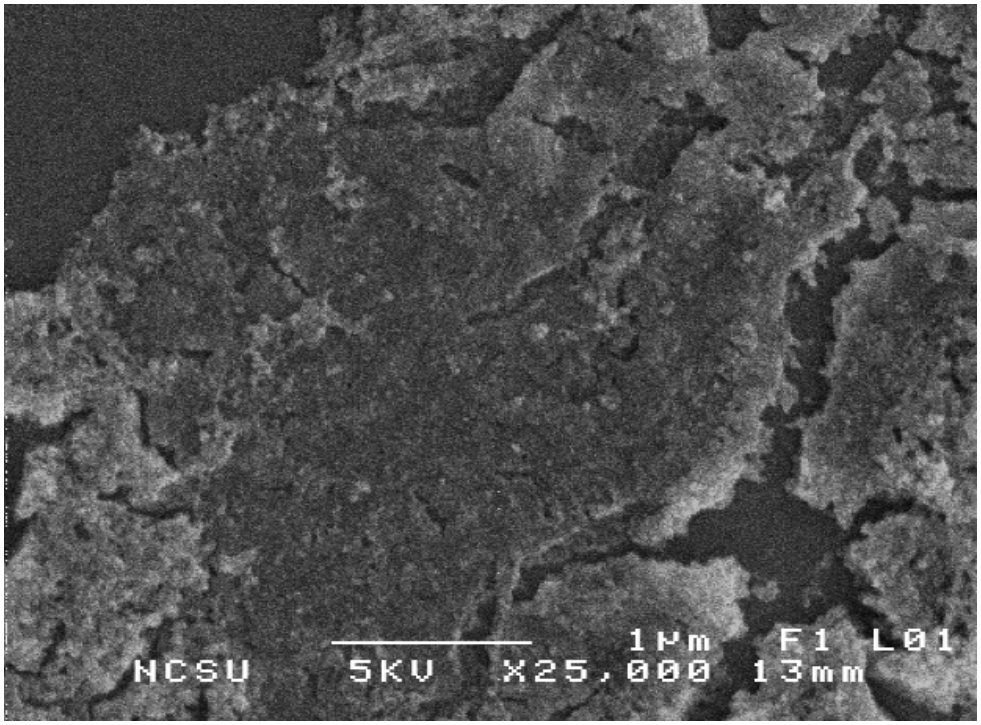

Fig.A.35. 1.00 / non / 13000 rpm / 50 times diluted.

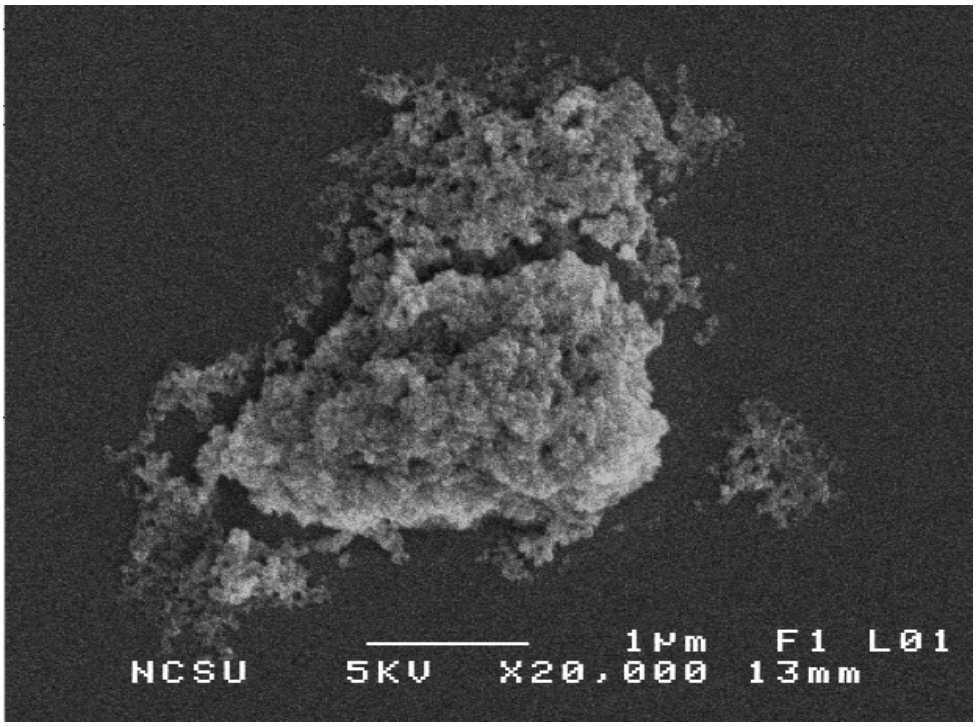

Fig.A.36. 1.00 / non / 13000 rpm / 50 times diluted.

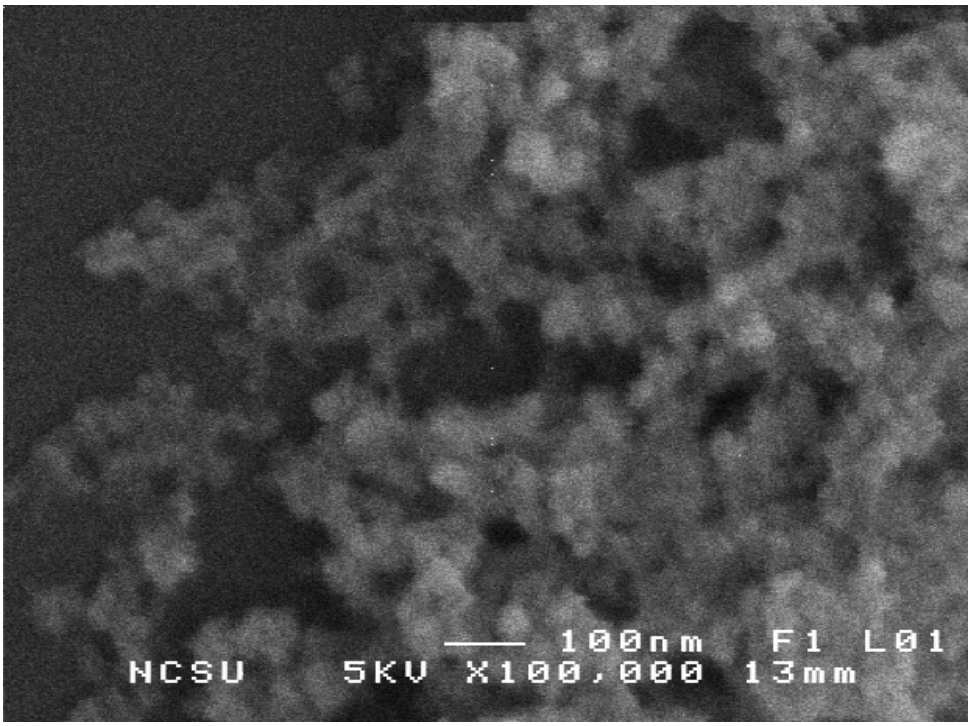

Fig.A.37. 1.00 / non / 13000 rpm / 50 times diluted.

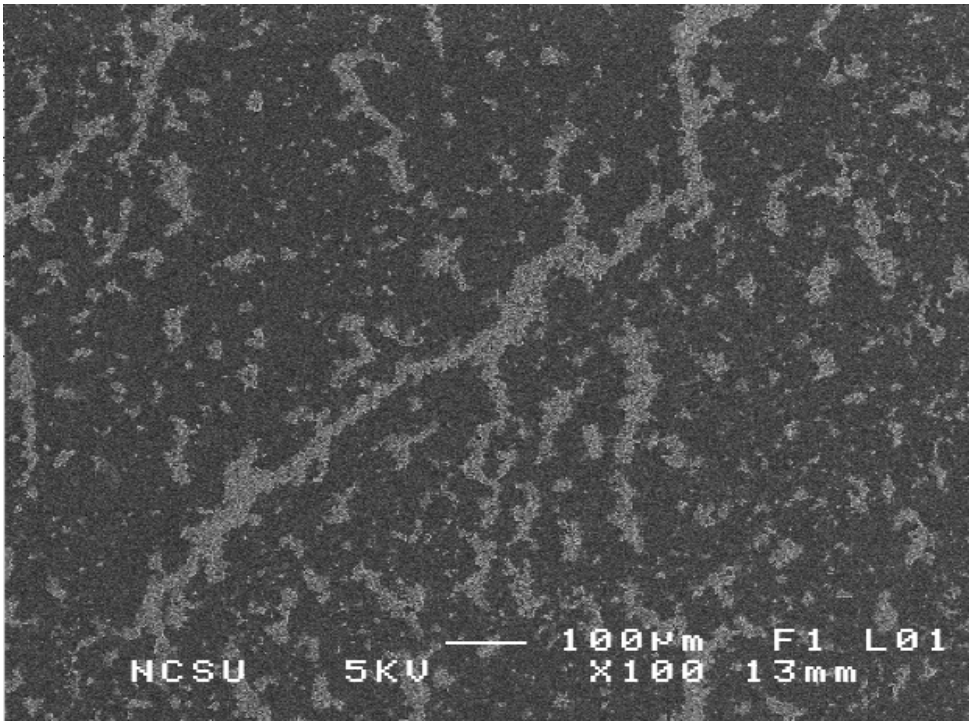

Fig.A.38. 1.00 / 25% / 13000 rpm / 50 times diluted.

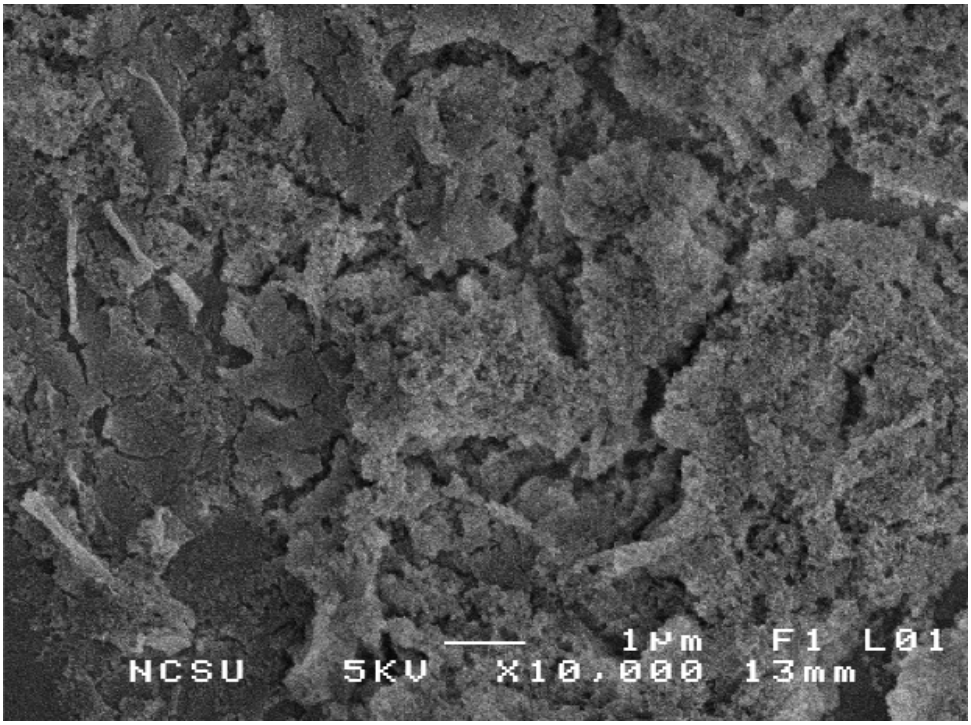

Fig.A.39. 1.00 / 25% / 13000 rpm / 50 times diluted.

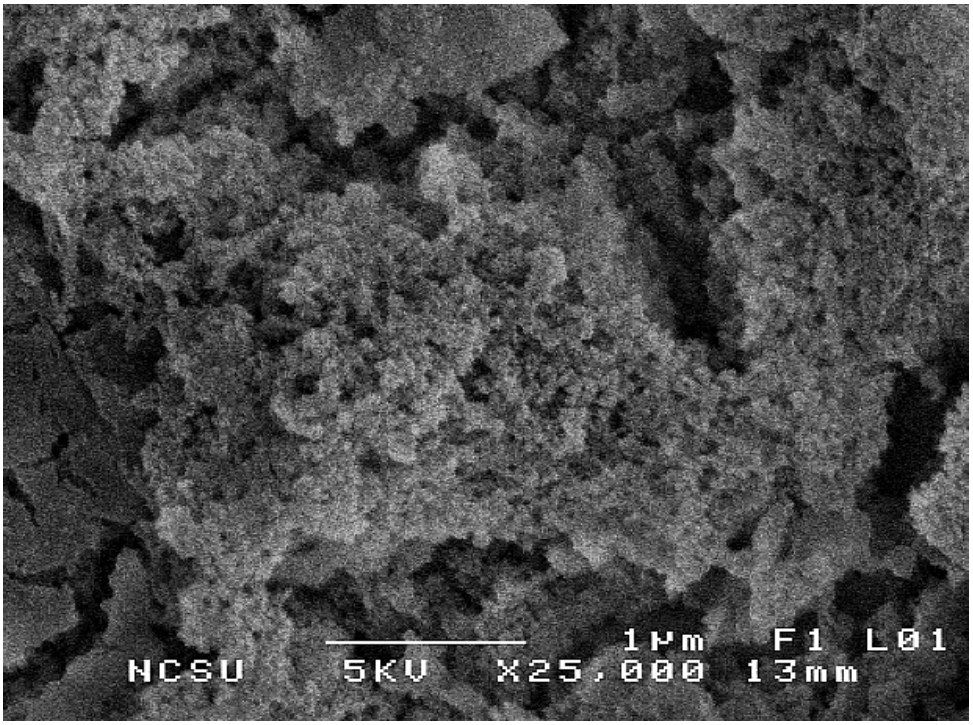

Fig.A.40. 1.00 / 25% / 13000 rpm / 50 times diluted.

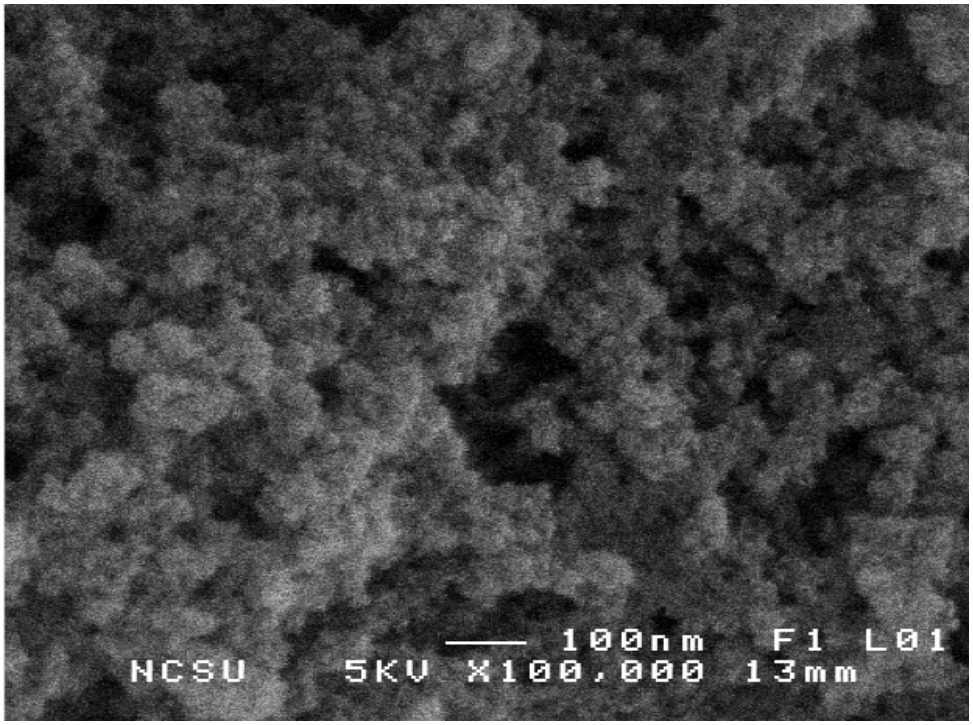

Fig.A.41. 1.00 / 25% / 13000 rpm / 50 times diluted.